

AD-A227 731

31 July 1990

Thesis/Dissertation

On the Developmental Dynamics of Sudden Stratospheric  
Warmings

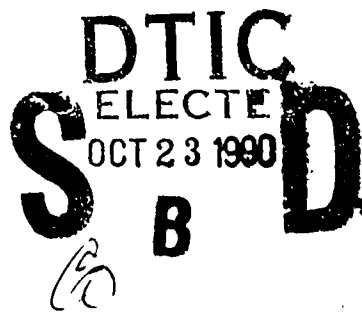
Ann R. Ostdiek

AFIT Student at: Creighton University

AFIT/CI/CIA - 90-079

AFIT/CI  
Wright-Patterson AFB OH 45433

Approved for Public Release IAW AFR 190-1  
Distribution Unlimited  
ERNEST A. HAYGOOD, 1st Lt, USAF  
Executive Officer, Civilian Institution Programs



90

UNCLASSIFIED

## Chapter 1

### INTRODUCTION

Sudden Stratospheric Warmings (SSWs) were first observed in 1952 by Scherhag over Berlin, (Andrews et al., 1987). Until recently, data on SSW were sporadic due to a total dependence on the sparse radiosonde/rocketsonde network. Since the advent of satellite mounted sensors which routinely probe the stratosphere, observational data has become much more abundant. While tremendous advances in the research on SSW have been made in the past decade, few operational meteorologists know much about them. This paper will provide an overview of research done in the following areas: what SSWs are; what synoptic events occur during SSWs; and the dynamics involved with SSWs.

Stratospheric warmings are characterized by the occurrence of dramatic temperature increases in the high latitudes of the stratosphere. There are four recognized categories of warmings: minor, major, final, and Canadian warmings. Atmospheric phenomena associated with SSWs include the presence of tropospheric blocking, unusually large amplitude growth of long wave numbers 1 and 2, and redistribution of ozone in the stratosphere. While eddy transfers of energy between the troposphere and stratosphere drive the dynamical processes of a SSW, ozone redistribution, the primary radiational influence on SSWs, is a function of vertical motions and equator-to-pole transports. There are four primary theories on how SSWs form: wave instabilities; critical layers; preconditioning; and resonance. These theories have been incorporated into mechanistic numerical models. These models are used to simulate SSWs in attempts to learn more about the dynamics involved. General circulation models (GCM) are enhanced by lessons learned from mechanistic modeling, and are used to try to forecast future SSW events.

While a SSW may seem to be an abstract, gee whiz, event to many meteorologists, they are of operational significance. SSWs cause a degradation in High Frequency (HF) radio wave propagation, a hard to forecast phenomenon which impacts all users of HF radio (e.g., military aircraft, amateur radio operators,

satellite links, etc.). Multi-million dollar aircraft flying through the stratosphere are adversely affected by SSWs. The drastic temperature changes that are encountered challenges not only the aircraft designer but also the meteorologist assisting him. The operational meteorologist must forecast not only the severity but also the location of clear air turbulence (CAT) that will be experienced in the area of the SSW. It is the encounter with this strong density discontinuity which is similar to a lower-tropospheric front that cause associated CAT at these altitudes (Haymond, 1967) not the presence of the jet stream (Lee et al., 1979) which is a primary cause of CAT in the troposphere. Whether or not the polar night jet reversed direction in response to the warming needs to be known so anticipated fuel consumption can be calculated. With the retirement of the SR-71 reconnaissance aircraft, one of the few planes which routinely fly through the stratosphere, most operational meteorologists will soon forget what little they know about SSWs. The National Aerospace Plane (NASP), when completed, will be leading the way for a whole new fleet of aircraft that will make their home in the stratosphere. They will routinely probe the environs of the SSW and, if we are not careful in the interim, all we've learned about this layer of the atmosphere could be lost and regained only through yet another era of trial and error.



Accession For	
NTIS GRA&I	<input checked="" type="checkbox"/>
DTIC TAB	<input type="checkbox"/>
Unannounced	<input type="checkbox"/>
Justification	
By _____	
Distribution/ _____	
Availability Codes	
Dist	Avail and/or Special
A-1	

On The Developmental Dynamics of  
Sudden Stratospheric Warmings

By  
Ann R. Ostdiek

Directed Independent Study Project  
Department of Atmospheric Sciences  
Creighton University

31 July 1990

## Table of Contents

1.	Introduction .....	1
2.	Categories of Sudden Stratospheric Warmings .....	3
2.1	Minor Warming .....	5
2.2	Major Warming .....	5
2.3	Final Warming .....	6
2.4	Canadian Warming .....	7
3.	SSW Mechanics - Observed .....	8
3.1	Amplitude Change of Planetary Wave Heights .....	8
3.2	Amplification of Waves 1 and 2 .....	9
3.3	Changes in the Stratosphere .....	11
4.	Energy Cycle and Radiational Processes .....	15
4.1	Energy Cycle .....	15
4.2	Radiational Processes .....	18
5.	Formation Theories .....	21
5.1	Wave Instabilities .....	21
5.2	Critical Layer .....	24
5.3	Preconditioning .....	26
5.4	Resonance .....	31
6.	SSW Mechanics - Models .....	34
6.1	Mechanistic .....	34
6.2	GCM .....	36
7.	Summary .....	40
8.	Conclusions .....	42

## Appendices

### Appendix A

Diagnostic Tools .....	43
------------------------	----

## Appendix B

Case Study .....	46
Major Warming .....	46
Minor Warming .....	65
Conclusion .....	82

## Illustration

Fig. 1. Schematic latitude-height section of zonal mean wind ( $\text{ms}^{-1}$ ) for solstice conditions. W and E designate centers of westerly and easterly winds respectively.	..... 3
Fig. 2. Zonal mean (a) winds ( $\text{ms}^{-1}$ ), and (b) temperature (K) at 10 mb for the period 12 January-27 February 1979.	..... 4
Fig. 3. 50 mb height chart during a minor warming.	..... 5
Fig. 4. 50 mb height chart during a major warming.	..... 6
Fig. 5. Eddy kinetic energy of long waves during January 1963.	..... 9
Fig. 6. Variation with latitude and time at the 50 mb level of a) the zonal wind, and b) the zonal mean temperature during the warming of 1957.	..... 11
Fig. 7. Daily amplitudes of the zonal harmonic a) wave number 1 and b) wave number 2 at $60^{\circ}\text{N}$ for the period December 1970 - January 1971.	..... 12
Fig. 8. Daily values of zonal harmonic temperature wave 1 at the 10 mb and 30 mb levels for a) major and b) minor warmings.	..... 13
Fig. 9. Schematic illustration of the annual mean energy cycle in the lower stratosphere (30 - 100 mb).	..... 16
Fig. 10. Energy cycles for the prewarming and warming stages.	..... 17
Fig. 11. Variation of the ozone mixing ratio at 0.01 mb during 1982 - 1983.	..... 20
Fig. 12. Vertical structure of monthly mean long waves at $50^{\circ}\text{N}$ for	

January 1958.	.....	22
Fig. 13. Time-height sections at $60^{\circ}\text{N}$ showing amplitude of the geo-potential perturbation and the mean zonal wind speed for the wave number 1 case.	.....	26
Fig. 14. Same as Fig. 13 but for wave number 2.	.....	26
Fig. 15. Eliassen-Palm cross sections for a pair of model simulations in zonal wave number 2 are generated which planetary waves of by applying two different lower boundary conditions.	.....	28
Fig. 16. a) Difference at 30 mb between the temperature at the north pole and the zonally averaged temperature at $60^{\circ}\text{N}$ ; b) amplitudes in meters of zonal harmonic geopotential height waves 1 and 2 at $60^{\circ}\text{N}$ and 30 mb.	.....	29
Fig. 17. Breaking planetary wave at 00Z on 27 January 1979, as shown by the height of the 10 mb constant pressure surface.	.....	30
Fig. 18. Shape of the material line, originally coincident with the $30^{\circ}\text{N}$ latitude circle at an altitude of about 31 km, and then advected by a wind field generated by a mechanistic simulation.	.....	30
Fig. 19. Anomaly correlations of height calculated from $20^{\circ}\text{N}$ to $82.5^{\circ}\text{N}$ using heights of standard pressure levels between 1000 - 200 mb.	.....	38
Fig. 20. Some integral curves of $F$ and contours of $D_F$ in units $10^{-4} \text{ ms}^{-2}$ for a) February 17, b) February 19, c) February 21, d) February 23, e) February 26, and f) February 28, 1979.	.....	44
Fig. 21. 30 mb height/temperature for January 1, 1985.	.....	47
Fig. 22. 30 mb height/temperature for January 2, 1985.	.....	48
Fig. 23. 30 mb height/temperature for January 3, 1985.	.....	49
Fig. 24. 30 mb height/temperature for January 4, 1985.	.....	50
Fig. 25. 30 mb height/temperature for January 5, 1985.	.....	51
Fig. 26. 30 mb height/temperature for January 6, 1985.	.....	52
Fig. 27. 30 mb height/temperature for January 7, 1985.	.....	53

Fig. 28. 30 mb height/temperature for January 8, 1985.	.....	54
Fig. 29. 50 mb height/temperature for January 1, 1985.	.....	55
Fig. 30. 50 mb height/temperature for January 2, 1985.	.....	56
Fig. 31. 50 mb height/temperature for January 3, 1985.	.....	57
Fig. 32. 50 mb height/temperature for January 4, 1985.	.....	58
Fig. 33. 50 mb height/temperature for January 5, 1985.	.....	59
Fig. 34. 50 mb height/temperature for January 6, 1985.	.....	60
Fig. 35. 50 mb height/temperature for January 7, 1985.	.....	61
Fig. 36. 50 mb height/temperature for January 8, 1985.	.....	62
Fig. 37. 30 mb height/temperature for January 20, 1985.	.....	66
Fig. 38. 30 mb height/temperature for January 21, 1985.	.....	67
Fig. 39. 30 mb height/temperature for January 22, 1985.	.....	68
Fig. 40. 30 mb height/temperature for January 24, 1985.	.....	69
Fig. 41. 30 mb height/temperature for January 25, 1985.	.....	70
Fig. 42. 30 mb height/temperature for January 26, 1985.	.....	71
Fig. 43. 30 mb height/temperature for January 27, 1985.	.....	72
Fig. 44. 30 mb height/temperature for January 28, 1985.	.....	73
Fig. 45. 30 mb height/temperature for January 29, 1985.	.....	74
Fig. 46. 30 mb height/temperature for January 30, 1985.	.....	75
Fig. 47. 30 mb height/temperature for January 31, 1985.	.....	76
Fig. 48. 50 mb height/temperature for January 28, 1985.	.....	77
Fig. 49. 50 mb height/temperature for January 29, 1985.	.....	78
Fig. 50. 50 mb height/temperature for January 30, 1985.	.....	79
Fig. 51. 50 mb height/temperature for January 31, 1985.	.....	80

## References

References	.....	83
------------	-------	----

## Chapter 2

### Categories of Sudden Stratospheric Warmings

A SSW is an event which causes a drastic temporary disruption of the zonal winter configuration of the stratosphere. High latitudes in the stratosphere experience temperature increases of over  $25^{\circ}\text{C}$  in less than a week. At the peak of the warming, the temperature can increase by as much as  $80^{\circ}\text{C}$ . Typically, within six weeks the atmosphere returns to a more normal configuration, ending the SSW. The onset of a warming is defined by the first appearance of a closed  $-35^{\circ}\text{C}$  isotherm at 10 mb (McQuirck and Douglas, 1988). The warming ends when temperatures warmer than  $-35^{\circ}\text{C}$  are no longer observed.

The normal winter westerly zonal mean flow of the stratosphere results from rising motion near the summer pole where maximum diabatic heating occurs. A coriolis torque is exerted on the meridional drift into the winter hemisphere and sinking near the winter pole occurs which generates zonal mean westerlies in the winter hemisphere (Andrews *et al.*, 1987). See Fig. 1. As equinox approaches, maximum heating migrates towards the equator. A poleward meridional drift occurs in both hemispheres and the Coriolis torque generates weak zonal mean

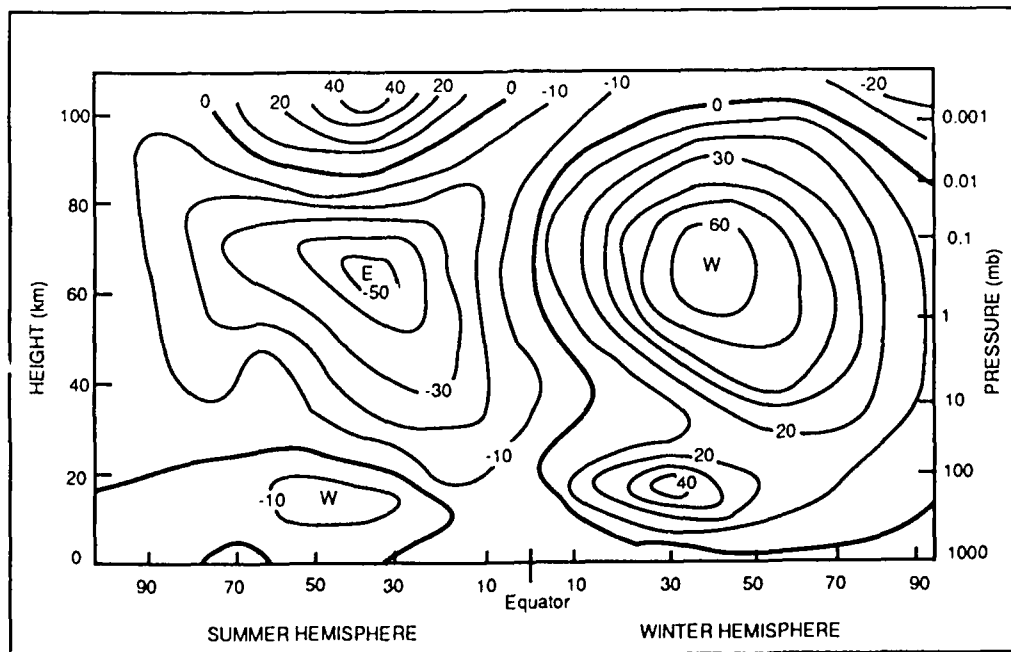


Fig. 1. Schematic latitude-height section of zonal mean wind ( $\text{ms}^{-1}$ ) for solstice conditions. W and E designate centers of westerly and easterly winds respectively. From Andrews *et al.* (1987)

westerlies in both hemispheres.

Sudden Stratopsheric Warmings which occur only in the winter hemisphere can drastically alter the climatologically normal circulation of the winter stratosphere (see Fig. 1). There are four types of warming events - minor, major, final and Canadian (Labitzke, 1977). They are distinguished by the changes in the mean wind flow and the behavior of the polar night jet, in the winter hemisphere. Figure 2 (Mechoso *et al.*, 1985) shows the zonal mean a) wind and b) temperature profiles at 10 mb for the January and February of 1979 SSW of mid-January, the return to a non-SSW circulation in early February, and the major SSW of late February.

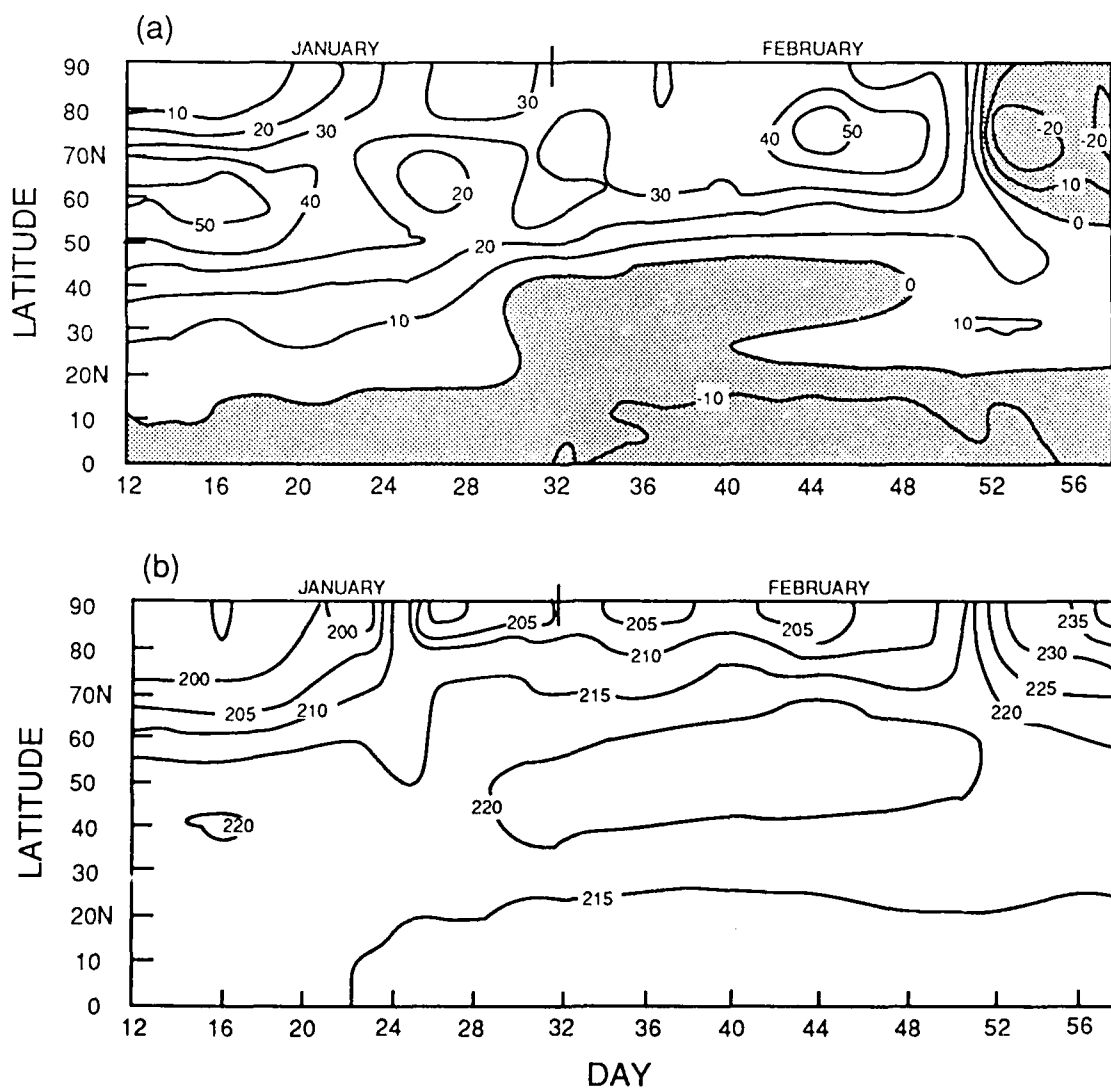


Fig. 2. Zonal mean (a) wind ( $\text{ms}^{-1}$ ), and (b) temperature (K) at 10 mb for the period 12 January-27 February 1979. From Mechoso *et al.*, (1985).

## 2.1 Minor warming

Minor warmings are the type most frequently observed in both the Northern and Southern Hemispheres. A minor warming shows at least a  $25^{\circ}\text{C}$  increase in temperature in the region at or above 10 mb, poleward of  $60^{\circ}$ . The zonal mean winds are from the west prior to, during, and after the warming event. Minor warmings usually occur a few times every winter. Figure 3 (between the 19,355 m and 19,260 m contour along  $60^{\circ}$  longitude) shows the 50 mb height chart for the minor SSW of mid-January 1979 reflecting a typical westerly flow. (While the most dramatic effects of a warming are seen in the upper (10 mb) stratosphere, the mid-stratosphere (50 mb) reflects the overall wind flow and temperature patterns.

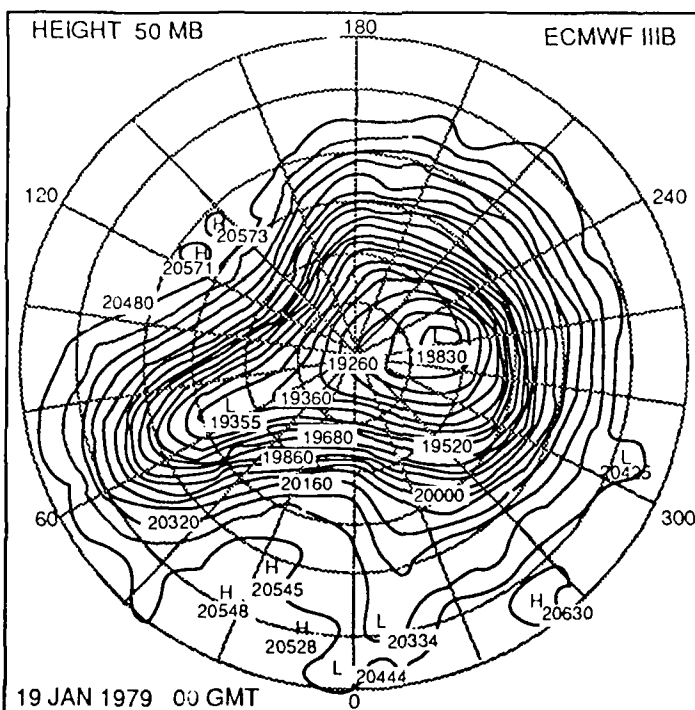


Fig. 3. 50 mb height chart during a minor warming. Typical flow pattern; westerly winds prevail.

(Appendix B, Minor Warming shows a case study of a late January 1985 warming event.)

## 2.2 Major warming

Major warmings are the most dramatic type of warming event. They are unique to the Northern Hemisphere. Relatively rare, they usually occur only once every two or three winters. As with a minor warming, there is a temperature

increase of at least  $25^{\circ}\text{C}$  poleward of  $60^{\circ}\text{N}$  at or above 10 mb. However, in a major warming there is also a breakdown of the polar night jet and a reversal of the mean winds from westerly to easterly between  $55^{\circ}\text{N}$  and  $75^{\circ}\text{N}$ . This reversal persists throughout the warming period, anywhere from one to four weeks (Andrews *et al.*, 1987). Figure 4 shows the 50 mb height chart for the major SSW of late February 1979. Notice the breakup of the polar night jet. The region of easterly flow depicts the area where the warming is occurring. After the event, normal winter radiative processes will eventually reassert themselves and allow westerlies to return and the polar night jet to reestablish itself. (Appendix B, Major Warming shows a case study of an early January 1985 warming event.)

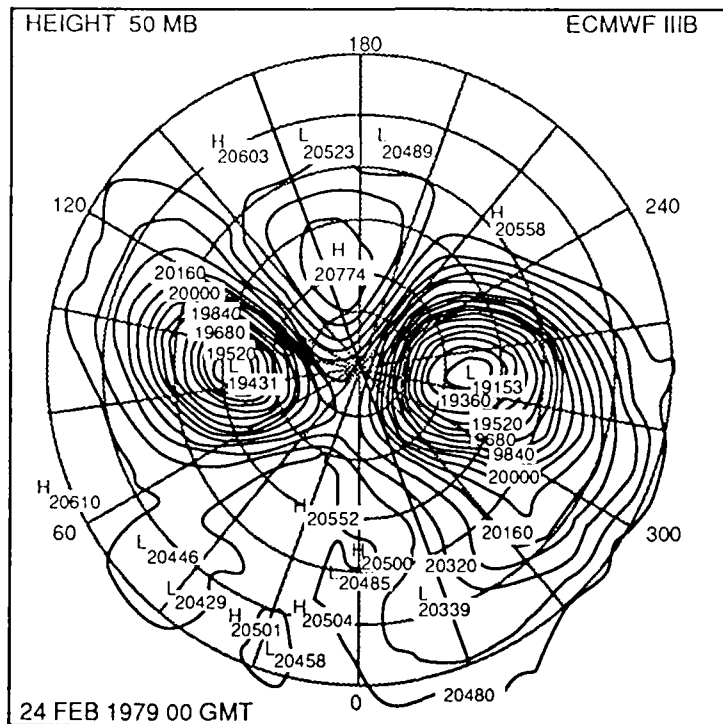


Fig. 4. 50 mb height chart during a major warming. The polar night jet breaks down and easterly cwinds prevail over the area of warming.

### 2.3 Final Warming

Final warmings are a special subset of major warmings (Labitzke, 1977). When a major warming occurs late in the winter it frequently becomes a final warming, in which the easterly mean flow remains after the event is over. Normally as spring approaches and sunlight slowly moves back into the polar latitudes, radiative processes cause the zonal flow in the high latitudes of the stratosphere

to reverse from westerlies to the easterly flow normal throughout the summer. When major warmings occur during the spring transition, the atmosphere may not revert back to the prewarming westerly flow, but instead, retain the easterly zonal flow of the warming event.

## 2.4 Canadian Warming

The fourth type of warming, a Canadian warming is actually a hybrid; a minor warming disguised as a major warming. At first, a Canadian warming looks like a major warming, in which the easterly winds replace the zonal westerly flow in the polar latitudes. However, a closer examination of this phenomenon shows that the westerly polar night jet has not really been destroyed, as in a major warming, but is displaced south of  $60^{\circ}\text{N}$  and, usually, relocated over southern Siberia. Canadian warmings set up when an intense strengthening of the Aleutian High forces the high to build into northern Canada. The warm air and easterly winds associated with the high displace the cold polar vortex, pushing it south into Siberia, causing easterly flow in the high latitudes (Labitzke, 1977). When the Aleutian High weakens, the polar vortex pushes northward and the stratosphere returns to its normal winter circulation.

## Chapter 3

### SSW Mechanics - Observed

Research in SSWs has primarily centered on the analysis of observational data in attempts to define the heat/energy balances of the tropospheric/stratospheric interface above which they form. These studies have looked primarily at three areas: amplitude change of planetary wave heights; amplification of wave numbers 1 and 2; and changes in the stratosphere through the lifetime of an SSW.

#### 3.1 Amplitude Change of Planetary Wave Heights

Various SSW heat balance and energy studies were done by Julian and Labitzke (1965), Mahlman (1969), Muench (1965), and Perry (1967). They found that an unusual growth in the amplitude of planetary height waves occur in the stratosphere prior to a warming. This increase is caused by the transfer of eddy kinetic energy into the stratosphere from the troposphere. Julian and Labitzke (1965) pointed out that SSWs normally commence in areas above intense tropospheric cyclonic activity with anticyclonic blocking conditions upstream. The pressure interactions increase the vertical motion of the eddies penetrating up into the stratosphere from the troposphere. It is the eddy heat fluxes which create the pole-to-equator temperature gradient reversals. These large planetary waves in the stratosphere cause strong, rapid, adiabatic changes in temperature to take place - the same drastic temperature changes associated with SSWs. Thus SSWs result from the penetration of tropospheric wave disturbances deep into the stratosphere.

Wave numbers 1 and 2 are ultra-long, planetary scale waves which are able to penetrate into the stratosphere from the troposphere. They are formed by forced flow over terrain and/or by differential heating between oceans and continents. See Fig. 5 (Perry, 1967).

Major upward transfers of energy in the mid-latitudes between the troposphere and the stratosphere can only occur when light westerlies prevail (Andrews *et al.*, 1987). The tropopause acts as a filter, allowing only energy from these ultra-long planetary waves to propagate upward into the lower stratosphere where they

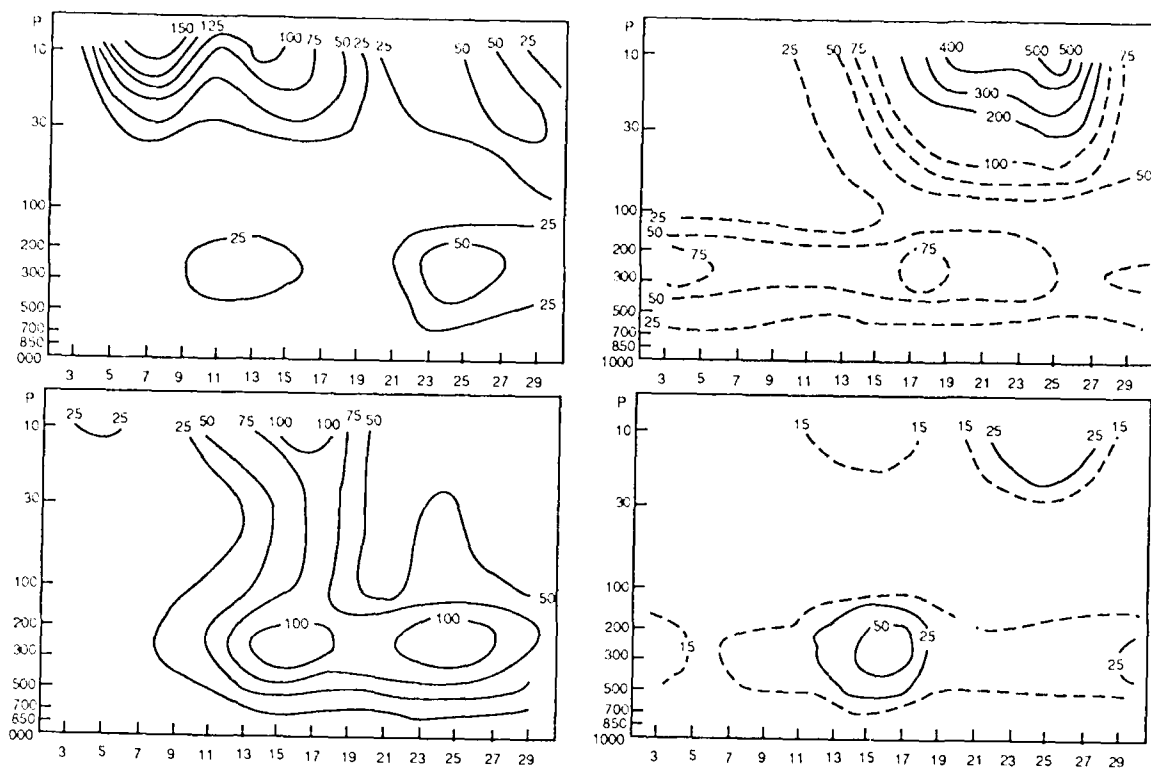


Fig. 5. Eddy kinetic energy of the long waves during January 1963. Upper left, wave 1; upper right, wave 2; lower left, wave 3; lower right, wave 4. Units  $10^4 \text{ erg cm}^{-2} \text{ mb}^{-1}$ . From Perry (1967).

become trapped beneath the stratospheric flow throughout most of the year. Only during spring and fall transitions, or briefly in the winter when the polar night jet weakens, can wave numbers 1 and 2 penetrate into the upper levels of the stratosphere. Charney and Drazin (1961) investigated how energy transfers associated with upward propagation of planetary wave disturbances occur between the troposphere and the stratosphere. They found that for stationary waves, waves whose phase velocity is zero with respect to the ground (i.e.,  $c = 0$ ), there is a maximum wind velocity,  $u_c$ , above which vertically propagating Rossby waves will not form (Andrews *et al.*, 1987). Vertical propagation is only possible when the wind velocity,  $u$ , is:

$$0 < u < u_c$$

For a typical static stability of  $5 \times 10^{-4} \text{ s}^{-2}$  at  $60^\circ\text{N}$ , they found that the maximum wind velocity was

$$u_c = 110/(s^2 + 3) \text{ ms}^{-1},$$

where  $s$  = wave number.

stratosphere. Charney and Drazin (1961) investigated how energy transfers

associated with upward propagation of planetary wave disturbances occur between the troposphere and the stratosphere. They found that for stationary waves, waves whose phase velocity is zero with respect to the ground (i.e.,  $c = 0$ ), there is a maximum wind velocity,  $u_C$ , above which vertically propagating Rossby waves will not form (Andrews *et al.*, 1987). Vertical propagation is only possible when the wind velocity,  $u$ , is:

$$0 < u < u_C.$$

For a typical static stability of  $5 \times 10^{-4} \text{ s}^{-2}$  at  $60^\circ\text{N}$ , they found that the maximum wind velocity was

$$u_C = 110/(s^2 + 3) \text{ ms}^{-1},$$

where  $s$  = wave number.

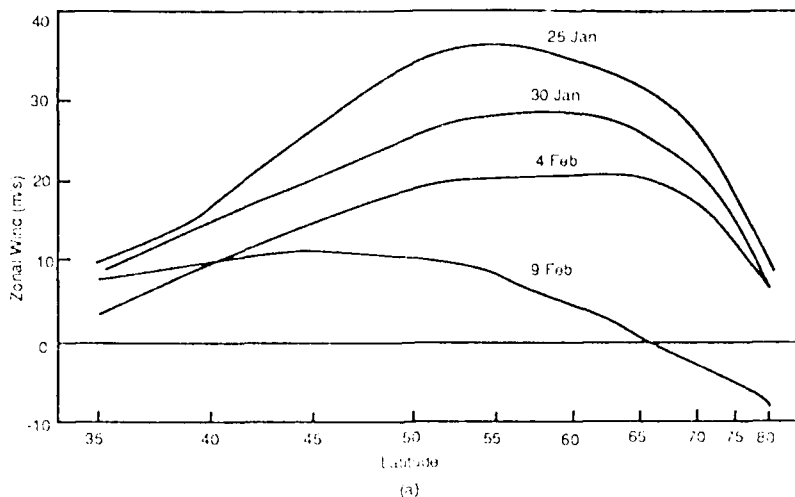
Below are the corresponding  $u_C$  values for wave number 1 through 4.

$s = 1$	$u_C = 28 \text{ ms}^{-1}$
$s = 2$	$u_C = 16 \text{ ms}^{-1}$
$s = 3$	$u_C = 9 \text{ ms}^{-1}$
$s = 4$	$u_C = 6 \text{ ms}^{-1}$

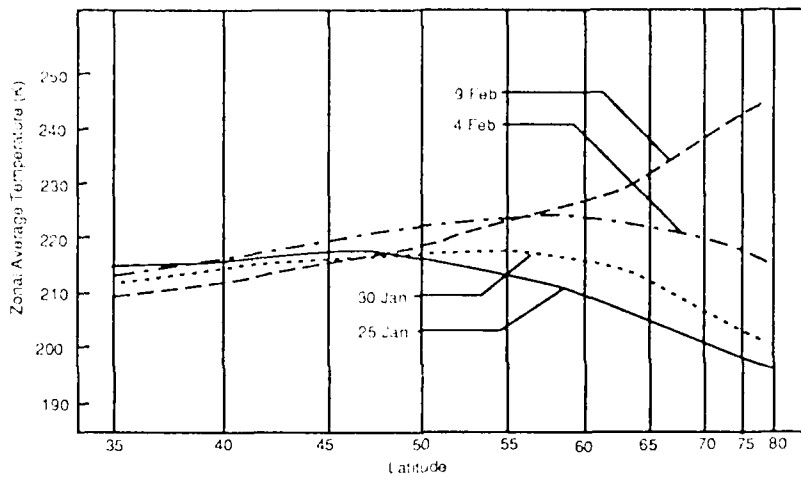
This indicates easterlies and strong zonal westerly winds (like those found in a well developed polar night jet) prevent transfers of large amounts of energy from the waves up into the stratosphere.

### 3.2 Amplification of Waves 1 and 2

Quiroz *et al.* (1975) found that a SSW is the result of an anomalous amplification of wave number 1 or 2 within the polar stratosphere. They observed an increase in the northward eddy heat flux which caused the zonal temperatures to rise in high latitudes and fall in low latitudes, disrupting the normal winter equator-to-pole temperature gradient of the stratosphere. This is all accomplished in a matter of days. The thermal wind balance is maintained, as an easterly wind shear caused by the new temperature gradient replaces the westerly wind shear found in the polar night jet. Coriolis torque acts on a secondary zonal meridional equatorward flow producing an easterly acceleration in the zonal wind. By applying



(a)



(b)

Fig. 6. Variation with latitude and time at the 50 mb level of (a) the zonal wind, and (b) the zonal mean temperature during the sudden warming of 1957. From Holton (1979).

the mass continuity equation to the secondary zonal flow, ascending motion in the zonal flow occurs at high latitudes and zonal mean sinking occurs in the lower latitudes. The type of circulation that would be expected from the new temperature distribution of warm poles and cool equator. See Fig. 6 (Holton, 1979).

Adiabatic temperature changes from air parcel motions partially cancel the temperature changes caused by the eddy heat fluxes. In minor warmings this cancellation prevents the destruction of the polar night jet and keeps the zonal wind westerly. In major warmings, however, the pole-to-equator temperature gradient reversal takes place through a deep enough layer (e.g., 60 mb through 10 mb) that adiabatic temperature changes are insignificant and air parcel motions

instead create an easterly shear. This shear is strong enough to destroy the polar night jet and cause the zonal wind to become easterly.

### 3.3 Changes in the Stratosphere

In an attempt to see how the stratosphere changed from its normal winter pattern during a SSW, Labitzke (1977) looked at observational data from the winters of 1964/65 through 1975/76. Using filtered data, she compared daily temperature differences, amplitude heights for wave numbers 1 and 2, and values of kinetic energy from  $50^{\circ}$  -  $80^{\circ}$ N for various levels of the stratosphere. Her results are presented in Figs. 7 and 8. She found that major warmings have two distinct phases in the lower to middle stratosphere:

**Phase 1: The Prewarming Phase.** Initially, a well developed cold polar vortex is present. An increase in kinetic energy between 30 mb and 10 mb occurs from 30 December 1970 through 5 January 1971 (Fig. 7, Curve A) and the temperature gradient from  $50^{\circ}$  -  $80^{\circ}$ N reverses and increases with altitude (Fig. 7b, Curve B). As the temperature of wave number 1 amplifies and peaks, the resulting increase at 10 mb is greater than at 30 mb (Figs. 7 and 8), indicating less

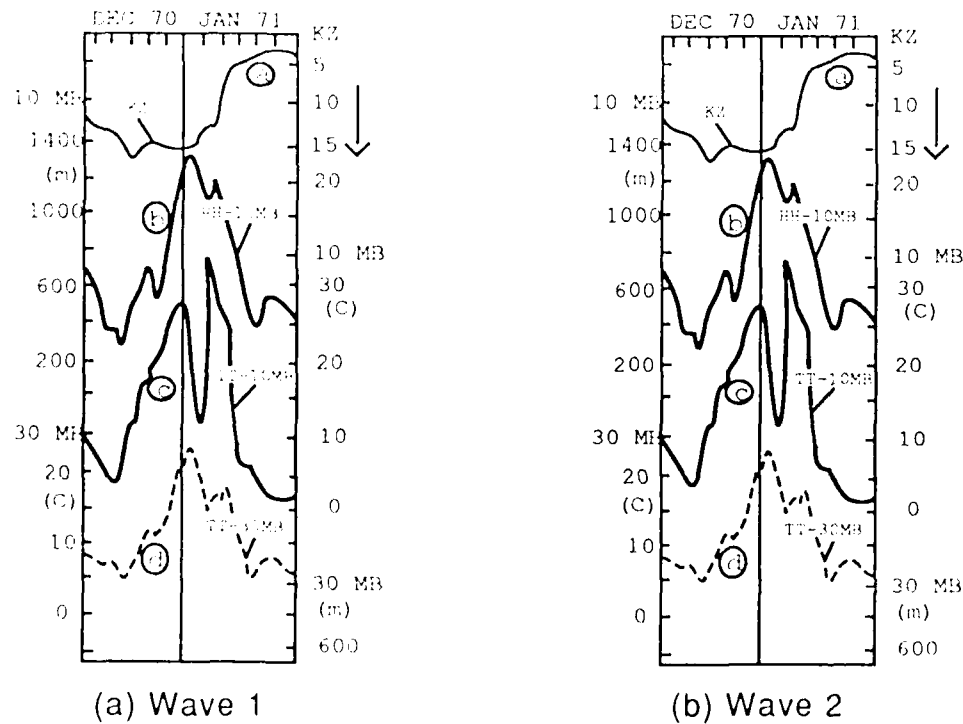


Fig. 7. Daily amplitudes of the zonal harmonic (a) wave 1 and (b) wave 2 at  $60^{\circ}$ N for the period December 1970 January 1971. Curve a: daily values of KZ ( $10^{-4} \text{ J m}^{-2}$ ), reversed scale; curve b: daily values of the amplitude (m) of the 10 mb zonal harmonic wave 1 (at  $60^{\circ}$ N); curve c: as in curve b except for 10 mb temperatures ( $^{\circ}\text{C}$ ); curve d: as in curve b except for 30 mb temperatures ( $^{\circ}\text{C}$ ). After Labitzke (1977).

energy is required for greater temperature changes at higher altitudes. The temperature rise causes the height field of wave number 1 to amplify and peak, and at the same time the height of wave number 2 declines to a minimum (Fig. 7).

**Phase 2: The Breakdown Phase.** Wave number 1 rapidly starts to decay on or about 10 January 1971 and wave number 2 quickly develops, splitting the stratospheric polar vortex (Fig. 7b, Curves C and D). The temperature gradient

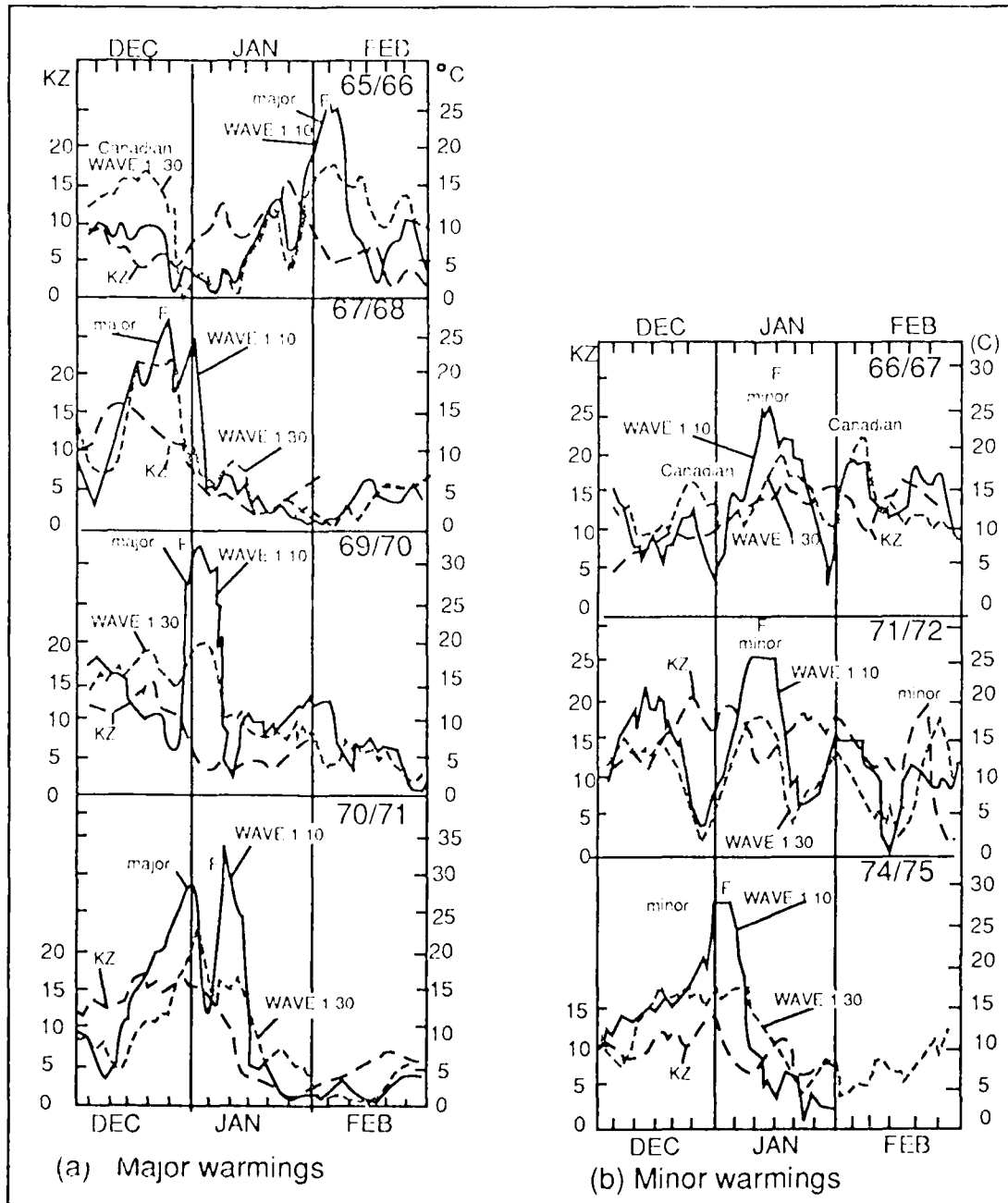


Fig. 8. Daily values of zonal harmonic temperature wave 1 ( $^{\circ}\text{C}$ ), at the 10 mb level (solid lines) and at the 30 mb level (dotted light lines); and daily values of  $\text{KZ} [10^4 \text{ J ms}^{-2}]$ , dashed lines]; F denotes the day with maximum upward flux of geopotential through the 50 m mb level. (a) major warmings, (b) minor warmings. After Labitzke (1977).

significantly as the atmosphere begins to return to normal.

Labitzke (1977) found that the main difference between major and minor warmings is not the amount of actual warming that occurs, but the difference in the amplitudes of the different waves (see Fig. 8). A 10:1 ratio between the amplitudes of wave number 1 and wave number 2 occurs during the prewarming phase of major warmings. For minor warmings this ratio is much smaller, being only 2:1. This implies that major warmings are much more likely to occur when there is a dramatic increase in amplitude in wave number 1. It appears that large amplitudes of wave number 2 during the prewarming phase retards the process which leads to the breakdown of the polar vortex (Labitzke, 1977).

## Chapter 4

### Energy Cycle and Radiational Processes

Circulation and temperature distribution in the stratosphere are driven by dynamical processes; the transfer of energy by eddies between the troposphere and stratosphere, and radiational processes. An examination of the energy cycle of the stratosphere is required in order to understand the dynamics involved in a SSW.

#### 4.1 Energy Cycle

Portrayed in Figs. 9 and 10 are the "Lorenz" annual mean energy cycles of the lower stratosphere (100 - 30 mb) (Fig. 9) and for the prewarming (Fig. 10a) and breakdown phases (Fig. 10b) of a SSW, respectively (Holton, 1979, 1976). Squares represent energy reservoirs and arrows indicate energy sources, sinks, and conversions.

$\bar{P}$  - Zonal mean available potential energy

$P'$  - Eddy available potential energy

$\bar{K}$  - Zonal mean kinetic energy

$K'$  - Eddy kinetic energy

$\bar{P} \cdot P'$  - Conversion of eddy available potential energy to zonal available potential energy

$\bar{P} \cdot \bar{K}$  - Conversion of zonal kinetic energy to zonal available potential energy

$P' \cdot K'$  - Conversion of eddy kinetic energy to eddy available potential energy

$\bar{K} \cdot K'$  - Conversion of eddy kinetic energy to zonal kinetic energy

$\bar{G}$  - Generation of zonal heating by the zonal available potential energy

$G'$  - Generation of eddy diabatic heating by the eddy available potential energy

The annual mean energy cycle of the lower stratosphere (Fig. 9, from Holton, 1979) portrays the primary energy conversions as being from eddy kinetic energy to eddy available potential energy. Eddy heat transport in the stratosphere, like that of the troposphere, is from the equator to the poles, but the temperature distribution of the troposphere and the stratosphere differ. In the stratosphere, the equatorial latitudes are cool and the mid-latitudes are warm, which is the reverse of the

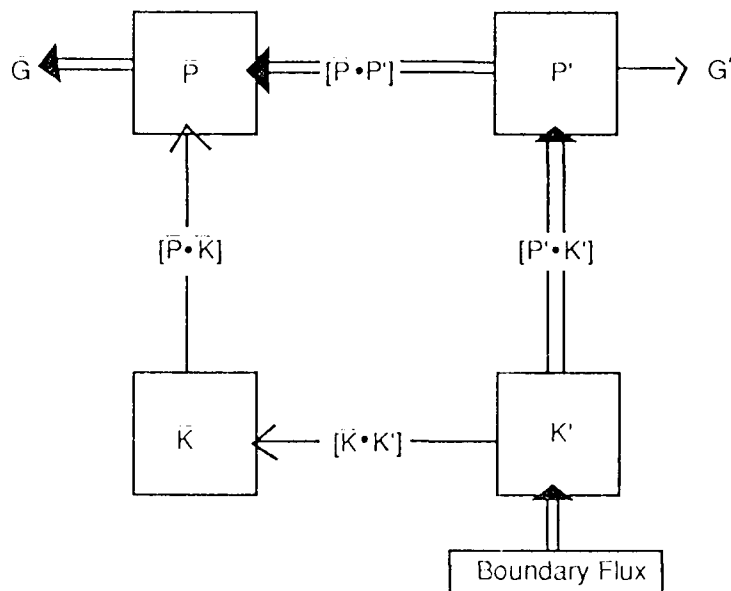


Fig. 9. Schematic illustration of the annual mean energy cycle in the lower stratosphere (30-100 mb). From Holton (1979).

between the middle and high latitudes reverses (temperature decreases with increasing latitude) and the temperatures at 10 mb start returning to normal (Fig. 7b, Curve B). The amount of kinetic energy in the stratosphere decreases distribution found in troposphere. Therefore, the stratospheric eddy heat transport is up the temperature gradient - going from cool air to warm air, not down from warm to cool. The path of the energy conversions within the eddies is determined by the meridional temperature gradient. Warm air within the eddies sinks,

converting eddy kinetic energy to eddy available potential energy. Advection of air within the eddies moves warm air poleward and cold air equatorward, converting eddy available potential energy to zonal available potential energy. A secondary mean meridional circulation sets up in connection with this poleward eddy heat flux. Rising motion occurs at both the cold polar and equatorial regions, with subsidence occurring in the warm mid-latitudes. A small conversion of zonal kinetic energy to zonal available potential energy results from this circulation.

Figure 10 (from Holton, 1976) shows the expected energy cycles for SSWs of wave number 1 and wave number 2 for both the prewarming (day=15) and the breakdown stages (day=22) of a SSW. During the prewarming phase there is a strong upward flux of eddy energy from the troposphere into the stratosphere for both

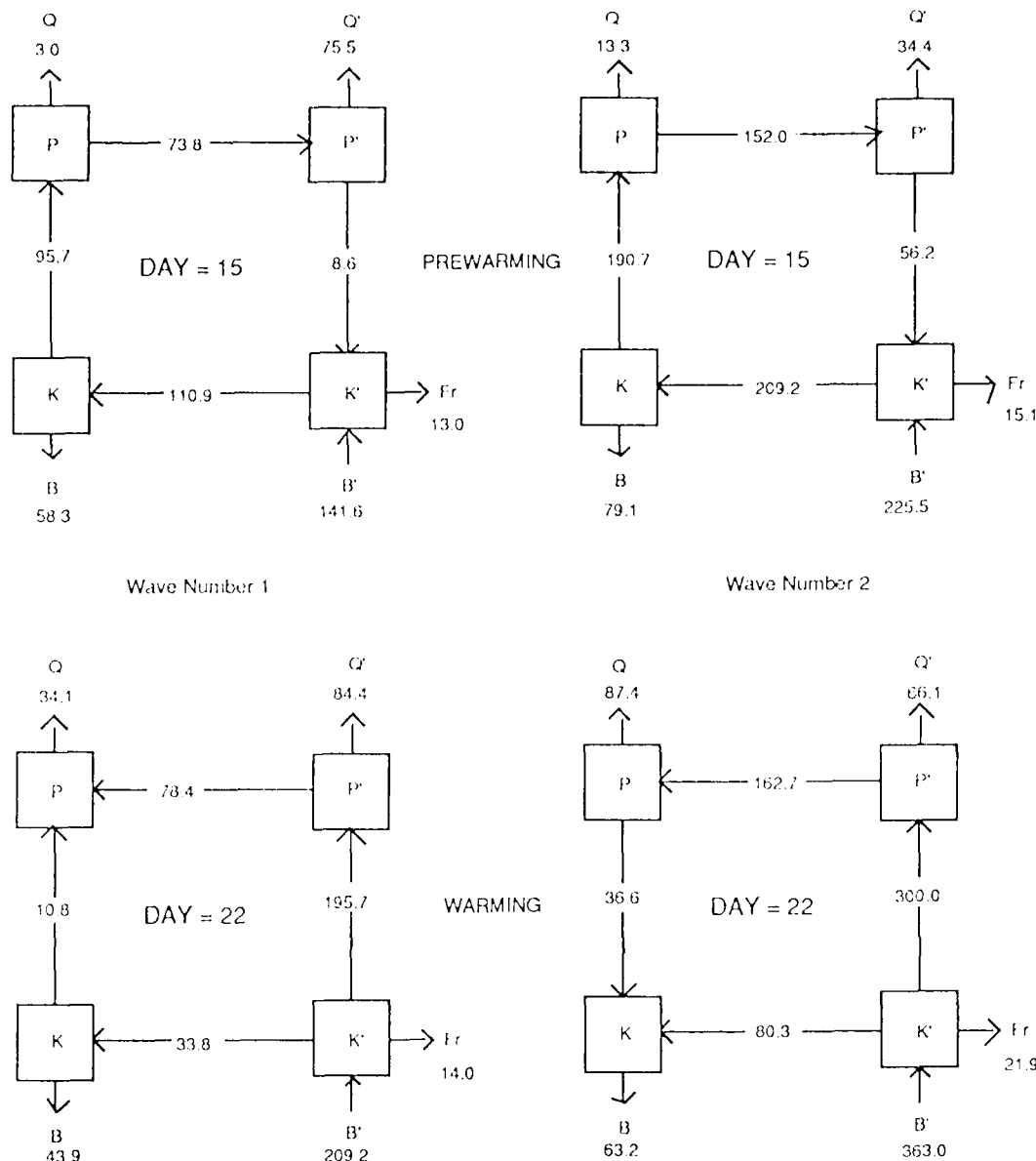


Fig. 10. Energy cycles for the prewarming and warming stages.  $B$  and  $B'$  are boundary fluxes,  $Q$  and  $Q'$  are radiative fluxes, and  $Fr$  designates frictional losses. Units: storage ( $\text{kJ m}^{-2}$ ), conversions ( $\text{mW m}^{-3}$ ). From Holton (1976).

wave numbers 1 and 2. Eddy kinetic energy is barotropically converted to zonal kinetic energy. The indirect mean meridional circulation converts kinetic energy to available potential energy. The zonal available potential energy is then baroclinically converted to eddy available potential energy. For wave number 2 there is a significant conversion of eddy available energy to eddy kinetic energy. During the breakdown phase, the baroclinic portion (conversion of available potential energy between mean and eddies) of the energy cycle reverses. Holton's results are in agreement with several previous observational studies (Julian and Labitzke, 1965; Mahlman, 1969; Muench, 1965; Perry, 1967).

Julian and Labitzke (1965) performed an in-depth examination of the energetics of the January 1963 SSW. They identified five major energy conversions associated with SSWs:

1. Generation of eddy available potential energy.
2. Conversion of eddy available potential energy to eddy kinetic energy.
3. Conversion of zonal kinetic energy to zonal available potential energy.
4. Conversion of eddy available potential energy to zonal available potential energy.
5. Conversion of eddy kinetic energy to eddy available potential energy.

They found that prior to and throughout the warming, sensible heat is transported down the temperature gradient through planetary wave numbers 1 and 2, creating eddy available potential energy. The polar night jet results from the transport of momentum into regions of the strongest westerly flow, which converts eddy available potential energy to eddy kinetic energy. When this conversion is coupled with a large transport of eddy energy from the troposphere, it results in a significant increase of eddy kinetic energy in the stratosphere - the start of the prewarming phase. The conversion of zonal kinetic energy to zonal available potential energy, combined with the export of energy back into the troposphere through boundary effects significantly decreases the amount of zonal kinetic energy present in the stratosphere. This causes a reversal of the temperature gradient. Continued poleward transfer of sensible heat results in a reversal of the energy transfer in the breakdown phase, and eddy available potential energy is then converted to zonal available potential energy.

#### **4.2 Radiational Processes**

Sudden amplification of planetary height waves is not the only stratospheric phenomena associated with SSWs. Changes in ozone concentration and distribution also occur. According to Tung and Yang (1988), the temperature changes which result from the dynamic eddy processes during a warming are different from temperature changes caused by radiational processes. Dynamic processes deal with

eddy energy conversions between the troposphere and stratosphere. Radiational processes deal with absorption of radiation by ozone and are restricted to the stratosphere.

As ozone is a major absorber of solar radiation, it effects the stratospheric temperature distribution. Dynamically induced changes are accompanied by the large scale forcing of planetary waves from the troposphere, while radiational changes are controlled by the ozone distribution of the stratosphere. The density of ozone in a column of the atmosphere is changed either through vertical motions within the column or the horizontal, equator-to-pole transport of ozone. The vertical motion of the column is determined by its temperature structure, which is kept from radiative equilibrium by irreversible wave transports of heat. Conservation of mass principles requires that the ozone-poor air penetrating up from the lower atmosphere displace the ozone-rich air to other latitudes. Downward motion in the lower stratosphere increases the density of an ozone column by transporting ozone-rich air away from its source region, over the equator, into higher latitudes. Evaluation of LIMS (Limb Infrared Monitor of the Stratosphere) satellite data shows surges of ozone-rich air are transported from their source region to polar latitudes during both major and minor warmings (Andrews *et al.*, 1987). The constant mixing ratio surfaces for stratospheric ozone have poleward and downward slopes. The steepness of these slopes in the spring is a product of a gradual wintertime ozone buildup resulting from the long photochemical timescale and rapid meridional transport. The stratospheric ozone mixing ratio shows behavior analogous to that shown in Fig. 11 from Andrews *et al.* (1987) for the mesospheric ozone mixing ratio distribution. The ozone concentration during the spring equinox is twice that of the solstices. This extreme variability can not be explained by photochemical processes alone. Dynamic transport processes must also be taken into account.

The equatorial quasi-biennial oscillation (QBO) of stratospheric winds is also an important ozone transport mechanism. Tung and Yang (1988) showed that ozone

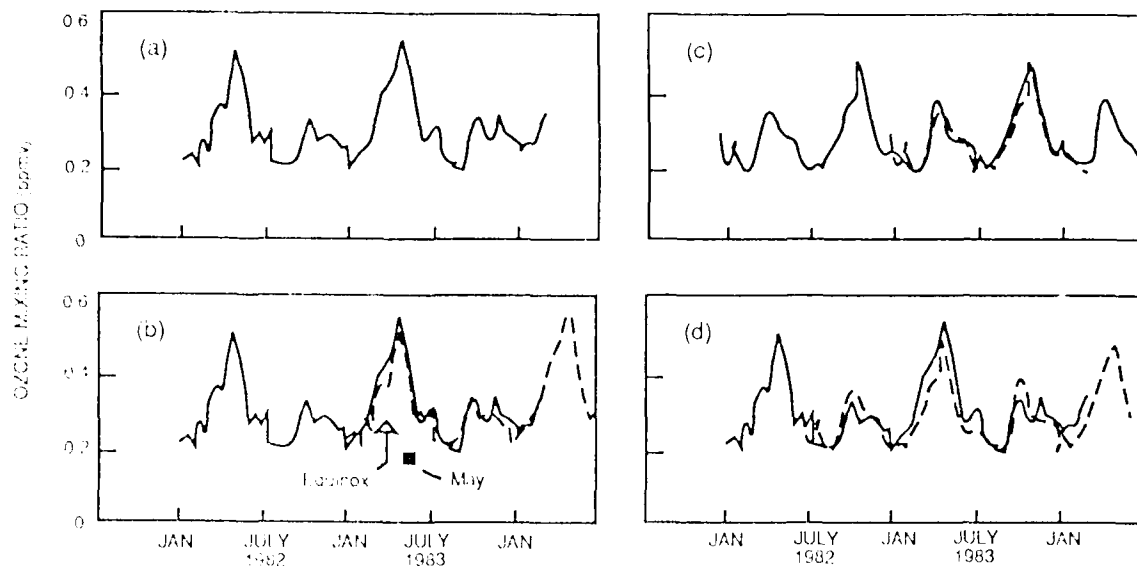


FIG. 11. Variation of the ozone mixing ratio at 0.01 mb during 1982-1983: (a) 45°N during 1982-1983; (b) 45°N with 1982 overlaid on 1983 (solid); (c) 45°S with 1982 overlaid on 1983 (dotted); (d) 45°N (solid) with 45°S (dotted) overlaid with a 6-month time shift. Note the remarkable regularity in the seasonal variation. From Andrews et al. (1987).

distribution patterns follow the stratospheric QBO. They found high ozone content over the poles during the QBO easterly phase and low ozone content during the westerly phase of the QBO. Reviewing all SSWs between 1951 and 1981, Labitzke (1982) found that of the 13 winters in the easterly phase of the QBO, 8 experienced a SSW. Considering that ozone, a radiation absorber, is most dense over the polar latitudes during the easterly phase, it is reasonable to expect the most frequent occurrence of SSW events to also occur during the easterly phase. Of the 16 winters in the westerly phase of the QBO only 4 had SSWs develop, and all 4 occurred during a solar maximum - a period when abnormally large amounts of solar radiation were incident upon the earth.

## Chapter 5

### Formation Theories

Figure 10 showed that the amount of eddy energy propagated up into the stratosphere is quite substantial compared to the amount created by the stratosphere's internal energy conversions. Therefore, it is appropriate to examine the theories of how planetary waves transport this energy. Looking at the different breakdown stages of the energy cycle illustrated in Fig. 10 it is obvious that the stratosphere reacts differently to wave number 1 than to wave number 2. Most SSWs are associated with a large amplification of wave number 1. Though wave number 2 related SSWs are less common, they tend to be more intense. Why does this happen? How does a SSW result from the growth of a planetary wave? To begin to answer these questions we must look at the different theories of how SSWs form. These theories can be divided into four major categories, those of wave instabilities, critical layers, preconditioning, and resonance.

#### 5.1 Wave Instability Theory

As shown in sections 3.1 and 3.2 by Andrews *et al.* (1987), Quiroz *et al.* (1975) and Labitzke (1977), only planetary long waves are suitable for transporting the energy required for SSWs. Muench (1965) attempted to determine how planetary waves force a coupling of the troposphere and the stratosphere. He performed several height field analyses from 1000 mb to 10 mb at 50°N (see Fig. 12). He found that wave numbers 1 and 2 (upper and lower right in Fig. 12) tilt westward with height (indicative of a poleward transfer of energy) and that the wave amplitudes increase with height. In contrast, wave numbers 3 and 4 (upper and lower left in Fig. 12) are essentially vertical, with very little tilt to either the west or east, and their amplitudes are fairly stable, showing little tendency to increase with height. Muench's results indicate that waves shorter than wave numbers 1 or 2 have virtually no impact in the stratosphere, so they can be ignored when dealing with stratospheric phenomenon.

Charney and Drazin (1961) claim that during winter wave numbers 1 and 2 are

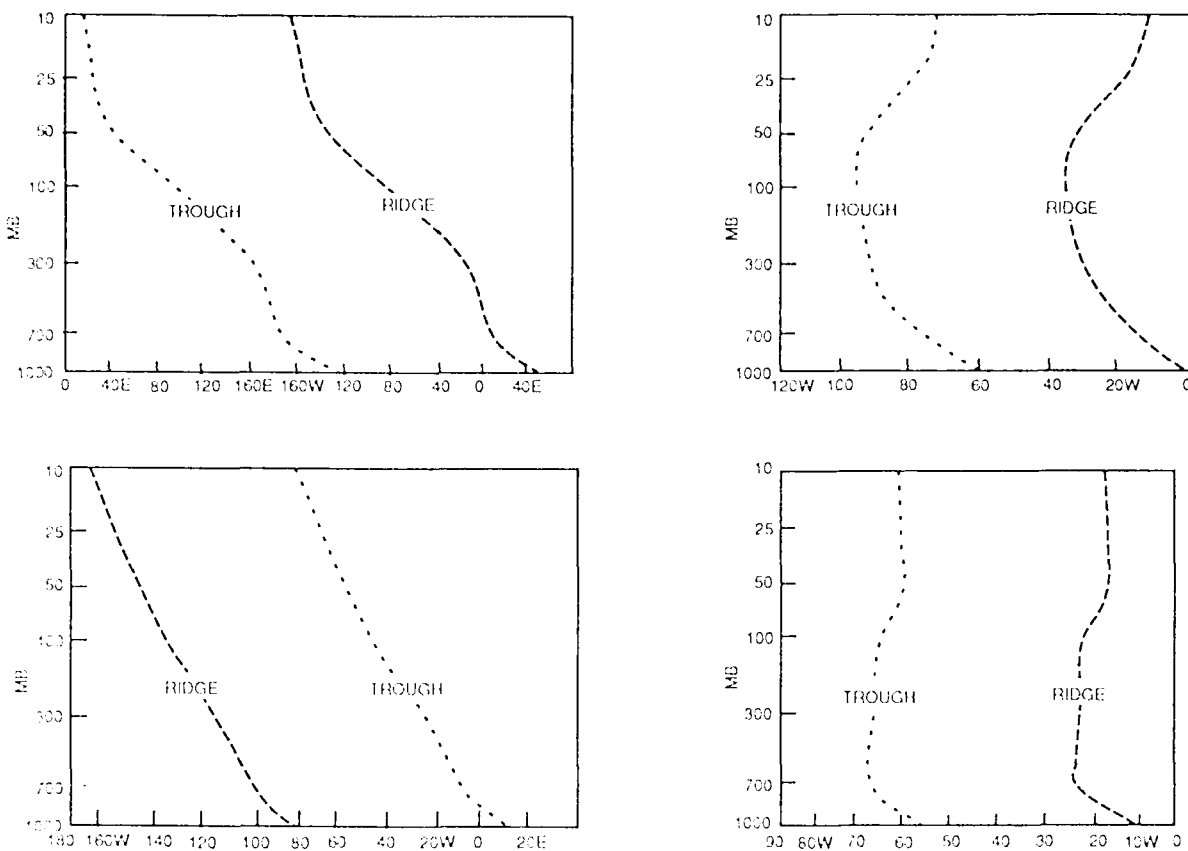


Fig. 12. Vertical structure of monthly mean long waves at 50°N for January 1958. Wave 1, upper right; wave 2, lower right; wave 3, upper left; wave 4, lower left. From Muench (1965).

baroclinically stable. They believe long waves which are forced to propagate upward can penetrate a considerable distance into the stratosphere, but the shorter, baroclinically unstable waves forced upward cannot. Unstable waves can only propagate upwards in the stratosphere when the mean winds in the middle and upper stratosphere are light and westerly (i.e., usually in the spring, just prior to the transition from the winter westerlies to the summer easterlies). Therefore, in most cases, baroclinically unstable waves in the winter will be reflected or damped as they move vertically through the tropopause. This is called the wave instability theory as it states that only stable waves can penetrate the stratosphere and form SSWs.

Muench (1965) devised a model of the stratosphere's winter circulation based on this idea. He made three assumptions.

- 1) Northern hemispheric orographic features act upon the troposphere forcing long wave disturbances which are quasi-stationary in space and periodic in time.

2) In the winter, the lower troposphere produces long waves whose energy conversions are similar to the energy conversions of baroclinically unstable short waves.

3) The speed of the vertical propagation of the energy is not a function of pressure, but is approximately constant with height.

Muench theorized that the initiation of a disturbance near an orographic source will cause vertical propagation of energy. Since attenuation of energy is a function of stability, the energy will be able to penetrate a considerable distance into the stratosphere before baroclinically unstable conditions, which will damp the wave, are approached. In order to conserve kinetic energy, the amplitude of the wave increases as density decreases. As the disturbance penetrates further into the stratosphere and encounters a less baroclinically stable environment, the wave energy is either further attenuated or reflected downward. According to Muench's second assumption, energy conversions in a long wave are similar to those of a baroclinically unstable short wave. Therefore, there is a northward transport of heat and a flux of momentum into the mean westerlies making the flow super-geostrophic. Super-geostrophic flow in the stratosphere will cause the mean westerlies to drift southwards in response to inertial instability. The southerly drift is stronger at higher altitudes. The less dense air at these altitudes allows the waves to reach greater amplitude creating stronger momentum and heat fluxes.

The secondary mean meridional circulation, previously discussed in section 4.1, sets up with rising motion over the poles, a southerly drift in the middle and high latitudes, and subsidence at the wave's southern boundary (around  $40^{\circ}\text{N}$ ). This subsidence produces a warming in the middle and low latitudes which leads to differential radiational cooling and the loss of eddy available potential energy. The ratio between the heat flux and momentum flux is a critical determinant of the effect of vertically propagating waves on the stratosphere. If there is an abnormally large amount of heat flux compared to momentum flux, then the weak meridional cell will set up; the poles will warm, the westerlies will weaken, and a

warming will begin.

## 5.2 Critical Layer Theory

Matsuno (1971) developed one of the first models that approximated the observed behavior of SSWs, based on the theory of a critical layer. A critical layer is the level at which the mean flow switches from westerly to easterly. The mean flow below is westerly, the mean flow above is easterly but, at the critical level between the two, the mean flow is neutral.

This theory is based on the fact that geostrophic planetary scale disturbances can only propagate upward when the mean flow is light and westerly, as shown in section 3.1 for vertically propagating Rossby waves. When the prevailing wind is easterly or strongly westerly, upward propagation ceases (Charney and Drazin, 1961) and a critical layer develops (Matsuno, 1971). A planetary wave encountering a critical layer is damped. As the wave is being damped, its energy is absorbed by the critical layer and its amplitude decreases rapidly. A large temperature gradient, either in the vertical or horizontal, develops around the critical level. Meridional heat transfer by planetary waves while constant in the westerly layer is zero at the critical layer (Matsuno, 1971).

Matsuno (1971) begins with a planetary wave propagating up into the stratosphere. As the wave encounters and interacts with the strong westerly polar night jet, the jet decelerates. As the wave's amplitude increases, the polar night jet and westerly flow continue to weaken, allowing mean easterlies to dominate the flow. With the appearance of these easterlies, a critical layer forms between the higher level easterlies and the lower level westerlies. The critical layer halts any further upward propagation of planetary wave energy, and creates a significant temperature disturbance, causing the mean temperatures to rise. As planetary waves continue propagating up into the stratosphere they are absorbed by the critical layer, further deceleration of the polar night jet occurs and the critical layer descends even further through the stratosphere. Intense warming occurs at high latitudes just below the critical level, while the mean temperature falls in the low latitudes.

Convergence of the poleward eddy heat flux forces the appearance of the secondary mean meridional circulation. As the Coriolis force acts on this circulation the mean easterly flow begins to accelerate and strengthen, locking in the advent of a SSW. The location of the critical layer is a function of the phase speed of the waves which created it. Since high latitude critical layers are more likely to occur when the tropical winds are easterly, SSWs can be facilitated by the presence of a deep layer of quasi-biennial easterlies (McIntyre, 1982). These deep layered quasi-biennial easterlies are associated with both the QBO and ozone redistribution mechanisms already shown to be closely tied to SSW formation (Section 4.2).

Holton (1976) created a model similar to Matsuno's model, also based on the concept of the critical layer. Holton did not find a downward propagation of the critical level, but instead found that the zero mean wind line, the interface between easterly and westerly flow in the vertical, occurred simultaneously at  $60^{\circ}\text{N}$  between 30 and 80 km (see Figs. 13 and 14). Inspecting the results for wave number 1 (Fig. 13) and for wave number 2 (Fig. 14), he concluded that the critical level interacts differently with each type of wave. For wave number 1, wave transience (a temporary oscillation that results in the damping of the wave) not critical layer interaction was the main cause of the deceleration of the polar night jet. For wave number 2, the convergence of horizontal momentum flux near a vertically oriented zero mean wind line causes poleward propagation of this line as the warming progresses. Holton cautions that these conclusions are based on the application of concepts developed for linear waves and are not necessarily valid when applied to SSWs.

In Matsuno's theory the significant factor was not the presence of critical lines, but the damping or transience and dissipation thought to be associated with them. Since transience and dissipation are now known to occur regardless of the presence of critical lines (Plumb, 1981), Matsuno's original theory on critical layers has been significantly modified. It is now believed that wave transience and dissipation from either wave

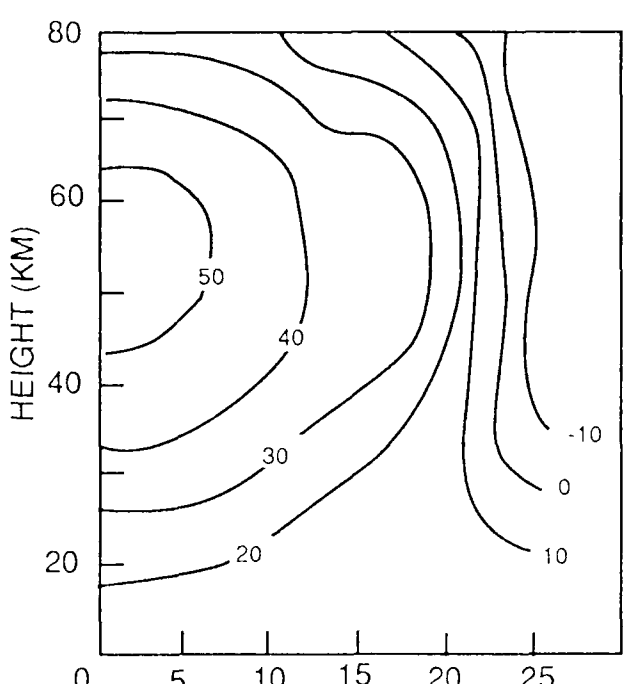
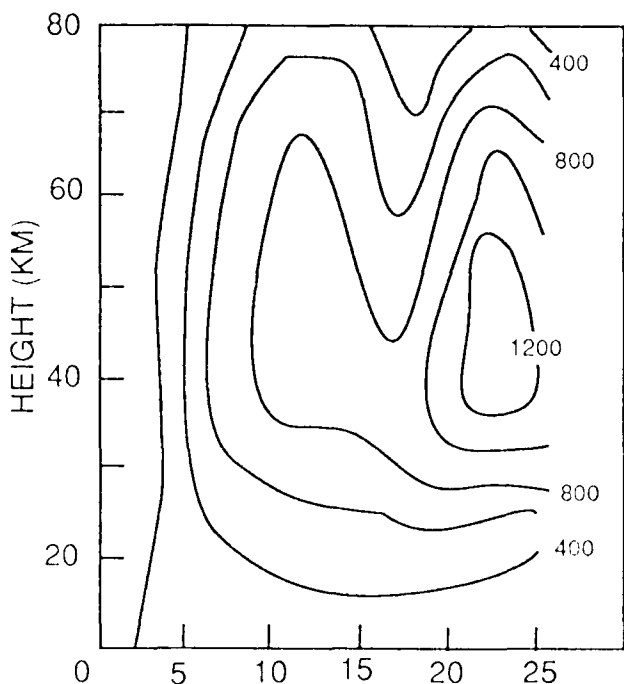


Fig. 13. Time height sections at  $60^{\circ}\text{N}$  showing amplitude of the wave geopoential perturbation (left, units of gpm) and the mean zonal wind speed (right, units of  $\text{ms}^{-1}$ ) for the wave number 1. From Holton (1976).

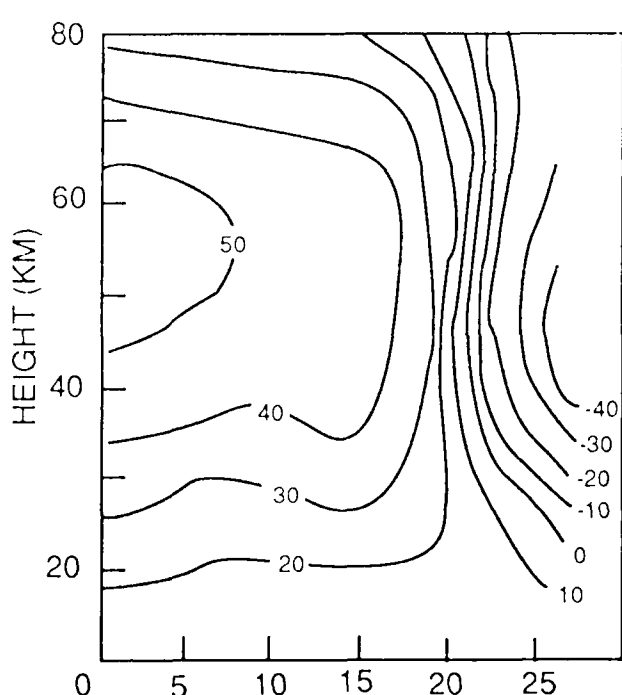
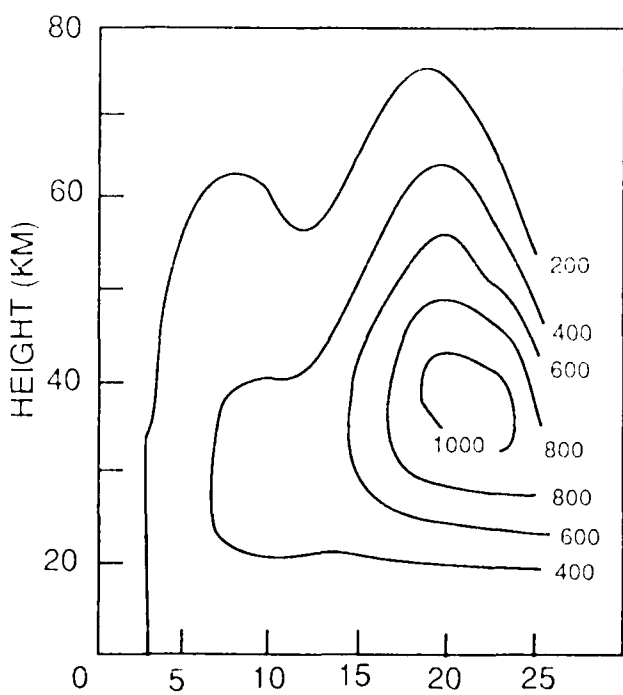


Fig. 14. Same as for Fig. 13 but for wave number 2.

reflection or a critical layer is the mechanism leading to the distortion and breakdown of the polar night jet.

### 5.3 Preconditioning Theory

The preconditioning theory originated from comparing the normal winter pattern of the stratosphere and the pattern created by a SSW. It is based on the

assumption that no single event could cause a drastic enough change in the pattern to create a SSW. A preconditioning of the stratosphere must occur in order for the normal winter pattern to be altered enough for a later pulse of energy to bring about the final alterations to the stratosphere required for a major warming (McIntyre, 1982). For a SSW to occur, stationary planetary waves must have extremely large amplitudes, westerly phase tilts (allowing energy transfer poleward and propagation of wave energy up from the troposphere), and a very strong focusing of energy into the regions poleward  $60^{\circ}\text{N}$ . Since the atmosphere is so thin at these altitudes and latitudes, the small mass and moment of inertia of the region increases the opportunities for the waves to dramatically effect the stratosphere (McIntyre, 1982).

The normal tendency of waves to propagate away from the poles, and into the much larger areas of the lower latitudes is called "defocusing" (McIntyre, 1982). Fig. 15 is an Elissen-Palm (EP) cross section which gives an excellent example of the defocusing of wave number 2 under normal winter conditions. (EP cross sections are diagnostic tools used to display primary eddy heat fluxes, quasi-geostrophic potential vorticity, and momentum on a single diagram.  $\mathbf{F}$  is the direction of energy propagation in the meridional plane (Dunkerton *et al.*, 1981). For more information on EP cross sections see Appendix A). The negative contours show where  $\mathbf{F}$  converges, where the group velocities of the waves converge, because of the wave's transience. Since defocusing tends to be pronounced for wave number 1 and even more so for wave number 2, it is understandable that major warmings occur rarely, as they must overcome the defocusing of the climatological mean circulation. Many researchers (Butchart *et al.*, 1982; Dunkerton *et al.*, 1981; Labitzke, 1981; Palmer, 1981; Quiroz *et al.*, 1975) have concluded that the stratosphere must be prepared in some special way for a major warming, especially a wave number 2 related warming. During preconditioning, some mechanism inhibits the defocusing effect allowing the waves to propagate upward into the polar cap. Since it is harder to redirect the more strongly defocused wave number 2, the

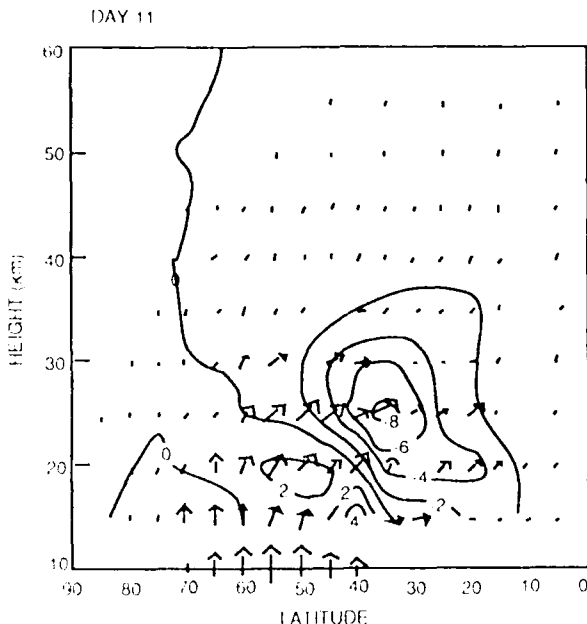


Fig. 15. Eliassen-Palm cross sections for a pair of model simulations in which planetary waves of zonal wavenumber 2 are generated by applying two different lower boundary conditions. The waves propagate on a basic zonal wind profile typical of what has usually been taken as a representative climatological mean. The arrows represent the Eliassen-Palm wave flux and the contours its divergence, plotted in accordance with the conventions described in Dunkerton et al. (1981). From McIntyre (1982).

requirements for preconditioning the stratosphere when this wave dominates are much more stringent than for wave number 1.

The 16 winter survey done by Labitzke (1981) for the winters 1964/65 through 1979/80 indicates that the main preconditioning requirement for major warmings is for the amplitude of height wave number 1 to increase to at least 700 meters in the middle stratosphere while height wave number 2 simultaneously declines to a amplitude of less than 300 meters. However, for a wave number 2 warming an additional requirement is made; the amplification of height wave number 1 must displace the polar night jet southward.

The breakdown of the jet will eventually follow the peaking of wave number 1, but the exact timing varies. Breakdown may occur immediately after the wave peaks or as long as two weeks after. Timing of the jet breakdown is dependent on whether wave number 1 or wave number 2 is involved. If wave number 1 maintains its large amplitude, or even weakens slightly only to experience a resurgence of energy and so restrengthen, the polar night jet will breakdown soon after the original peaking of the wave. The nature of the wave's evolution, whether it is continuous or pulsed, appears to have little influence on the warming, as SSWs

occur from both (McIntyre, 1982).

If wave number 2 is involved, the complete breakdown of the polar night jet usually takes longer. The stratosphere has already been preconditioned and the polar jet displaced south by wave number 1. The temperature gradient has begun to reverse. All that is needed is for wave number 2 to be forced upward while wave number 1 continues to weaken and diminish. The development of wave number 2 is accompanied by the splitting of the polar night jet and its eventual, complete breakdown (Labitzke, 1981). Figure 16 from McIntyre (1982) shows the time variations of the wave amplitudes and latitudinal temperature contrasts within the polar region at 30 mb during the January/February 1979 SSW. This was a wave number 2 dominated warming. It was an unusual SSW in that there was an exceptionally long, 4 week, delay between the preconditioning by wave number 1 and the final pulse from wave number 2. Dunkerton *et al.* (1981) explain this delay by a

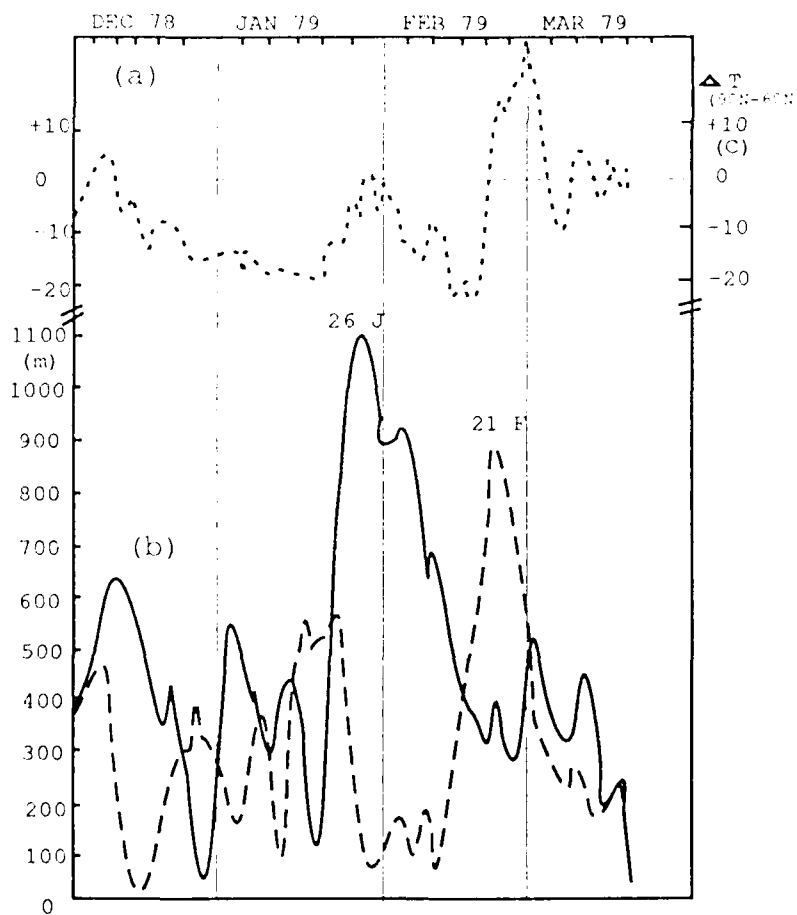


Fig 16. (a) Difference at 30 mb, around 24 km altitude, between the temperature at the north pole and the zonally averaged temperature at 60°N; (b) amplitudes in meters of zonal harmonic geopotential height waves 1 and 2 (broken line) at 60°N and 30 mb . From Labitzke (1981).

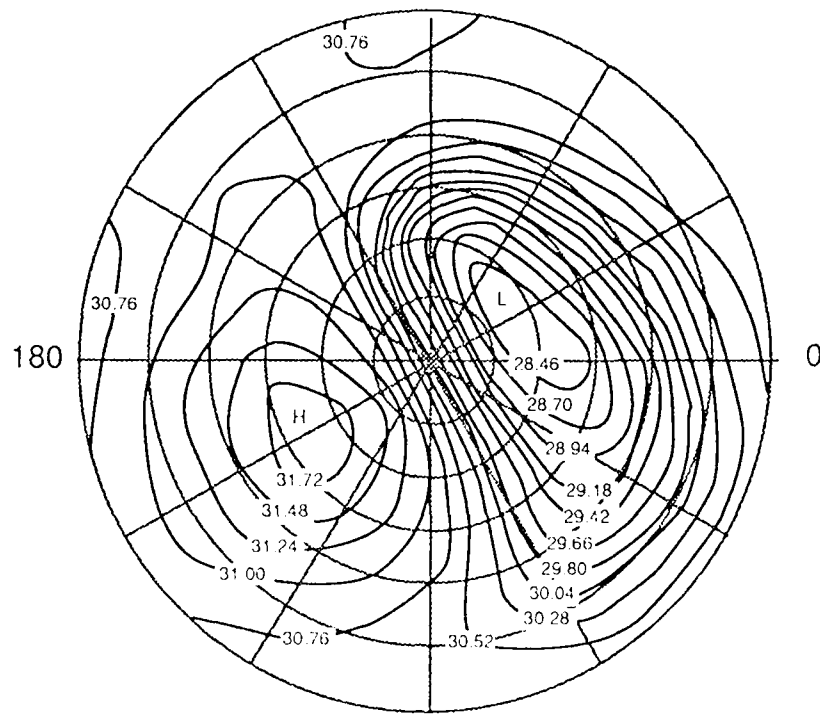


Fig. 17. Breaking planetary wave at 00Z on 27 January 1979, as shown by the height of the 10 mb constant-pressure surface. Contour interval is 24 dekameters;  $H=32.09$  km,  $L=28.42$  km. Latitudes north of  $30^{\circ}\text{N}$  are shown. From Pick (1979).

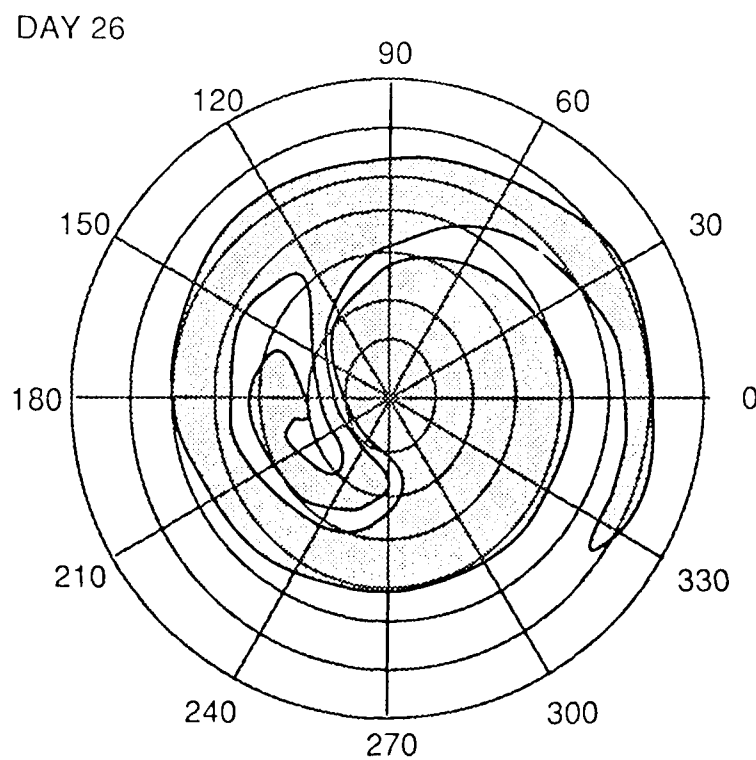


Fig. 18. Shape of a material line, originally coincident with the  $30^{\circ}\text{N}$  latitude circle at an altitude of about 31 km, and then advected by a wind field generated by a mechanistic model simulation. Whole northern hemisphere is shown. From Hsu (1981).

lack of wave number 2 forcing mechanism earlier in the event.

The January/February 1979 warming can be used to summarize the preconditioning theory in more synoptically oriented terms (see Fig. 17). As a wave number 1 disturbance grew to large amplitudes in late January 1979, it displaced the main polar vortex southward cutting off the Aleutian High. A central core of potential vorticity contours was also displaced south of the pole. Most potential vorticity contours outside the central core were eroded by the wind field connected with the cutoff Aleutian High (Fig. 18), leaving very weak potential vorticity gradients outside and extremely sharp gradients at the boundaries of the surviving central core. In mid-February (Fig. 16), when wave number 1 decayed, the potential vorticity cell began migrating back towards the pole. Wave number 2 was finally forced upward and began focusing into the polar region, thereby adding the final ingredient necessary to finish eroding the potential vorticity, completely destroying the polar night jet and culminating in a SSW.

#### 5.4 Resonance Theory

When a traveling planetary wave becomes stationary, it interacts with quasi-stationary waves induced by topography and differential heating of land/ocean mass (Grose and Haggard, 1981). Resonance, the enhancement resulting from interaction between two waves, will force the planetary wave to grow. The amplitude height of a wave in the stratosphere will be determined by the amount of tropospheric forcing applied to it at the bottom of the stratosphere (McIntyre, 1982). Tung and Lindzen (1979) derived the linear resonance condition as:

$$\phi_{z^*}^{(0)} + [1/2 - (\bar{\mu}_{z^*}^{(0)})/\bar{\mu}(0)] \phi^{(0)} = 0 \quad \text{at } z^* = 0 \quad (5)$$

where:  $z^*$  is the vertical height above the lower boundary

$\phi_{z^*}$  is the new geopotential height of the forced stationary wave

$\bar{\mu}_{z^*}$  is the mean wind component at the vertical location

$\bar{\mu}$  is the lower boundary mean wind

$\phi$  is the lower boundary geopotential height

The linear resonance condition requires a wave to be either internally trapped in the

vertical, or be transient near the lower boundary, before it can undergo resonant growth. In order for wave numbers 1 and 2 to be resonant, a secondary stratospheric westerly jet must be present at 40 km. This forces waves above the mid-stratosphere to be transient (Kanzawa, 1980).

The linear resonance condition has been relaxed by Plumb (1981). He states that the strongest growth in wave amplitudes will occur when the mean state of the atmosphere is "near" resonance, not "in" resonance. A stationary wave forced by topography to grow will effect the atmosphere and bring the mean state of the atmosphere even closer to resonance - giving rise to a positive feedback process Plumb calls "self-tuning". This implies that a free traveling planetary wave will slow down, allowing wave growth, as it encounters a mean state approaching resonance. As this forced wave becomes stationary, interference with it will cause the entire planetary wave disturbance to grow and hence impact upon the mean state of the surrounding atmosphere.

There are two distinct versions of the resonance theory (McIntyre, 1982):

1. The troposphere and stratosphere act as one resonant cavity. Occasionally this cavity approaches resonance and large wave amplification occurs. This version is applicable to the large, planetary scale wave numbers 1 and 2. They extend from the surface, through the troposphere, and far up into the stratosphere during SSWs. At times, these waves appear to organize themselves into free normal modes, which implies the existence of a deep hemispheric - scale cavity extending into both the troposphere and stratosphere.

2. Resonant cavities are of a smaller horizontal scale and are limited to the troposphere. During the northern hemisphere winter, the North Atlantic and North Pacific act as separate resonant cavities which are independent of each other and of the stratosphere. The stratosphere responds to the upward forcing produced by these resonant cavities. When the Atlantic and Pacific large-amplitude anomalies are of opposite sign, wave number 1 will be strongest and penetrate furthest into the stratosphere. When the two oceans have the same anomaly sign, wave number 2

will have the strongest impact on the stratosphere. The key point of this version of the resonance theory is that it allows forcing of the stratosphere to occur without changing the resonance field of the cavity. Unlike the first version, no self-tuning occurs within the cavity.

No one theory completely explains what causes SSWs but the resonance theory comes closest. This theory is really a combination of the other three. Like the instability theory, resonance begins with an orographically induced wave interacting with a stationary wave forcing the planetary wave to grow. The "self-tuning" process gives rise to a feedback mechanism, which pre-conditions the atmosphere by causing a slow down, allowing the atmosphere to prepare itself for what is to come. As the wave propagates up into the stratosphere it reaches the critical layer, or mean zero wind line, forcing the breakdown of the polar night jet.

## Chapter 6

### Modeling

Researchers have incorporated these theories into their models. They may design their numerical models around just one theory or may use parts of many theories.

There are two types of numerical models used by researchers in their attempts to simulate SSWs and learn more about the dynamics involved in warmings. These are the mechanistic (hypothesis-testing) models and the general circulation models (GCM). Mechanistic models used are usually restricted to the stratosphere and require some sort of upward forcing of the upward propagating planetary waves be inserted at the bottom level of the model (O'Neill, 1980). In contrast, GCMs usually have both the troposphere and stratosphere represented and use either climatology or observed data as their initial conditions. They then try to produce a warming "naturally", without implementing any artificial forcing.

#### 6.1 Mechanistic

Matsuno (1971) developed one of the first mechanistic models able to produce many of the observed characteristics of major warmings. His was a quasi-geostrophic model which allowed propagation of a single planetary wave and watched the wave's interaction with the winds. This model was based on the critical layer theory discussed earlier. Matsuno hypothesized that the upwardly propagating planetary waves would interact with the mean flow and cause it to slow. This effect would be extremely prominent at higher elevations where the low atmospheric density would weaken the polar night jet to such an extent that a critical level would appear. The critical level would absorb the wave's energy, producing further weakening of the jet and subsequent descent of the critical level. A large temperature gradient would form near the critical level, producing a secondary mean meridional circulation and directing the eddy heat flux poleward. Coriolis torque acting on the secondary circulation and convergence of the eddy heat flux would produce the easterly acceleration required for a SSW (Grose and Haggard,

1981).

Some problems were observed by Matsuno with his model, the most distinct being that wave number 2 did not penetrate deep enough into the stratosphere, making the warming occur too late.

Holton, like Matsuno, is an early pioneer of the SSW mechanistic models. Holton (1976) used a primitive equation model with a finite-difference grid in the latitude-height plane and spherical coordinates for longitude. His results provided a different explanation of warming development than Matsuno's, in that no indication of a descending critical level for the wave number 1 SSW was found. Holton concluded that wave transience, not critical level interaction with the mean flow, was the primary reason for the slowing of the mean flow. He also found that horizontal eddy momentum flux had an important role in acting to balance the Coriolis torque. The significance here was that the residual between the flux and the torque was an order of magnitude smaller than the Coriolis torque. This difference was large enough to cause a net deceleration in the westerlies (Grose and Haggard, 1981).

A more recent mechanistic model is that of Butchart *et al.* (1982). It differs greatly from the earlier models of Holton and Matsuno in that it is a global (not just hemispheric) three-dimensional primitive equation model. Both the stratosphere and mesosphere are included and the lower boundary layer is set at 100 mb. The observed 100 mb wave number 2 height fields from the January/February 1979 SSW were used as the forcing mechanism. They found that wave-wave interaction (interaction between waves with different wave numbers) was not significant in their simulation. Their successful simulation of the SSW was due to: (1) using the observed (not climatological) wind structure for the initial forcing and; (2) imposing a longitudinal phase speed for the waves propagating up from the lower boundary. They found that during the prewarming phase the propagation of planetary waves (represented by integral curves of the EP flux) is related to the mean refractive index.

A major problem experienced by Butchart *et al.* (1982) was their model handled the polar night jet poorly in the prewarming stage, allowing large deviations from the observed conditions. The use of a weak radiation scheme probably resulted in the weak circulation simulated by the model prior to the warming. Although this model clearly experienced some problems, the results obtained from it added another significant step toward our understanding of the dynamics involved in a SSW.

Mechanistic models, while vital for research, are not very useful for providing operationally useful SSW forecasts. For this, GCM models are necessary. Over the years, many researchers have tried to forecast, or at least simulate, a SSW with GCMs (Grose and Haggard, 1981; Mechoso *et al.*, 1985; Miyakoda *et al.*, 1970; O'Neill, 1980). The first successful forecast of a SSW was made for the January/February 1979 warming by an experimental version of the high-resolution forecast model at the European Centre for Medium Range Weather Forecasting (ECMWF) (McIntyre, 1982).

## 6.2 GCM

The first successful experimental model to forecast a SSW was developed by Simmons and Strufing (1983). It was a modified version of the global, primitive equation spectral model used for operational production at ECMWF. They employed a hybrid vertical coordinate scheme which followed the modeled orography at low levels, but gradually flattened out to become constant pressure surfaces in the stratosphere. The highest levels at which the winds and temperature were forecast were 50 mb, 25 mb, or 10 mb, for various model runs. The variation in level height was due to their attempt to assess the impact of the location of the upper boundary limit. They found the evolution of a warming below 10 mb to be fairly insensitive to what was happening in the upper stratosphere and mesosphere.

This model gave fairly accurate forecasts on SSWs for out to ten days. To quantify their results, Simmons and Strufing (1983) compared the model results with the observed conditions and with persistence. Persistence assumes that

whatever the current conditions are, they will remain indefinitely into the future. Figure 19 shows the percent of the height anomaly correlations between observed conditions and the model forecast conditions (light solid line), and between observed conditions and the persistence forecast (heavy solid line). An anomaly of 50 - 60% usually defines the limits of useful predictability. The forecast made for 16 January was the best, while the 17 February forecast was the worse. All model forecasts were much better than persistence.

Since Simmons and Strufing (1983) proved the usefulness of using GCM based products to forecast SSWs, more sophisticated models have been designed. Blackshear *et al.* (1987) used a primitive equation model with spherical geometry and a sigma coordinate system. It has 12 levels that extend from the surface to 57 km. Its diabatic heating term includes ozone absorption of solar ultraviolet radiation and long-wave cooling which is represented by a Newtonian approximation. They initialized the model with winter solstice conditions and a specified mean flow. Seasonally dependent parameters were kept at the solstice values until the atmosphere achieved a quasi-steady mean state.

Two distinct SSWs occurred spontaneously during the simulation. Both warmings exhibited a prewarming feature where the geopotential height of a well developed wave number 1 exceeded 1500 m at 70°N in the upper stratosphere. This development of wave number 1 was a reflection of orography and land-sea thermal contrasts creating a tropospheric forcing on the wave. This forcing caused the cold polar vortex in the stratosphere to be displaced. Thus, preconditioning the stratospheric polar latitudes for further model warming.

While many GCMs exist today with the capability of making SSW forecasts which are superior to persistence, few operational forecasters can use them. These models are generally used only at weather "think tanks" or "factories", and are turned on only by special request (Simmons and Strufing, 1983). This means there are few products out there for use by the operational forecaster who deals with the stratosphere on a daily basis. STRATALERTS issued by the Space Environmental

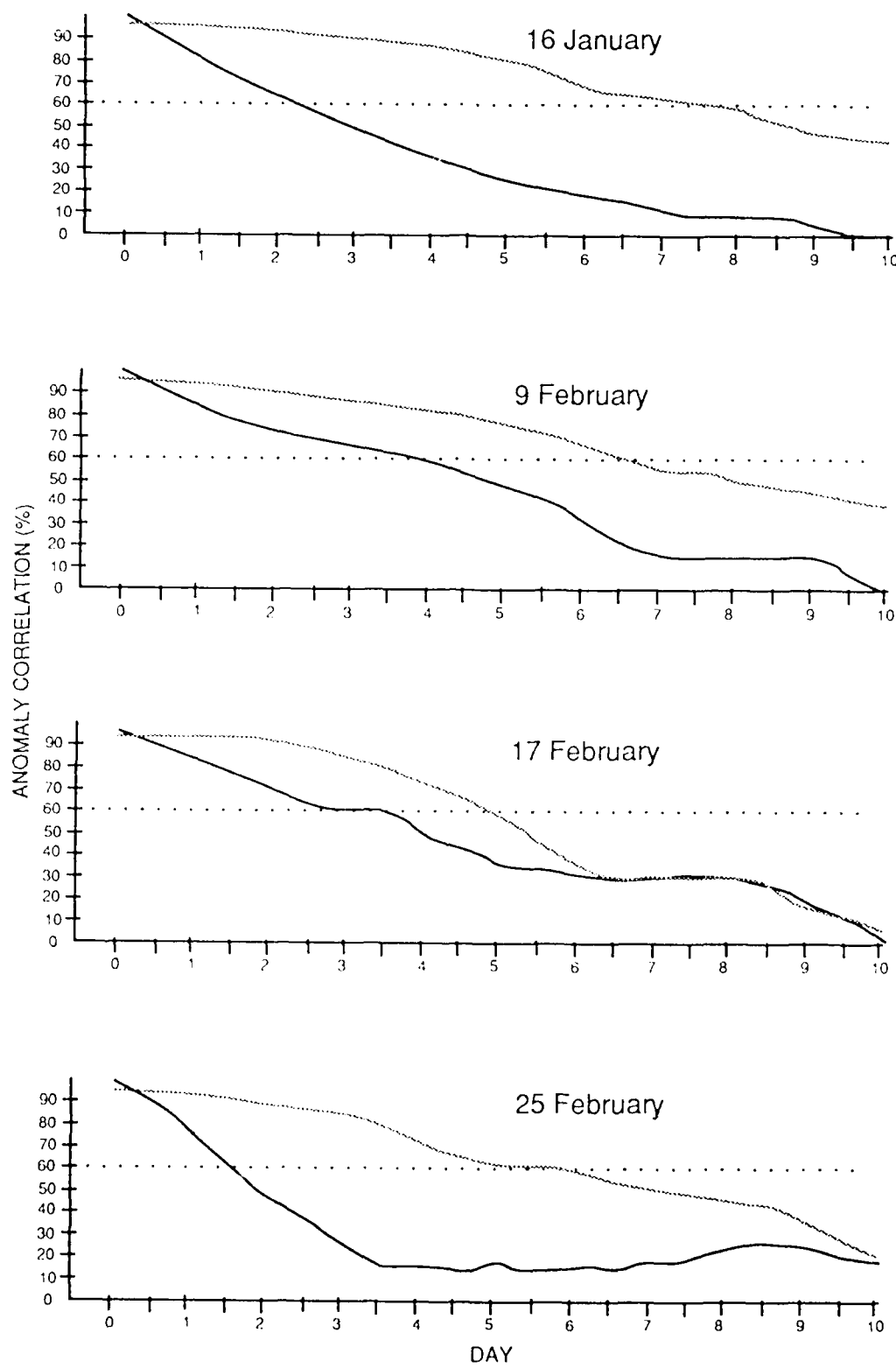


Fig. 19. Anomaly correlations of height (%) calculated for the area from  $20^{\circ}\text{N}$  to  $82.5^{\circ}\text{N}$  using heights of standard pressure levels between 1000 and 200 mb. The initial dates of the forecasts are shown. For each date the heavy solid line indicates a persistence forecast, the light solid line the numerical forecast with a 50 mb top level. After Simmons and Strufing (1983).

Service Center in Boulder, Colorado, but originating from the Free University of Berlin, are available. These, however, just state whether or not a warming is occurring and where; they do not forecast SSW occurrence. Twelve hour analysis charts for 100 mb, 50 mb, 30 mb, and 10 mb are available from the National Weather Service, but again, they are analyses, not forecasts. What is needed is for a more refined GCM capable of forecasting SSWs to be developed and continually run with wide dissemination of its products.

## Chapter 7

### Summary

SSWs consist of a sudden, dramatic increase in temperature within the polar regions of the stratosphere, frequently accompanied by complete destruction of the polar night jet and reversal of the mean flow to easterly winds. There is an unusual amplitude growth of planetary wave numbers 1 and 2 prior to a warming, during which they penetrate deep into the stratosphere. The eddy heat fluxes which bring about the temperature reversal are transported from the troposphere up into the stratosphere by the upward propagating waves. The reversed temperature gradient causes flow from cooler to warmer temperatures creating the easterly shears which begin the breakdown of the polar night jet. As the warming continues, the polar night jet is completely destroyed and the westerly flow reverses to easterlies.

There are four theories, which when combined, help explain the basic causes of SSWs. The first is the wave instability theory wherein baroclinically unstable waves are damped as they move through the troposphere. As the stable waves approach instability, they penetrate deeply into the stratosphere and supply the energy required for SSWs. Second, is the critical layer theory. Here, it is wave transience or dissipation resulting from either a critical layer or wave reflection that causes the reversal to easterly mean winds and the start of a warming. The third theory is that of preconditioning. This is based on an assumption that the stratosphere's normal winter circulation is not easily changed and requires some preconditioning before a true SSW can set up. The preconditioning stage consists of an increase in wave number 1's height amplitude while wave number 2's amplitude descends to a height minimum. This brings about the required temperature gradient reversal. To bring on a SSW, wave number 1 must continue pouring energy into the upper stratosphere for an extended period or, if wave number 1 diminishes, wave number 2 must grow. This allows the required circulation pattern to form. The last theory is that of wave resonance. This assumes that the planetary waves interact

with the quasi-stationary waves induced by topography and land/ocean differential heating. This wave interaction results in an upward forcing of the planetary waves through the troposphere and deep into the stratosphere supplying energy required for SSWs.

No one theory in itself provides a complete explanation of all the mechanics involved in SSWs. Most of these theories are complimentary; pre-conditioning provides the required environment necessary for resonance, wave instability allows a critical layer to form, etc.. Feedback mechanisms throughout the stratosphere are essential for warmings to occur.

Each theory partially explains the dynamics of SSWs and can be used by itself, or in combination with the others, to create models which simulate SSWs. Mechanistic models are primarily used for research and to test theories about the dynamics involved. General Circulation Models (GCMs) are used to make forecast products. The first successful SSW forecast made was for the January/February 1979 warming. Since then, more sophisticated GCMs have been designed and implemented. Unfortunately stratospheric forecast products are not routinely available to operational forecasters.

## Chapter 8

### Conclusions

Much work has been done in the theoretical realms to explain and model SSW formation, but little of the research has been directed at producing products and simulations which can be used to reliably forecast the event. The GCM modeling to date has produced promising avenues to such products. Their holistic approach to atmospheric modeling has already shown some success in forecasting SSWs, but refinements are still needed. As we push the limits of operational aerospace craft further into, and through, the stratosphere, parallel work in developing tools to accurately forecast the environmental conditions which will be encountered must be pursued. Where are the most intense temperature gradients located within the warming? How steep are the gradients? How quickly does the wind reversal from westerlies to easterlies occur? How strong are the easterlies? These are questions that need to better understood before we begin to routinely fly aircraft through the stratosphere.

What about the ionosphere? What exactly happens to the ionosphere during an SSW? This paper did not address this subject beyond stating that HF propagation is severely degraded throughout the warming. Almost all research on SSWs has been done with an academic, not operational, outlook. Operationally oriented research needs to also be accomplished. It's time we found the answers to some of these questions so customers of SSW forecasts can begin designing tomorrow's planes and communication equipment to withstand the impacts currently felt during SSWs.

## APPENDIX A

### Diagnostic Tools

Eliassen-Palm (EP) cross sections are diagnostic tools used by many researchers to analyze both actual SSWs and simulated warmings. EP cross sections display primary eddy heat fluxes, quasi-geostrophic potential vorticity, and momentum on a single diagram. They show both the vertical and meridional propagation of planetary waves in a manner directly related to the wave's effect on the mean state of the atmosphere. No assumptions about wave steadiness are involved (Dunkerton *et al.*, 1981). EP cross sections are latitude-height cross sections of the EP wave flux,  $\mathbf{F}$ , and its divergence,  $\nabla \cdot \mathbf{F}$  (Andrews *et al.*, 1987).  $\mathbf{F}$  is the direction of wave propagation in the meridional plane.  $\nabla \cdot \mathbf{F}$  is the eddy forcing of the mean flow of the transformed Eulerian mean equations.

The Eulerian-mean primitive equations, in spherical geometry, can be written as follows (Andrews *et al.*, 1987):

$$\bar{\mu}_t - f \bar{v}^* - \bar{X} = (\rho_0 a \cos \phi)^{-1} \nabla \cdot \mathbf{F} = D_f \quad (1)$$

The transformed mean momentum equation.

$$\bar{\theta} + \bar{\omega}^* \theta_{oz} - \bar{Q} = 0 \quad (2)$$

The quasi-geostrophic transformed mean thermodynamic equation.

$$(a \cos \phi)^{-1} (\bar{v}^* \cos \phi)_\phi + \rho_0^{-1} \rho_0 \bar{\omega}^* = 0 \quad (3)$$

The continuity of mass equation.

$$f \bar{\mu}_z + (R/aH) e^{-Kz/H} \bar{\theta}_\phi = 0 \quad (4)$$

The thermal wind equation.

where:  $f = 2 \Omega \sin \phi$

$$\mathbf{F} = [0, -\rho_0 a \cos \phi v' \mu', \rho_0 a \cos \phi f v' \theta' / \theta_{oz}]$$

$$\nabla \cdot \mathbf{F} = -(\rho_0 \bar{v}' \mu')_y + (\rho_0 f_0 \bar{v}' \theta' / \theta_{oz})_z$$

and:  $a$  = radius of the earth       $f$  = Coriolis parameter

$f_0$  = Coriolis parameter at  $45^{\circ}\text{N}$

$t$  - used as a subscript indicates a time derivative

$\bar{\mu}$  = mean of the  $x$  component of velocity

$\bar{v}^*$  = mean of the y component of velocity in spherical coordinates  
 $\bar{\omega}^*$  = mean of the vertical component of velocity in spherical coordinates  
 $z$  = vertical distance  
 $H$  = mean scale height  
 $\bar{Q}$  = diabatic heating term  
 $R$  = gas constant for dry air  
 $\bar{X}$  = mean meridional stream function  
 $\bar{\theta}$  = mean potential temperature  
 $K = R/c_p$ ; ratio of gas constant to the specific heat constant at a constant pressure

$\phi$  = latitude

$p_0$  = standard sea level pressure

$\Omega$  = angular speed of rotation of the earth

The above set of equations not only derives the EP flux and its divergence, but also provides a useful description of the interaction of the large-scale motions of the middle and upper latitudes. This equation set allows the use of the Eliassen-Palm theorem because the flux divergence is zero under non-acceleration conditions (Dunkerton *et al.*, 1981). Therefore, it is possible not only to get information on the net direction of wave propagation, but also on where non-acceleration conditions are being violated. Areas of numerous non-acceleration condition violations indicate the presence of a critical level.

It may be easier to conceptualize what is happening in the EP cross sections if  $\mathbf{F}$  is thought of as being related to the group velocity of the waves;  $\nabla \cdot \mathbf{F}$  as related to the change in angular momentum; and  $D_f$  as the northward flux of the quasi-geopotential vorticity (Dunkerton *et al.*, 1981). The normal winter stratospheric pattern has planetary wave energy propagating up into the stratosphere from the troposphere and turning equatorward (Andrews *et al.*, 1987). Figure 15 demonstrates this on an EP cross section. The arrows represent  $\mathbf{F}$  and the contours represent  $\nabla \cdot \mathbf{F}$  (McIntyre, 1982). During the prewarming and breakdown phases of a

SSW significant changes occur with both the EP flux,  $\mathbf{F}$ , and the quasi-geopotential vorticity flux,  $D_f$ . The arrows in Fig. 20 show the "integral curves" of  $\mathbf{F}$  (curves that are everywhere parallel to  $\mathbf{F}$ ) for several days of a warming which gives the direction of vertical propagation of planetary wave energy. The contour lines are  $D_f$  and show areas where  $\mathbf{F}$  converges (stippled and negative) along with areas where  $\mathbf{F}$  diverges (white and positive). Convergence of  $\mathbf{F}$  indicates a rapid rise in temperature which, according to the thermal wind equation (4), requires a rapid deceleration of the mean flow (Palmer, 1981). Figures 20a-c represent the prewarming phase and 20d-f the breakdown phase.

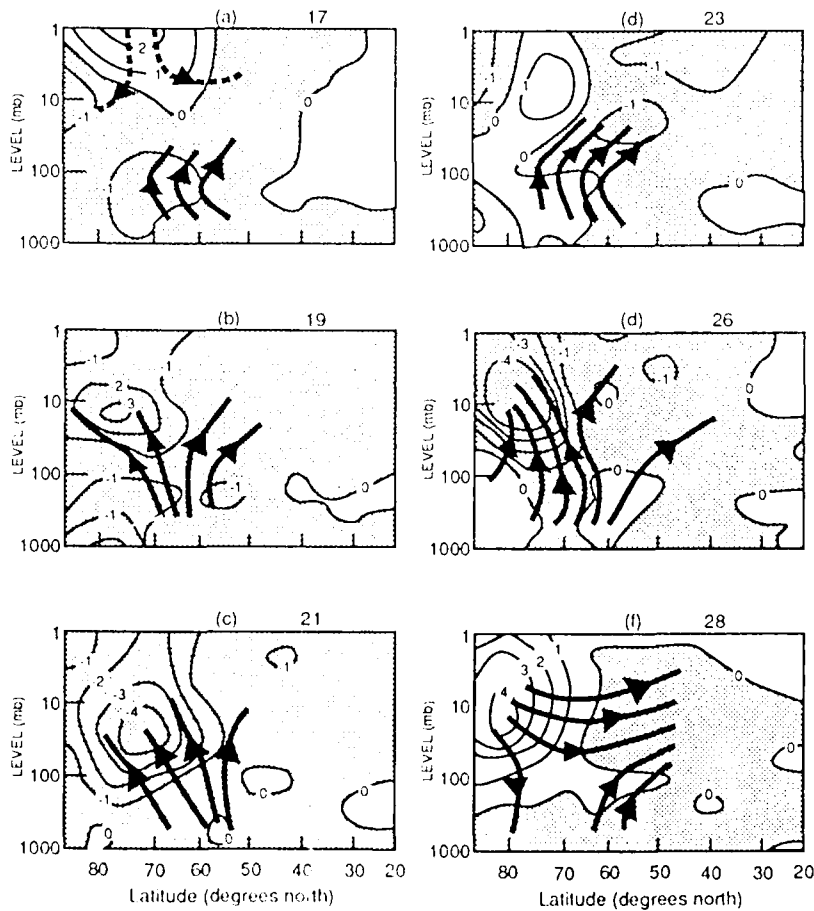


Fig. 20. Some integral curves of  $\mathbf{F}$  and contours  $D_f$  in units  $10^{-4} \text{ ms}^{-2}$  (negative values stippled) for (a) February 17, (b) February 19, (c) February 21, (d) February 23, (e) February 26, and (f) February 28, 1979. Dashed integral curves are dominated by wave 1 contributions to  $\mathbf{F}$ , full curves by wave 2 contributions. From Palmer (1981).

Figure 20a, the cross section for 17 February shows a region of  $\mathbf{F}$  flux convergence in the high-latitudes ( $60^{\circ}$ - $80^{\circ}$ N) of the troposphere and flux divergence in the polar latitudes of the stratosphere. The diverging dashed integral

curves represent a diminishing of previous wave number 1 activity in the area. The downward direction of the curves indicates the eddy heat fluxes are moving equatorward. The converging solid integral curves indicate a stronger eddy activity associated with wave number 2 pushing up from the troposphere. In Fig. 20b, 19 February, the EP flux is converging in the high latitudes of the mid-stratosphere. The integral curves show the flux is split; half the flux is focusing into the polar regions while the rest continues moving equatorward. As expected with convergent areas of EP flux, the mean flow is undergoing deceleration. By 21 February, Fig. 20c, we see an intensification of the flux convergence into the high latitudes of the mid-stratosphere ( $D_f = -4$ ). There is a strong focusing of the flux towards the pole. The amplitude of wave number 2 grew 170 m in two days at 10 mb at  $65^{\circ}\text{N}$  (Palmer, 1981), which implies that the transience of growing waves is responsible for the intensification of EP flux convergence. By 23 February, Fig. 20d, an area of flux divergence is present in the high latitudes throughout the depth of the atmosphere. The integral curves show the stratospheric wave flux pointed south. The deceleration of the mean flow experienced a short lull. However on 26 February, Fig. 20e, the flux convergence reappears in the high latitudes and the deceleration of the mean flow resumes. On 28 February, Fig. 20f, the warming is almost over and the stratospheric circulation is returning to normal. The divergence of the flux occurs in the high latitudes of the stratosphere and the integral curves are all, once again, pointing equatorward (Palmer, 1981).

## Appendix B

### Case Study

January 1985 was an active month for SSWs. The month began in the middle of a major warming event and ended with a minor event. Data obtained from the 30 mb and 50 mb height/temperature charts for both events will be reviewed in this case study. Warmings are characterized by an increase in temperature by  $25^{\circ}\text{C}$  and a breakdown of the polar night jet with westerlies reversing to easterlies. (See sections 2.1 and 2.2.) Assuming the average 30 mb and 50 mb temperature for January 1985 is  $-63^{\circ}\text{C}$  and  $-60^{\circ}\text{C}$  (taken from January 1-31, 1985 1200 GMT 30 mb and 50 mb height/temperature charts) then an increase in temperature to  $-48^{\circ}\text{C}$  and  $-45^{\circ}\text{C}$  or greater (respectively) indicates a warming event. The presence of westerly winds identifies the event as a minor warming, while the presence of easterly, not westerly, winds identifies the event as a major warming. In this study restrictions were tighten to require a reported temperature to read at least  $-45^{\circ}\text{C}$  in order to be included in this report. Due to cost data was only obtained for the month of January 1985; a month known for having both a major and minor warming event. The northern hemisphere 1200 GMT 30 mb and 50 mb height /temperature charts were analyzed for the entire month. Since only 0000 GMT and 1200 GMT charts are available for the stratosphere and diurnal temperature variations are slight due to cost restrictions only 1200 GMT charts were used. The 30 mb and 50 mb levels were chosen since these are the charts most frequently used by operational forecasters when trying to predict/determine the occurrence of SSWs. This study will demonstrate what the forecaster is working with, how a warming is identified, and what the customer impacts will be from the event.

#### **Major Warming**

A major warming event was already in progress as 1985 began (Figs. 21 - 36). On January 1 two separate warm cells were evident. Figure 21 shows the more intense cell was located over eastern Siberia at 30 mb with a maximum temperature of  $-43^{\circ}\text{C}$  and average winds being south-southeasterly at 85 knots. The second cell,

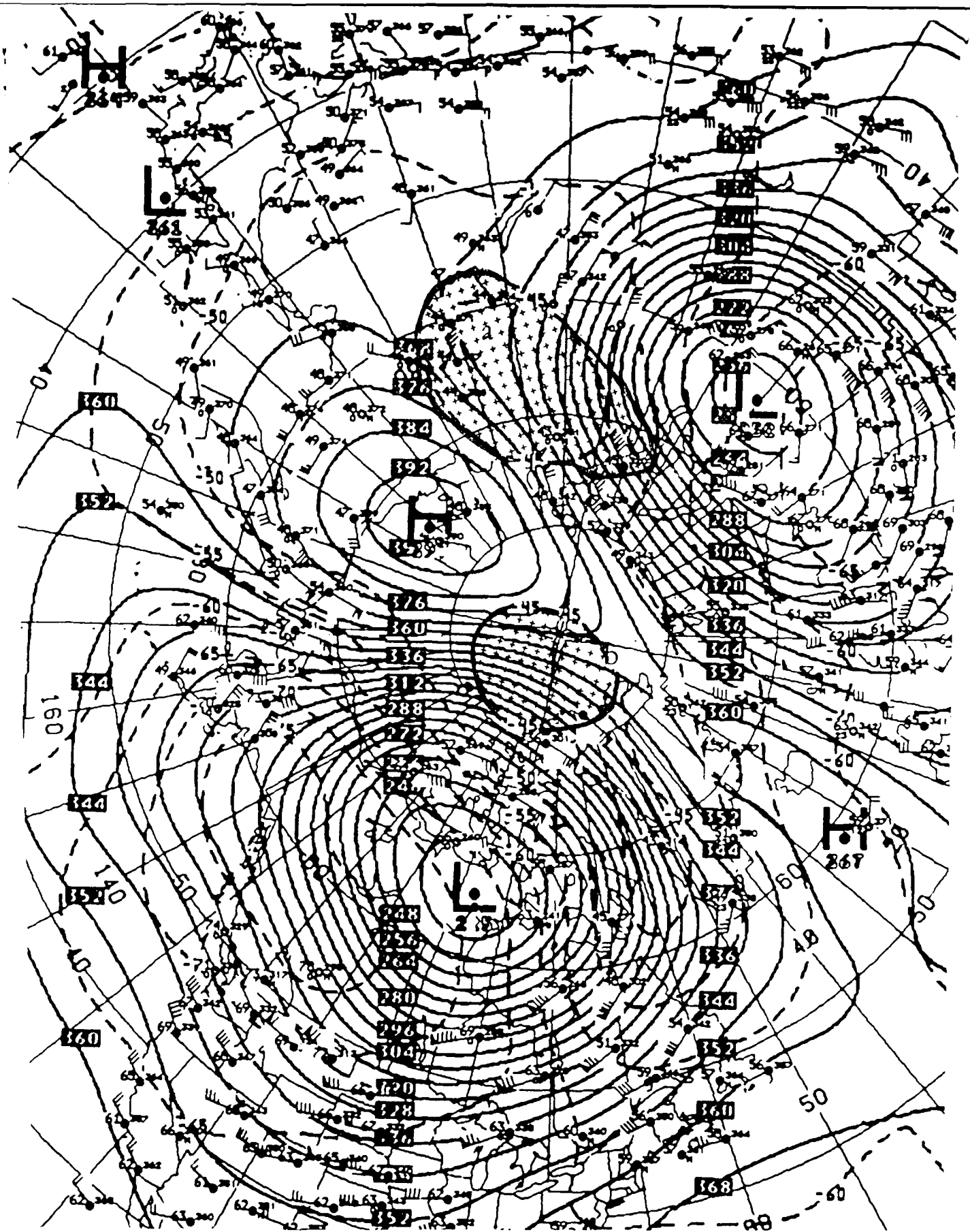


Fig. 21. 30 mb height/temperature for January 1, 1985. Isotherms dashed lines, isoheights solid lines. Shaded areas indicate region where warming event is located.

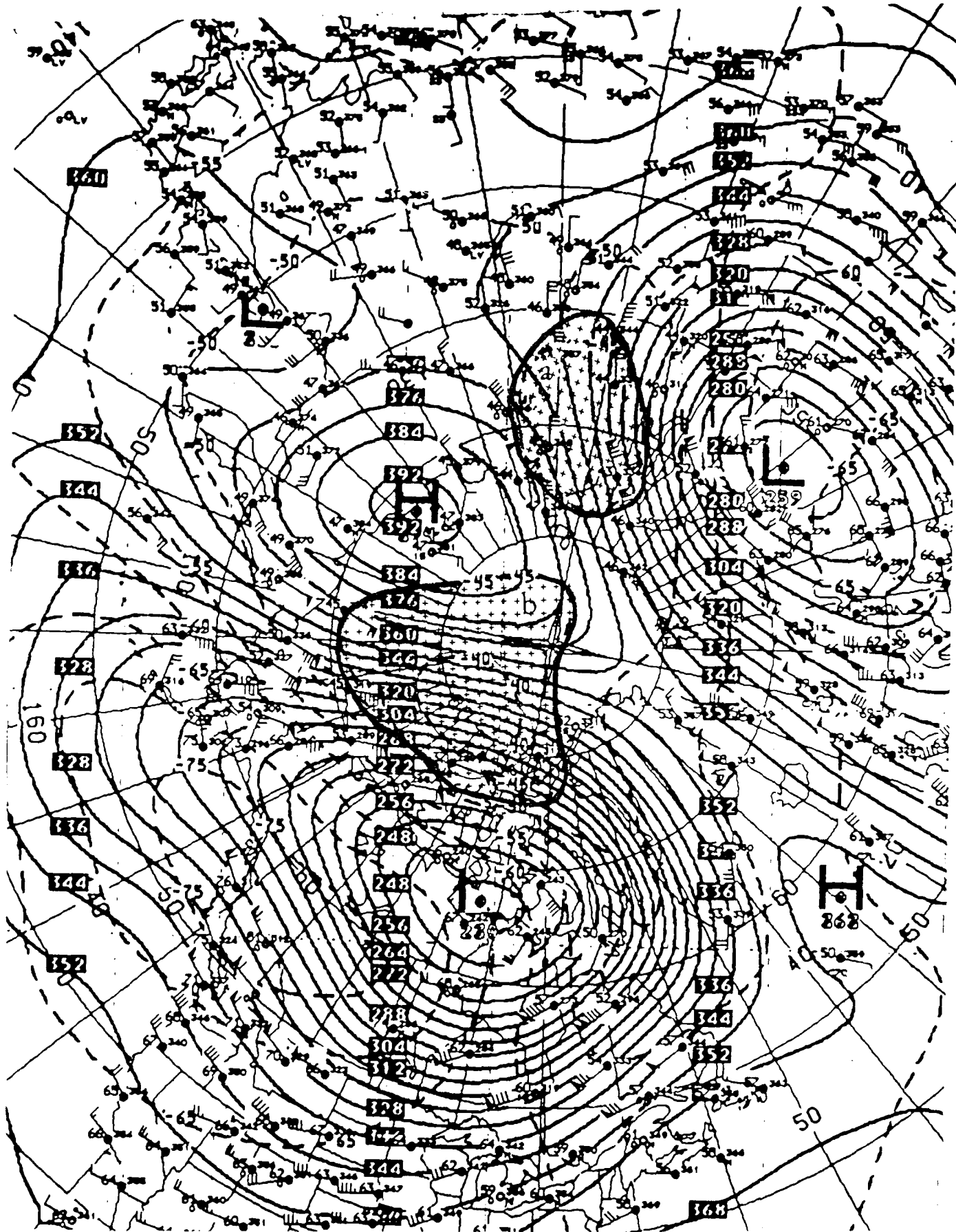


Fig. 22. 30 mb height/temperature for January 2, 1985.

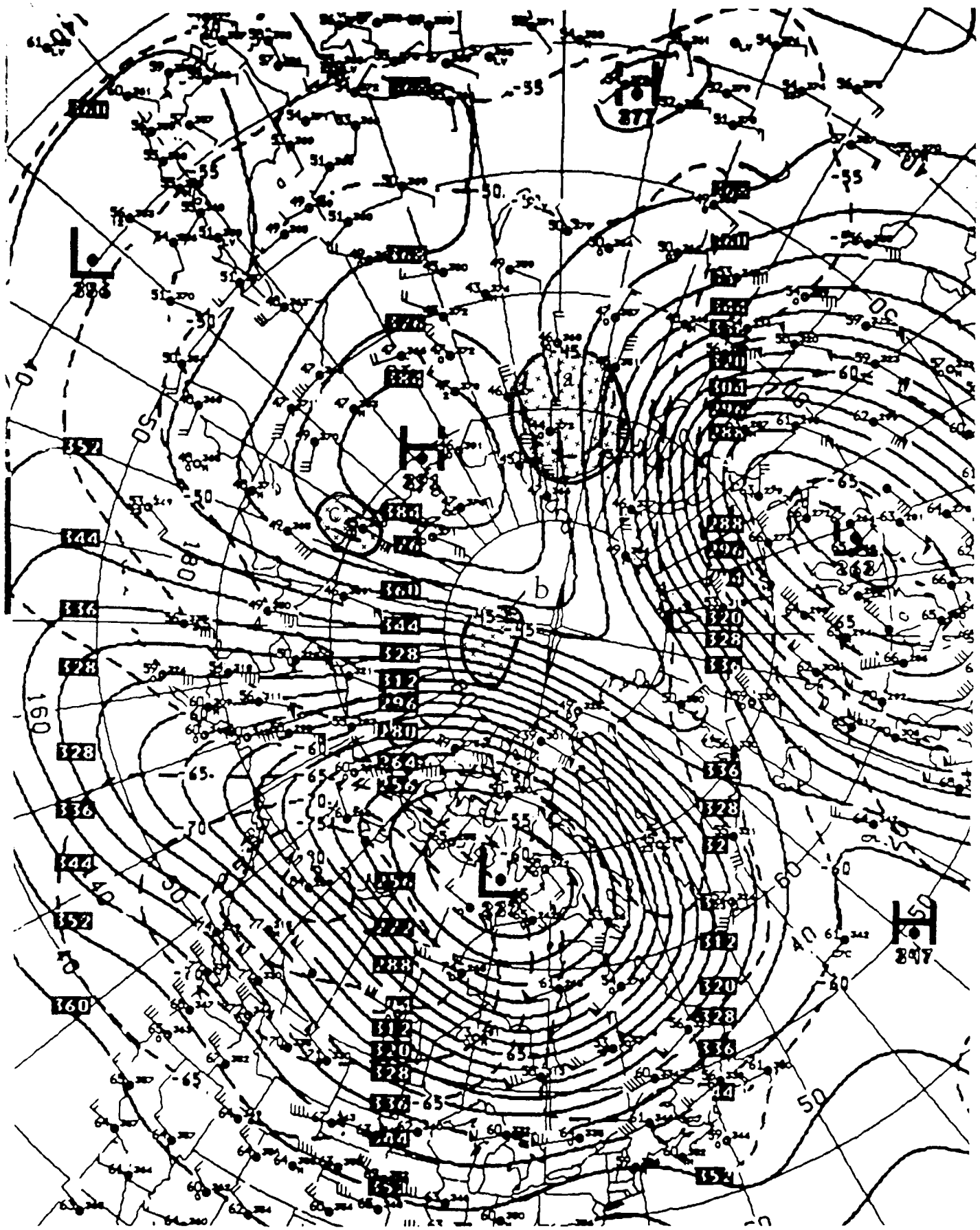


Fig. 23. 30 mb height/temperature for January 3, 1985.

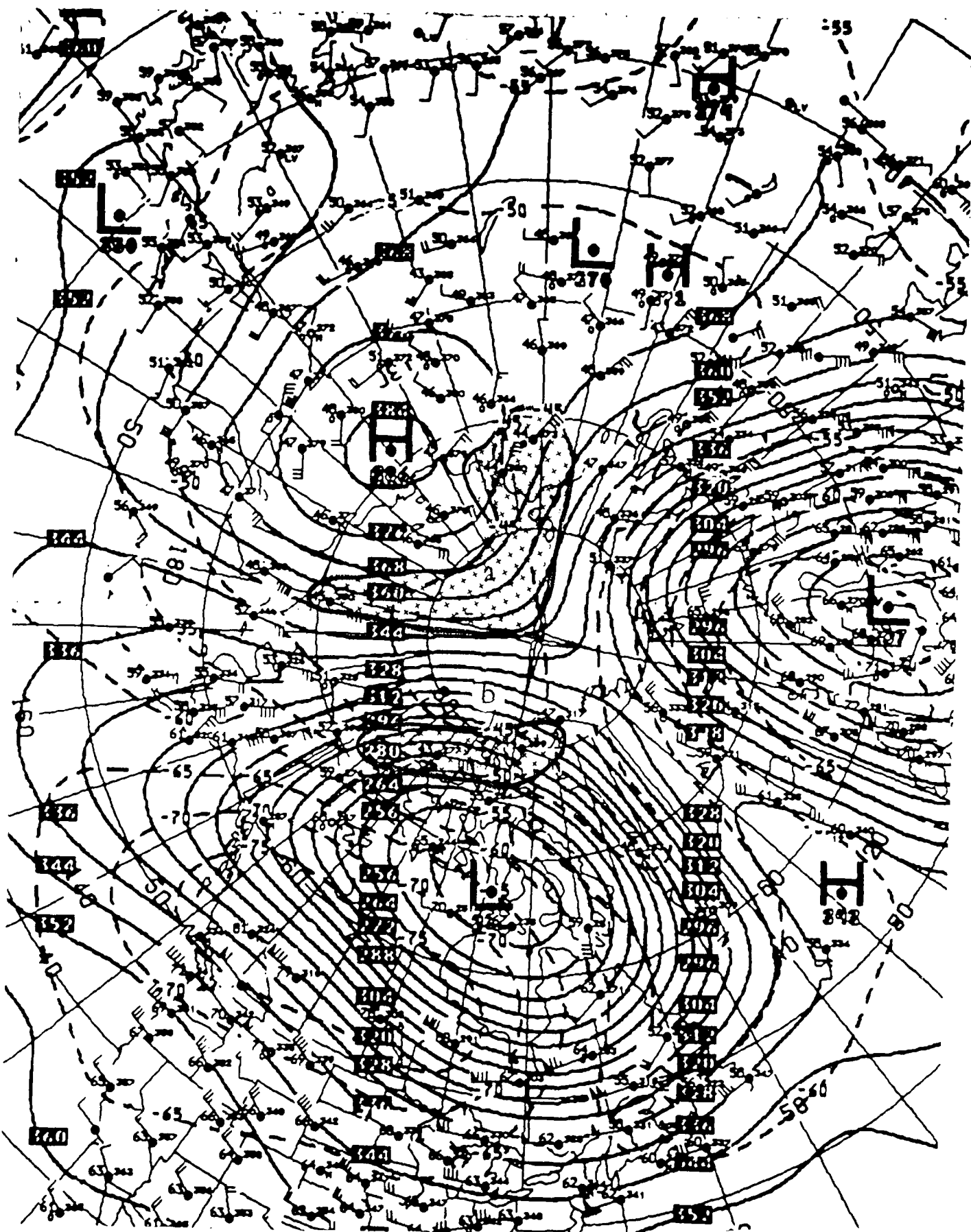


Fig. 24. 30 mb height/temperature for January 4, 1985.

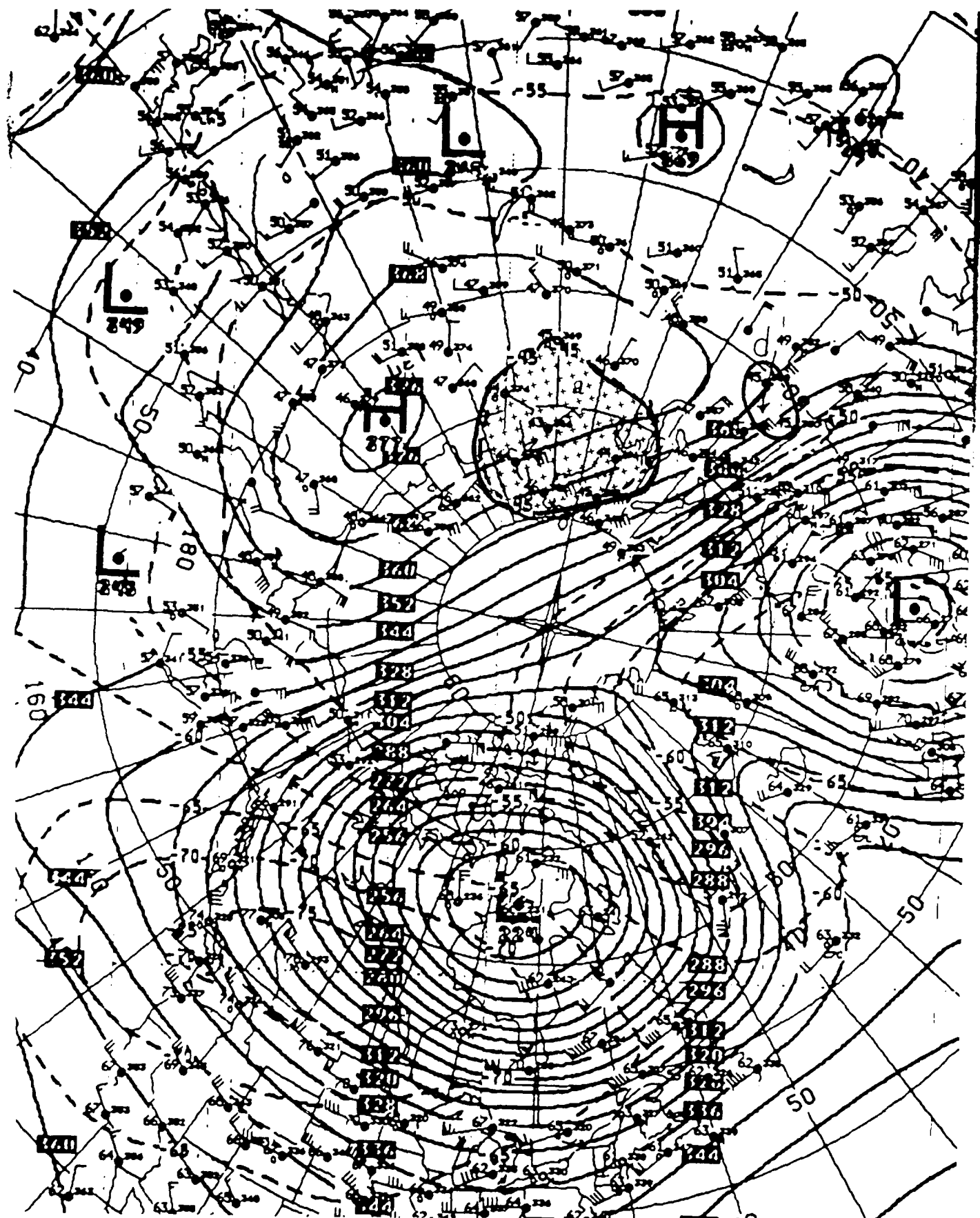


Fig. 25. 30 mb height/temperature for January 5, 1985.

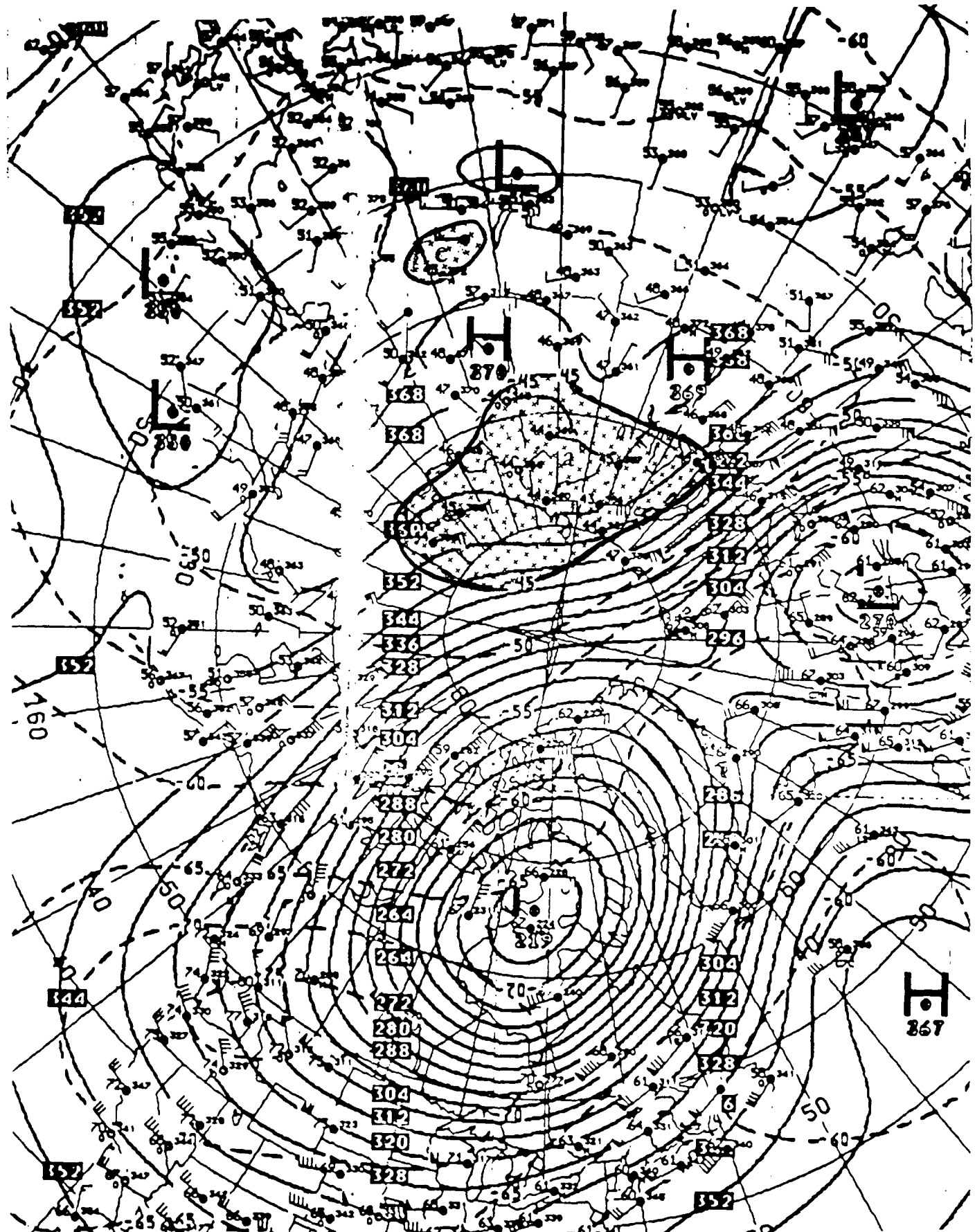


Fig. 26. 30 mb height/temperature for January 6, 1985.

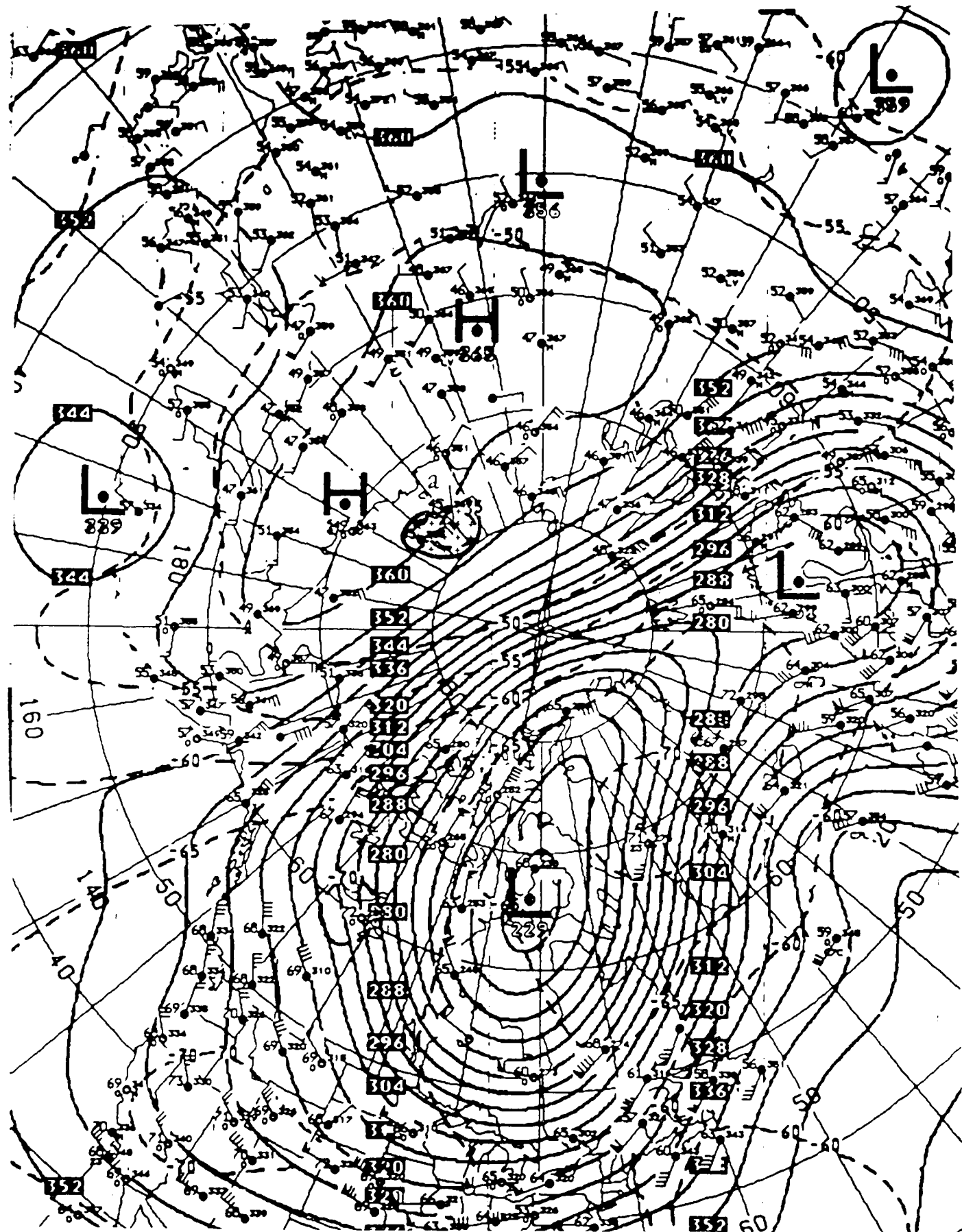


Fig. 27. 30 mb height/temperature for January 7, 1985.

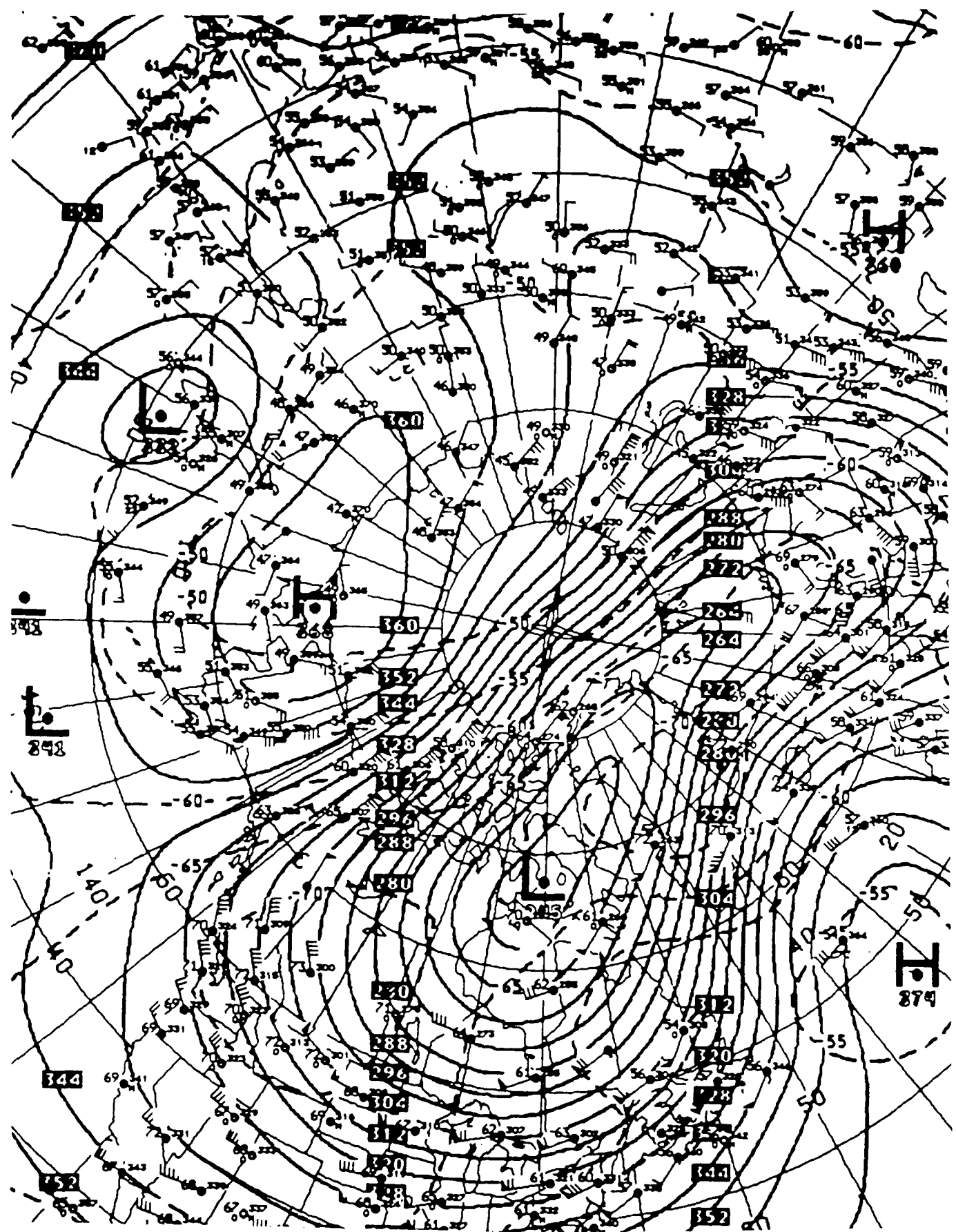


Fig. 28. 30 mb height/temperature for January 8, 1985.

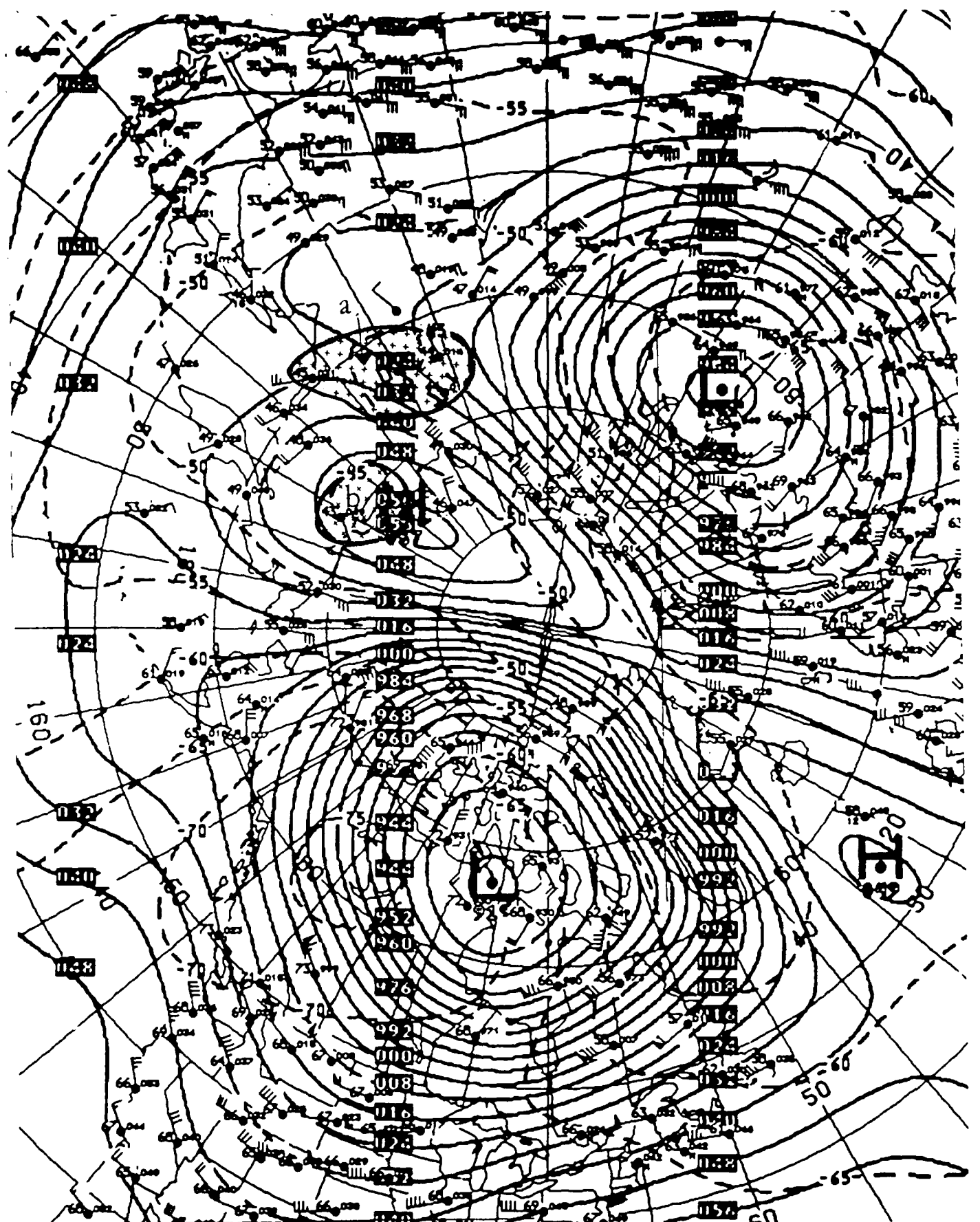


Fig. 29. 50 mb height/temperature for January 1, 1985.

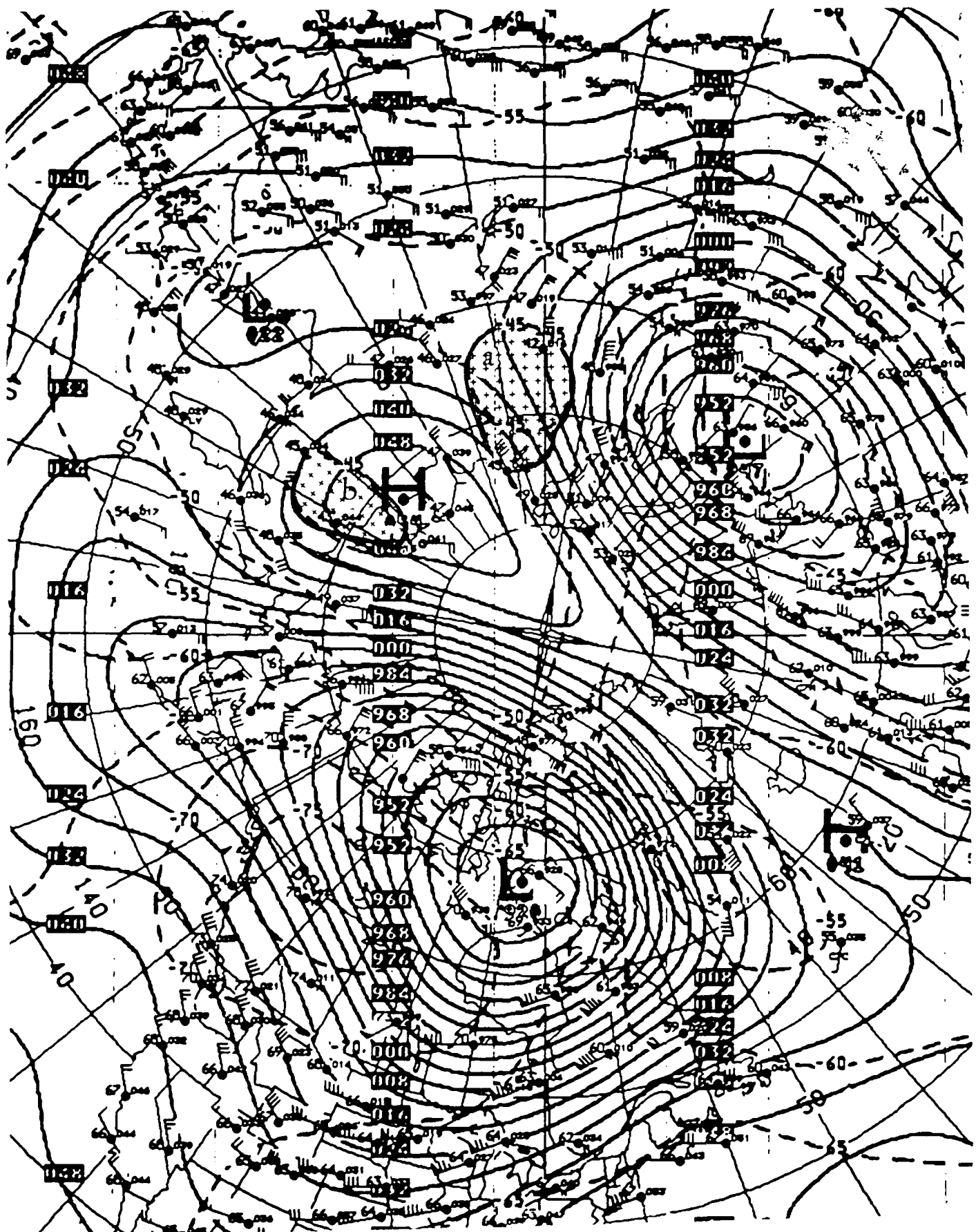


Fig. 30. 50 mb height/temperature for January 2, 1985.

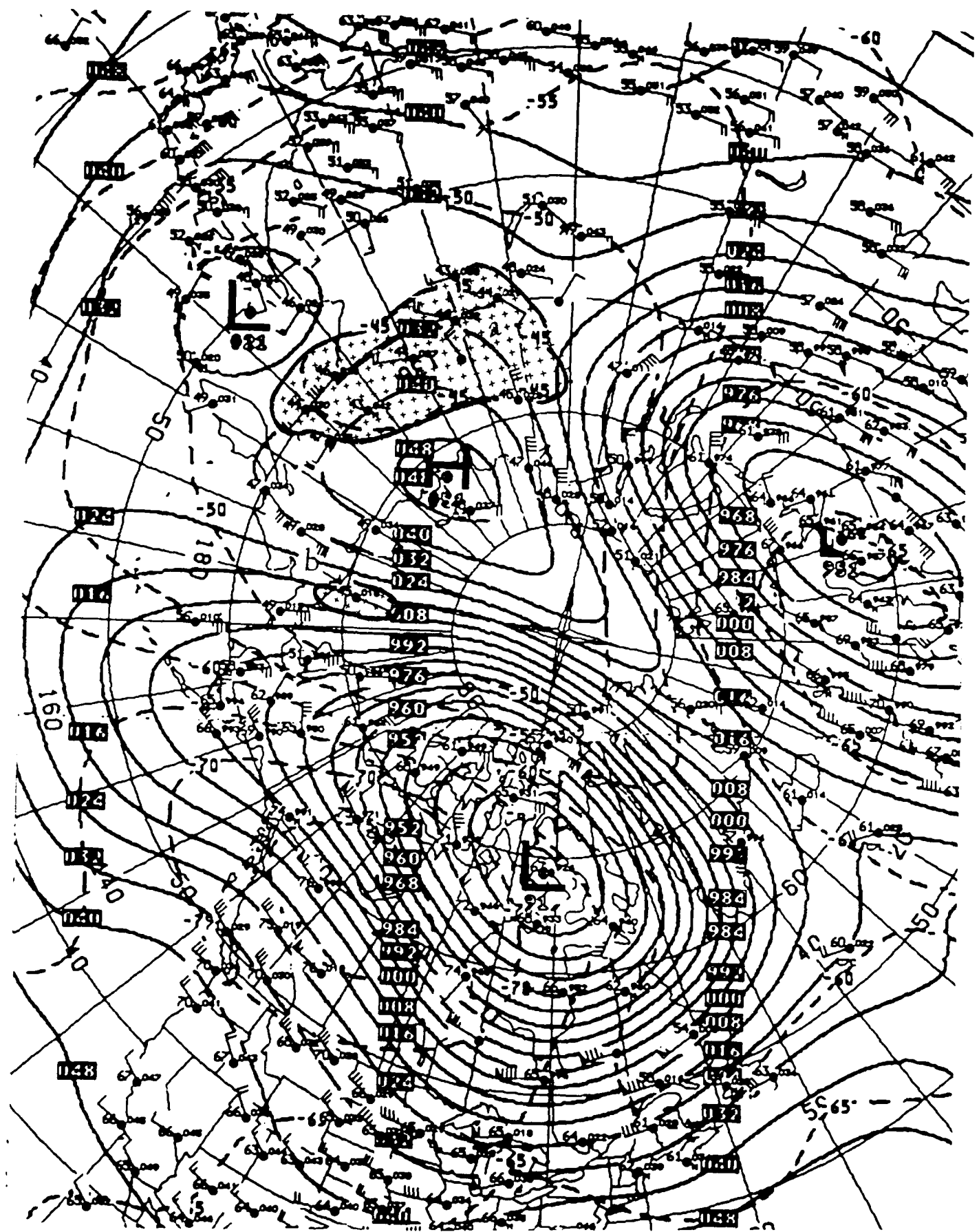


Fig. 31. 50 mb height/temperature for January 3, 1985.

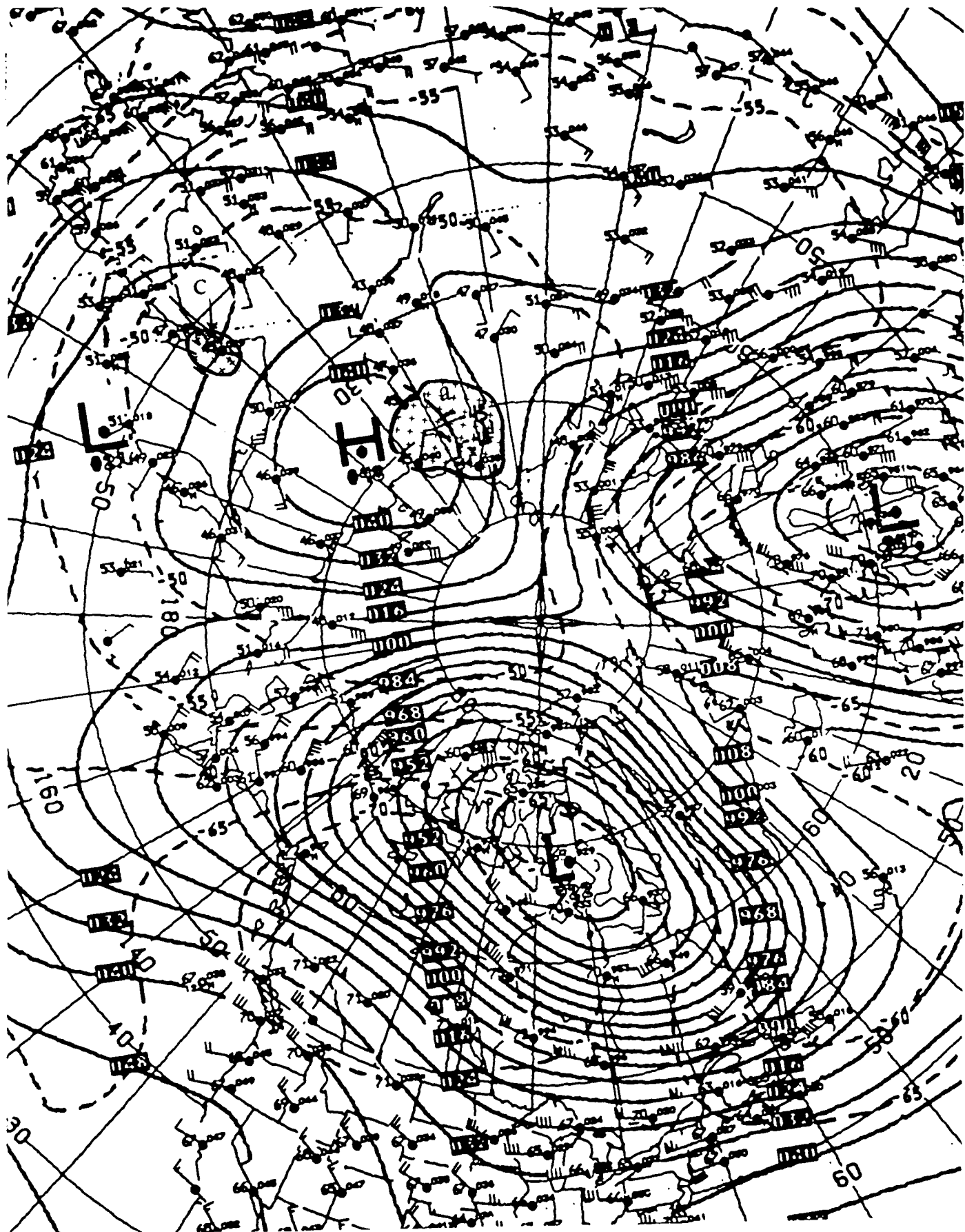


Fig. 32. 50 mb height/temperature for January 4, 1985.

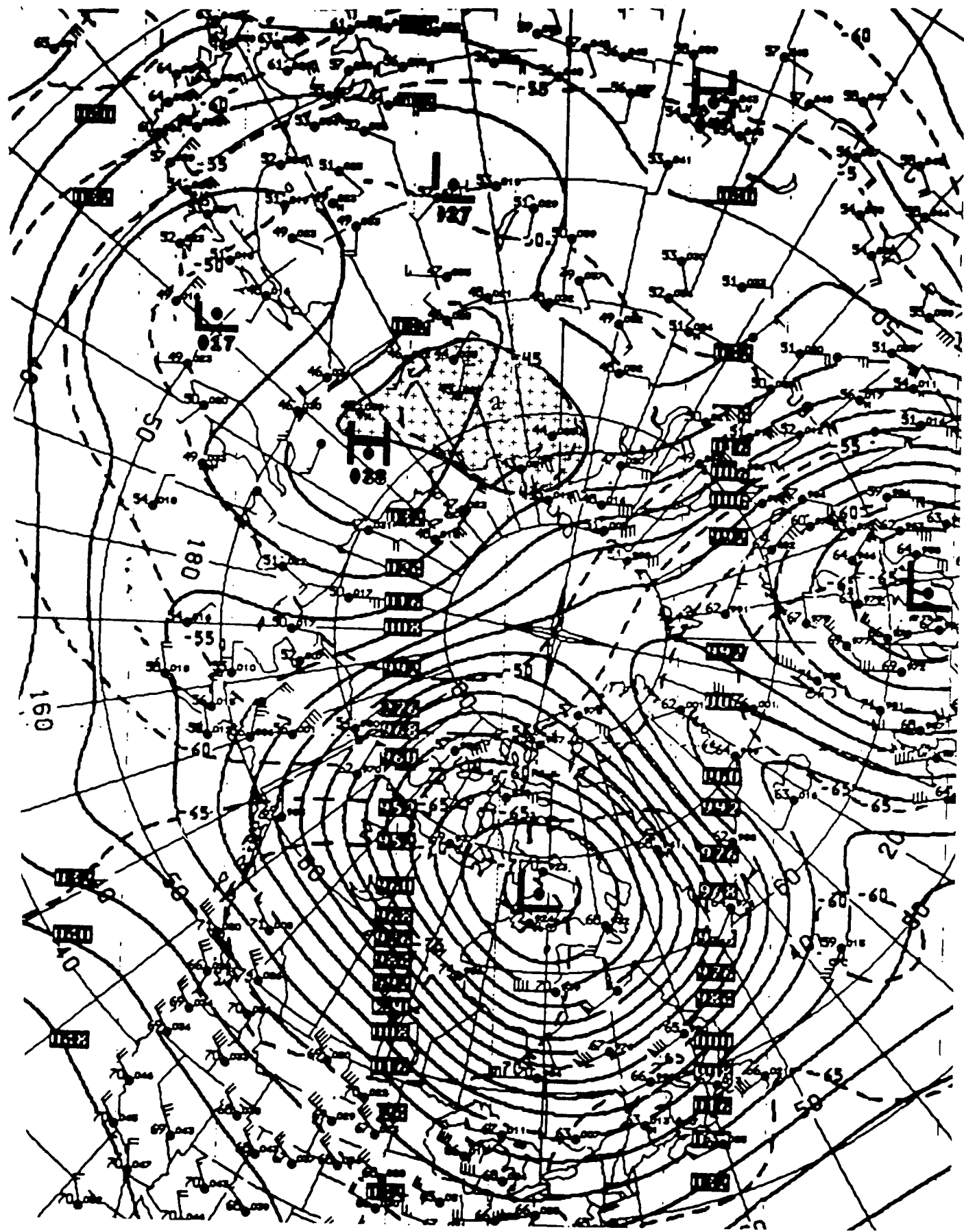


Fig. 33. 50 mb height/temperature for January 5, 1985.

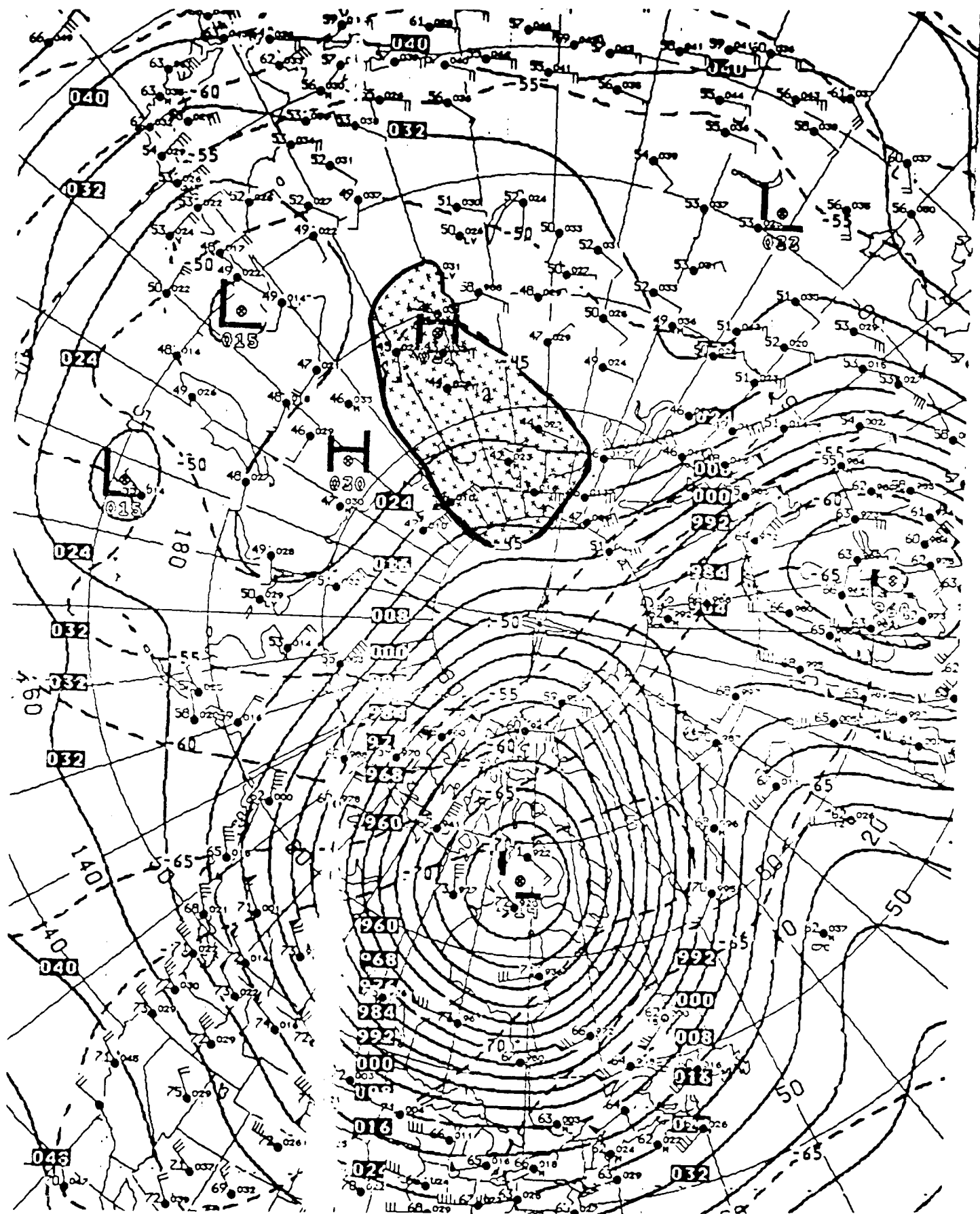
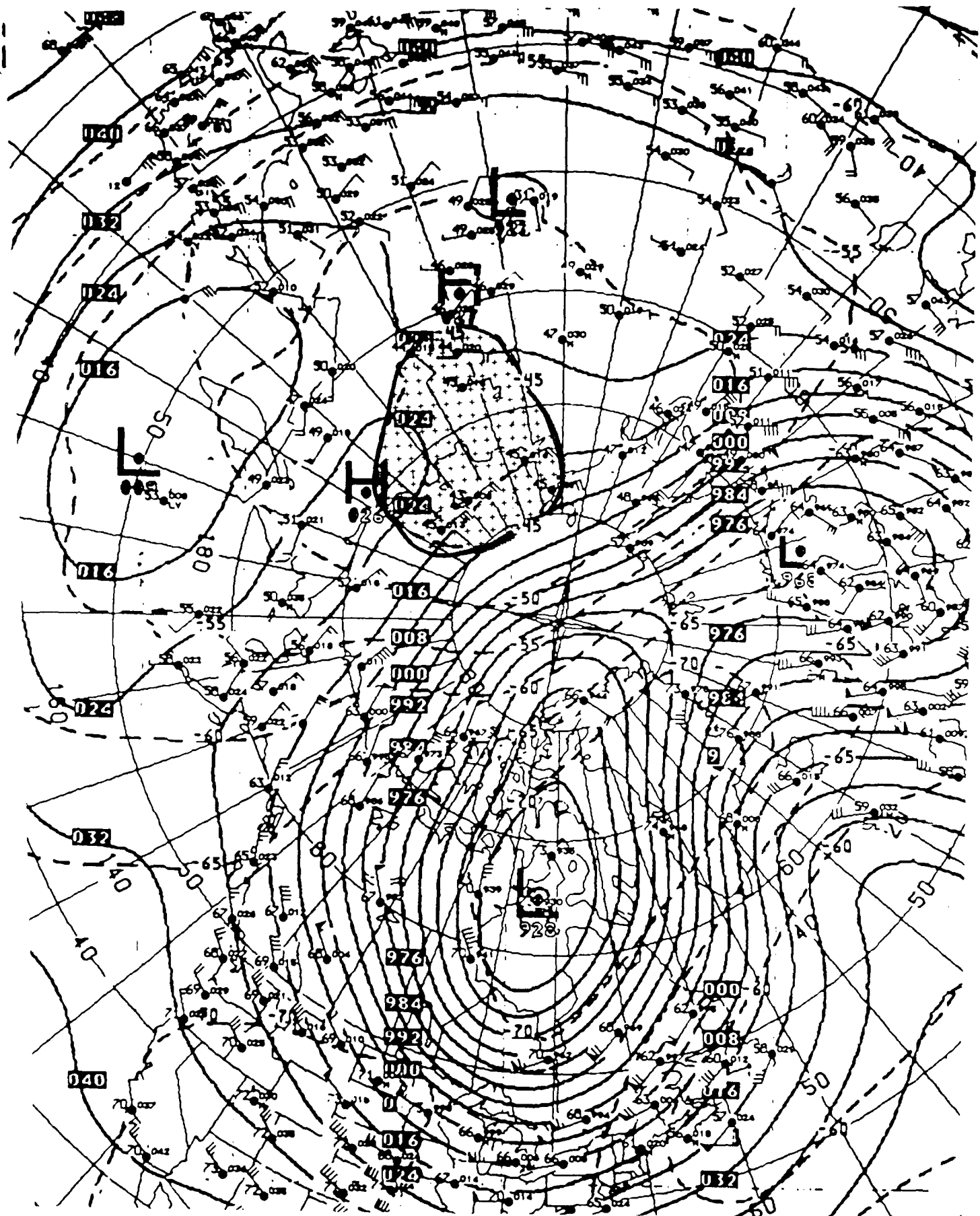


Fig. 34. 50 mb height/temperature for January 6, 1985.



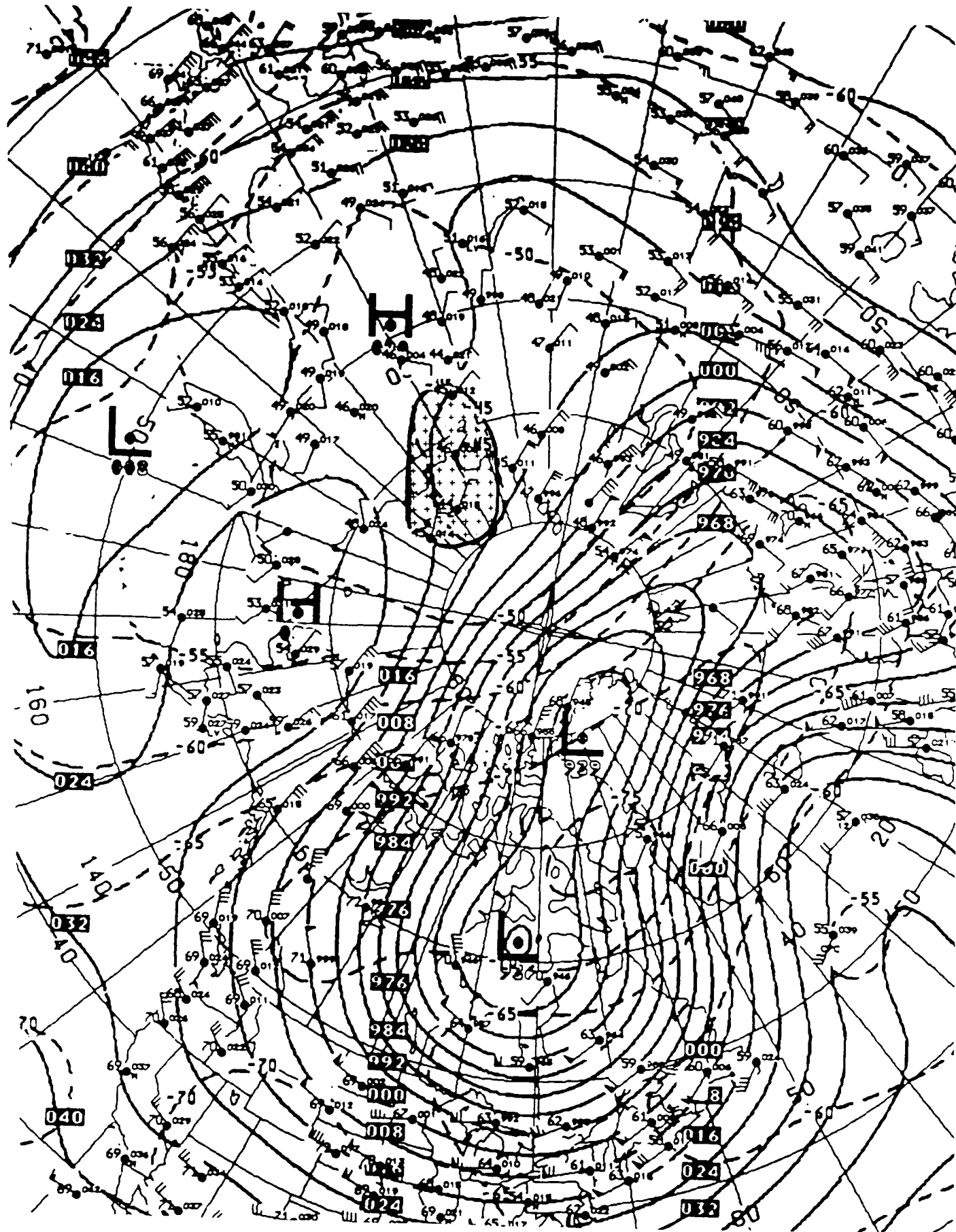


Fig. 36. 50 mb height/temperature for January 8, 1985.

just slightly less intense, north of the Beaufort Sea had temperatures as warm as -45<sup>0</sup>C and easterly winds averaging 70 knots - a major warming was occurring. Figures 21-28 show how this warming appears at 30 mb from when it's picked up on January 1, see Fig. 21, until it's end on January 8, Fig. 28. Figures 29-36 depict this same event but at 50 mb. The 50 mb warming differs from what's happening at the 30 mb level in the winds around the event and in the type wave pattern that dominates the hemisphere. The 50 mb winds are not as strong as those found at 30 mb in the height of the warming and the wave 2 pattern remains in place 24 hours longer before breaking down. This results in the 50 mb warm temperatures also being present 24 hours longer than the 30 mb -45<sup>0</sup>C or greater temperatures. Listed below is a summary of the significant data found in Figs. 21-36.

#### 30 mb Chart Results

<u>Date</u>	<u>Cell</u>	<u>Max Temp</u>	<u>Wind Dir &amp; Speed</u>	<u>Latitude</u>	<u>Longitude</u>	<u>Wave#</u>
Jan 1	a	-43 <sup>0</sup> C	SSE 85 kt	60-75N	130E-090E	2
Jan 1	b	-45 <sup>0</sup> C	E 70 kt	80-90N	030W-170E	2
Jan 2	a	-44 <sup>0</sup> C	S 50 kt	60-75N	130E-080E	2
Jan 2	b	-37 <sup>0</sup> C	E 100 kt	75-90N	080W-120E	2
Jan 3	a	-44 <sup>0</sup> C	S 35 kt	65-75N	110E-085E	2
Jan 3	b	-45 <sup>0</sup> C	E 80 kt	80-85N	130W-090E	2
Jan 3	c	-45 <sup>0</sup> C	E 40 kt	70N	165E-155E	2
Jan 4	a	-44 <sup>0</sup> C	S 35 kt	70-80N	180W-090E	2
Jan 4	b	-43 <sup>0</sup> C	E 70 kt	75-85N	080W-140W	2
Jan 5	a	-43 <sup>0</sup> C	S 20 kt	65-80N	120E-070E	Breaking
Jan 5	d	-45 <sup>0</sup> C	S 20 kt	60-65N	060E-050E	Breaking
Jan 6	a	-43 <sup>0</sup> C	WSW 30 kt	65-80N	160E-060E	Breaking
Jan 6	e	-45 <sup>0</sup> C	E 15 kt	55-60N	125E-115E	Breaking
Jan 7	a	-45 <sup>0</sup> C	W 15 kt	75-80N	150E-130E	1

### 50 mb Chart Results

<u>Date</u>	<u>Cell</u>	<u>Max Temp</u>	<u>Wind Dir &amp; Speed</u>	<u>Latitude</u>	<u>Longitude</u>	<u>Wave#</u>
Jan 1	a	-44° <sup>0</sup> C	SE 50 kt	60-65N	140E-120E	2
Jan 1	b	-43° <sup>0</sup> C	E 20 kt, W 20 kt	75-80N	165E-145E	2
Jan 2	a	-42° <sup>0</sup> C	S 30 kt	60-70N	115E-100E	2
Jan 2	b	-43° <sup>0</sup> C	E 30 kt, W 20 kt	60-75N	160E-150E	2
Jan 3	a	-43° <sup>0</sup> C	S 25 kt, E 35 kt	60-70N	150E-100E	2
Jan 3	b	-45° <sup>0</sup> C	N 35 kt	65-75N	180W	2
Jan 4	a	-44° <sup>0</sup> C	S 20 kt	65-75N	135E-105E	2
Jan 4	c	-43° <sup>0</sup> C	E 20 kt	50-55N	140E	2
Jan 5	a	-44° <sup>0</sup> C	S10 kt, E10 kt, W20 kt	60-75N	145E-095E	2
Jan 6	a	-42° <sup>0</sup> C	W 30 kt	55-80N	140E-090E	Breaking
Jan 7	a	-43° <sup>0</sup> C	W 20 kt	60-80N	160E-100E	Breaking
Jan 8	a	-44° <sup>0</sup> C	SW 15 kt	65-80N	150E-120E	1

At the start of January 1985 the 30 mb and 50 mb charts, Fig.s 21 and 29 respectively, showed a major warming already in progress. Two distinct areas, a and b, met the major warming criteria. HF propagation over these areas was degraded at this time. Any plane flying over the artic circle at these altitudes would have encountered a drastic 180° wind shift with wind speeds averaging 70 knots in both directions. On January 2, Fig. 22, the warming associated with area a had lost most of its eastward component, becoming predominately southerly flow. the warming associated with area b reached its peak intensity with temperatures as warm as -37°<sup>0</sup>C and easterly winds at 100 knots. This warm cell lasted only two more days, Figs. 23 and 24, before completely disappearing. While it managed to retain its easterly winds, its temperature profile echoed that of area a. Area a took much longer to dissipate. A couple small "hot spots" developed (Fig. 23 area c and Fig. 25 area d) and were absorbed and were absorbed by area a during its last few days of existence. With the dissipation of area b came the breakdown of wave 2 which had dominated the northern hemisphere up to the fifth of the month. The breakdown was complete

by 7 January which was the last day of the warm temperatures at 30 mb.

The warming at 50 mb reflected what was occurring at 30 mb but was not identical to the 30 mb profile. Wave 2 did not start breaking down at 50 mb until January 6, Fig. 34, and completed the breakdown in only two days vice the three days it took at 30 mb. As with the one day lag for the wave 2 break down, the warm spot at area a also lagged the 30 mb level and was still present on January 8, a full day after it had disappeared off the 30 mb chart. Another major difference between the two levels is that the winds throughout the 50 mb level were much less intense (with the January 1, Fig. 29, 50 knot wind being the strongest) than those found at 30 mb. Since the polar night jet normally resides between 10 mb and 30 mb lighter winds are expected at this level. However, what is surprising is that the warm temperatures were about the same at both levels.

#### **Minor Warming**

The minor warming event that occurred January 20-31, Figs. 37-51, differed from the major warming in several ways. First and most obvious, is that the polar night jet did not break down. Second, is that the 30 mb winds are noticeably weaker. There is no significant difference in the wind intensity at 50 mb. The last big difference is the type of wave pattern that dominates the northern hemisphere differs greatly between the two levels. At 30 mb the warming starts as wave 2 dominates the hemisphere (Fig. 37) but wave 1 soon takes over (Fig. 41) only to be replaced by wave 2 as the month ends (Fig. 47). At 50 mb a wave 3 pattern is present throughout the minor warming (Figs. 48-51). The presence of the wave 3 pattern is a good indicator that this will not develop into a major warming since major warmings are only associated with waves 1 and 2. Wave 3's do not normally carry enough energy to force the reversal of the polar night jet.

With all the differences between the two types of warmings, major and minor, there are practically no differences when just temperature profiles are considered. Given no other data, except temperature, it would be impossible to differentiate between the two.

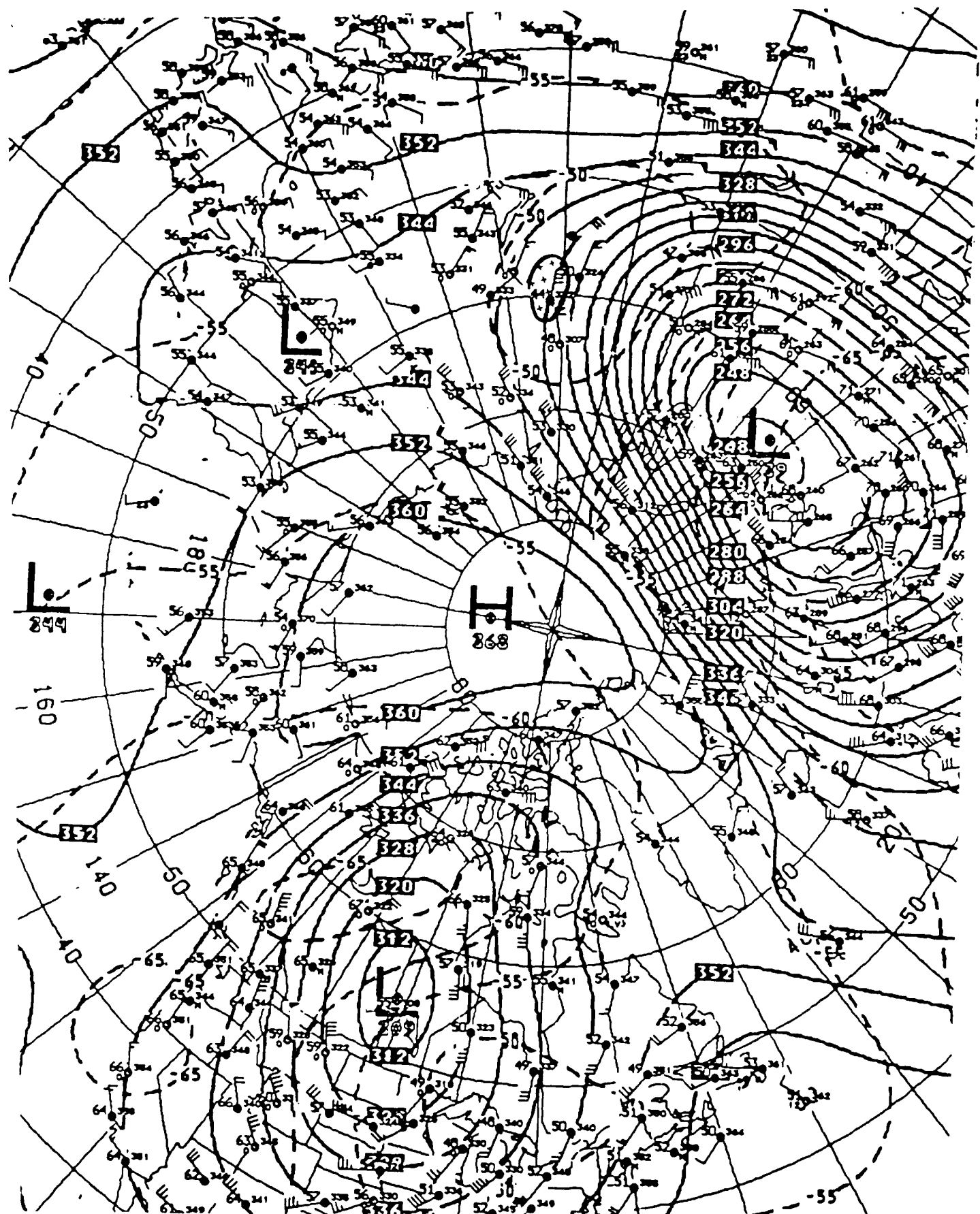
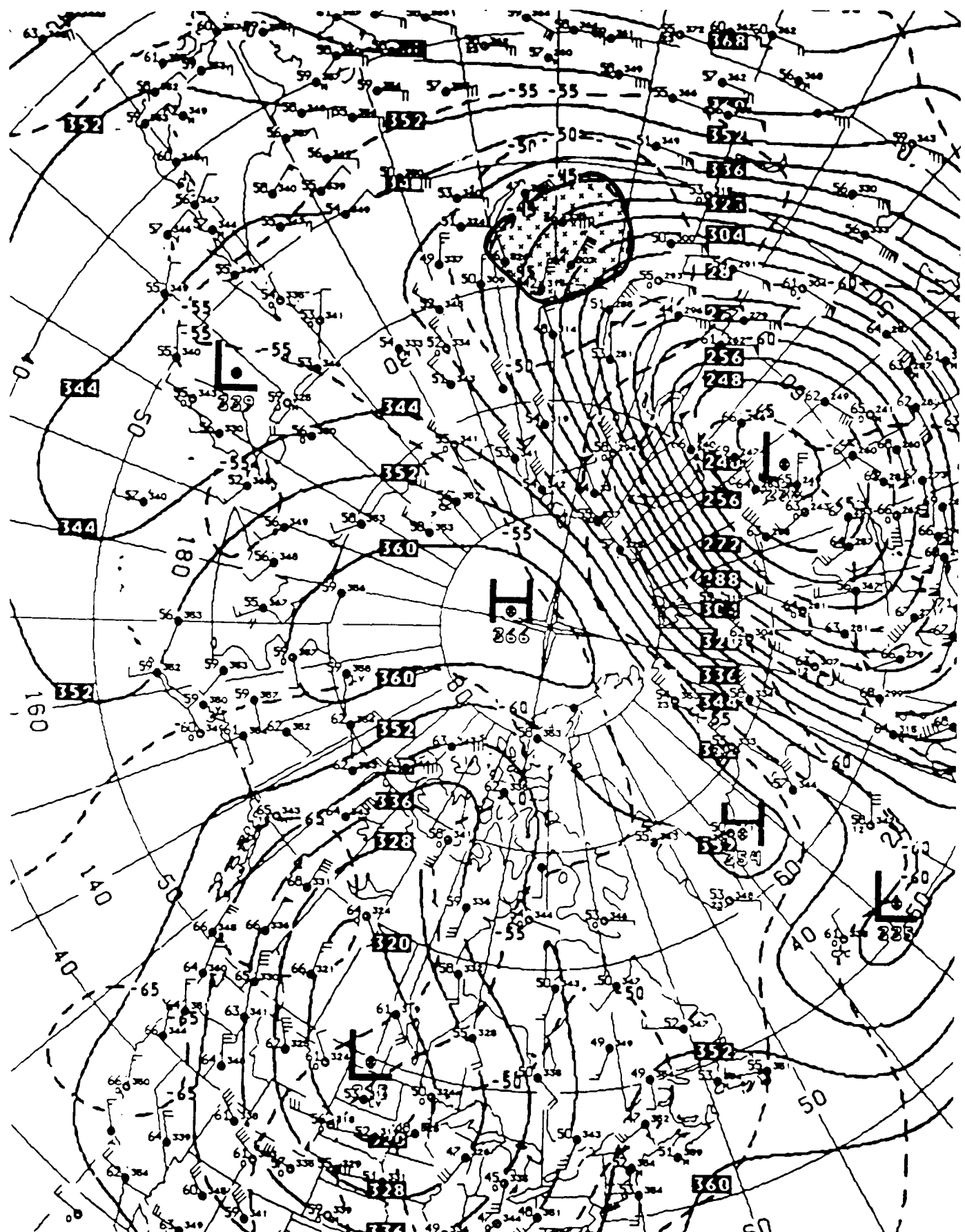


Fig. 37. 30 mb height/temperature for January 20, 1985.



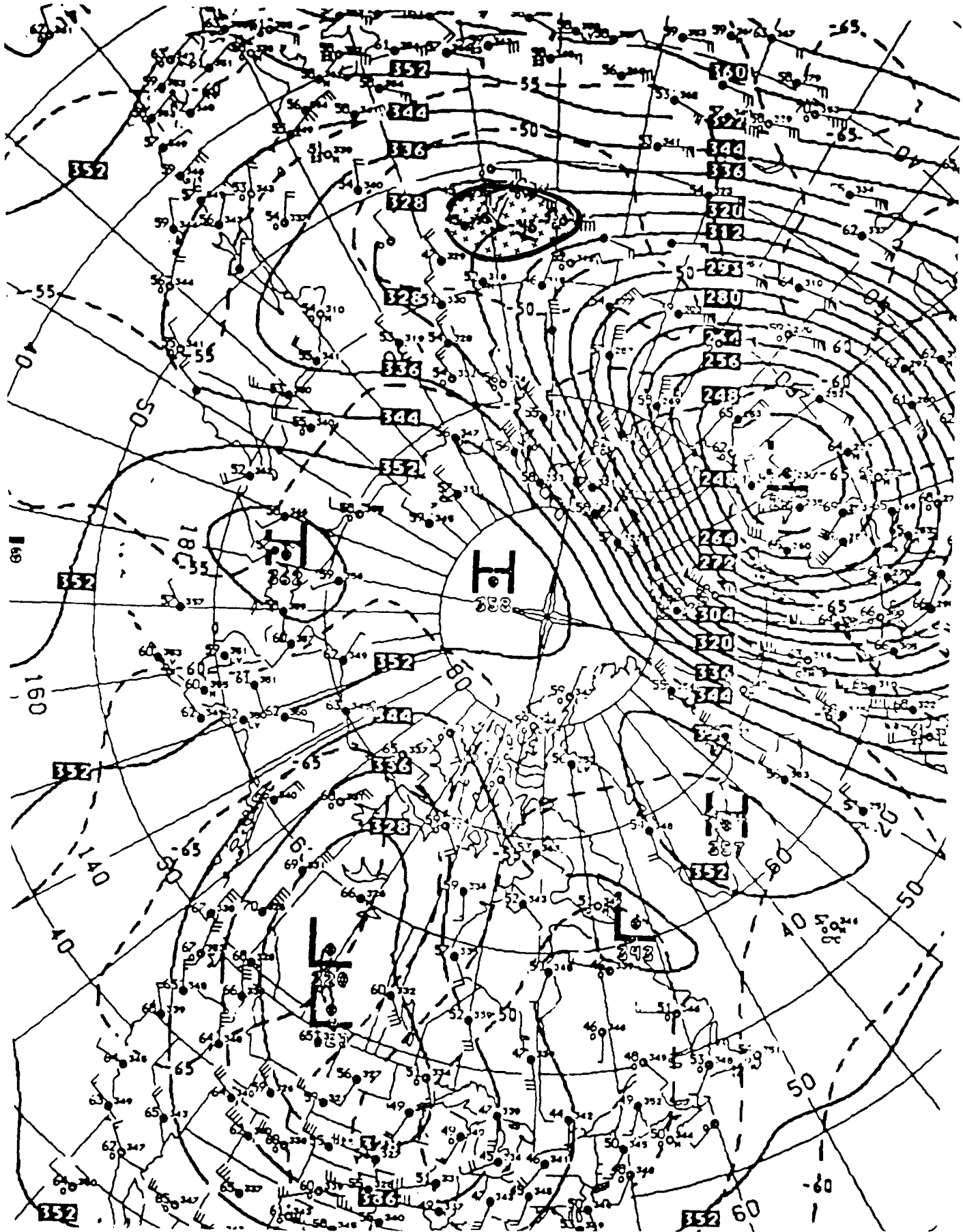


Fig. 39. 30 mb height/temperature for January 22, 1985.

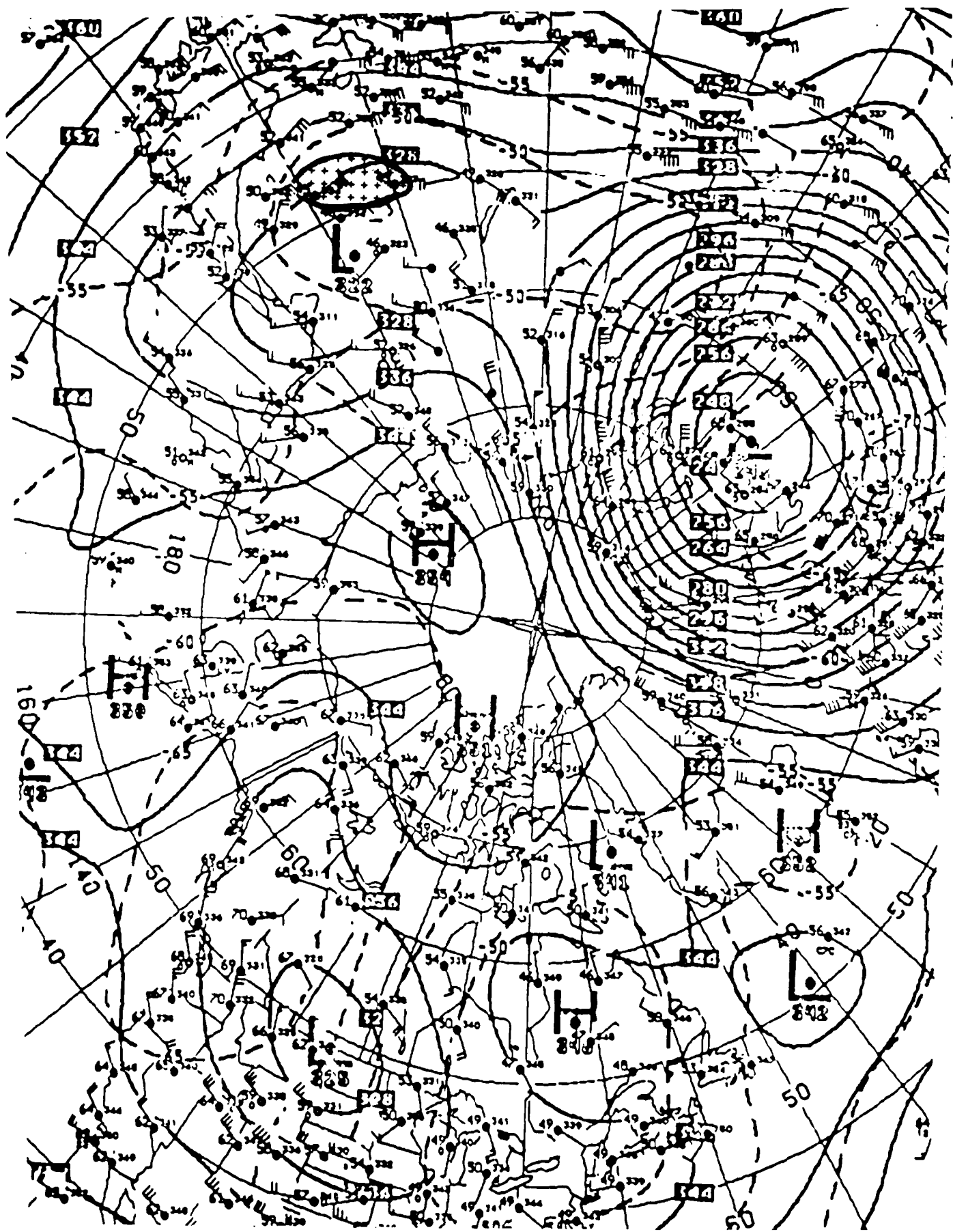
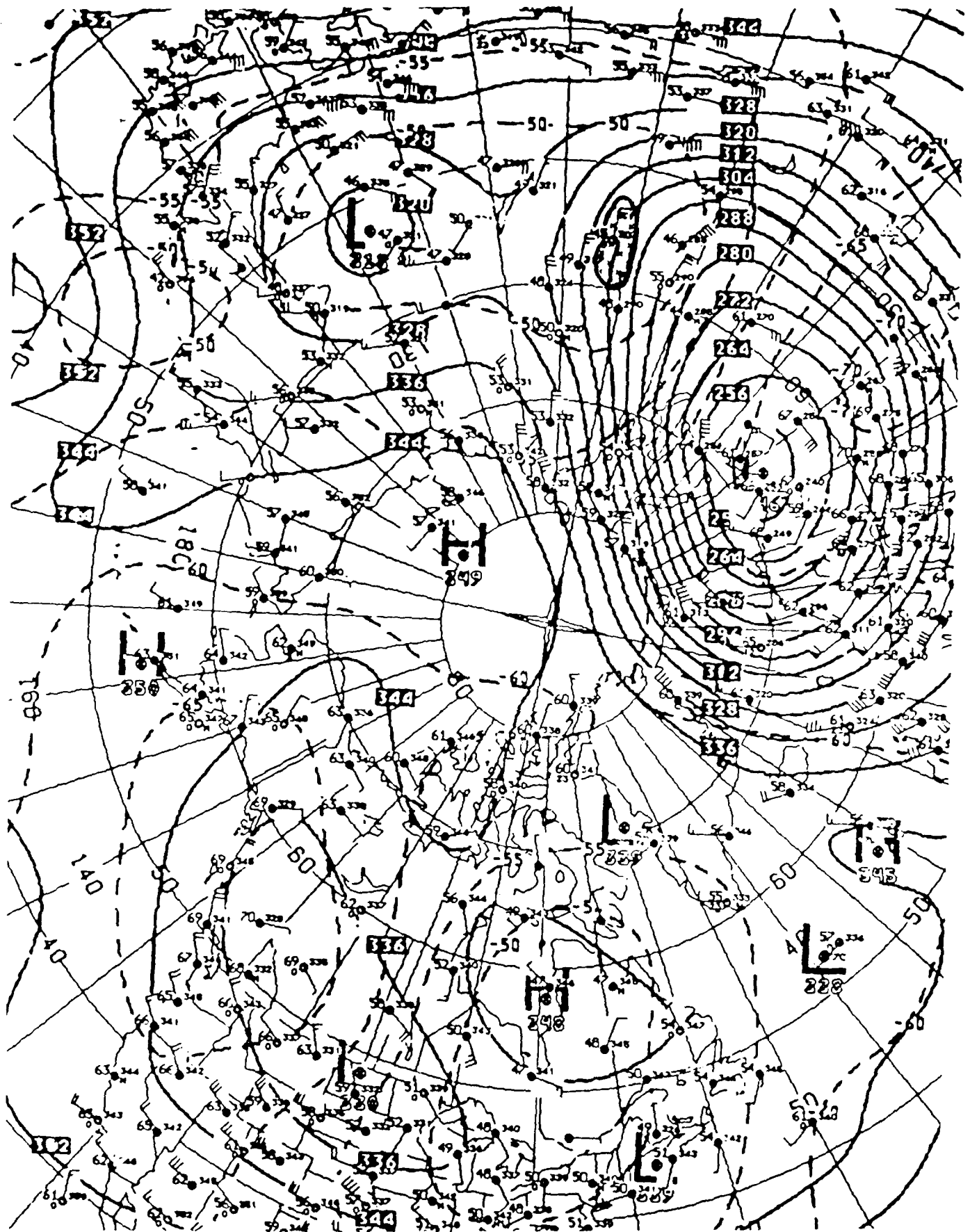


Fig. 40. 30 mb height/temperature for January 24, 1985.



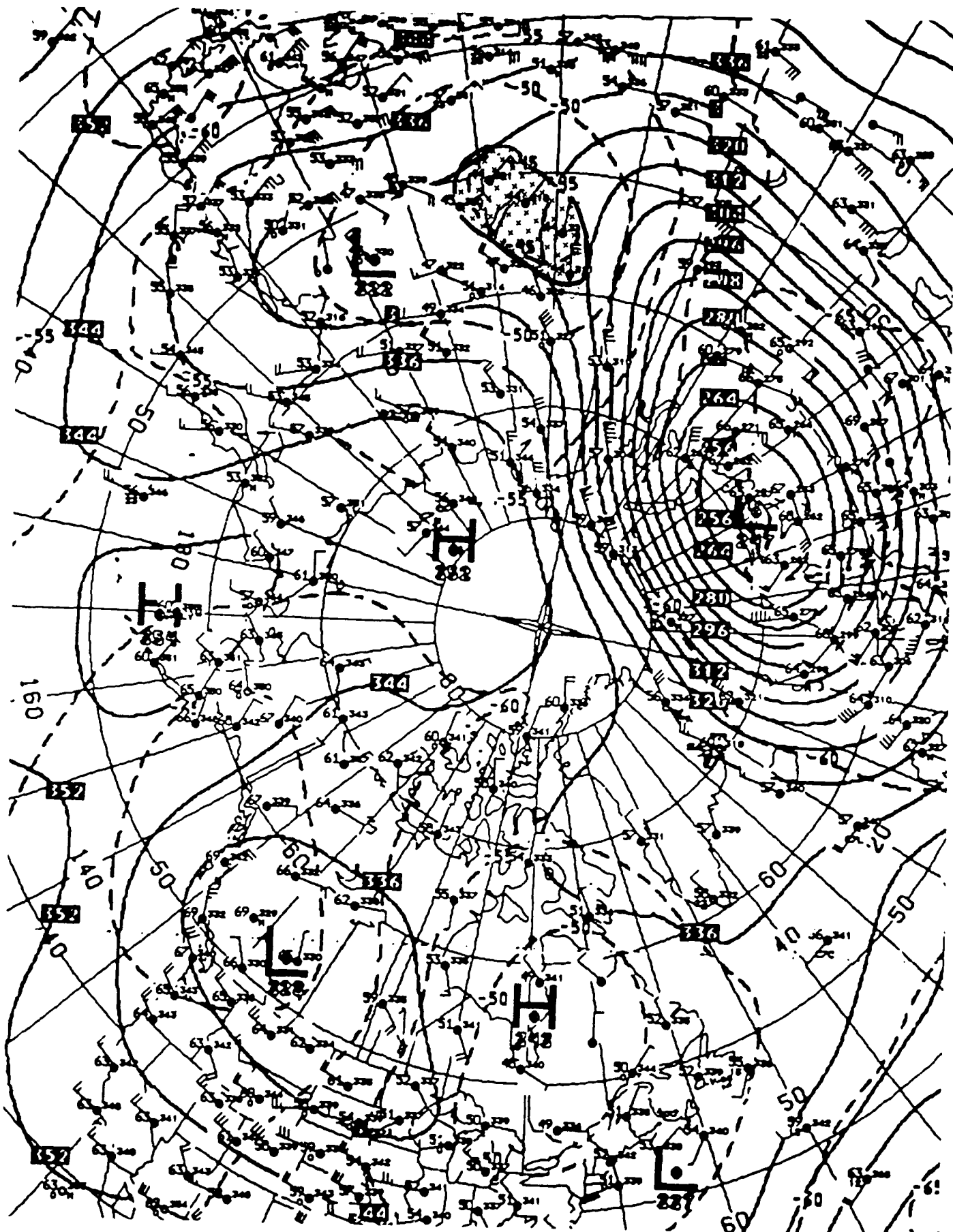


Fig. 42. 30 mb height/temperature for January 26, 1985.

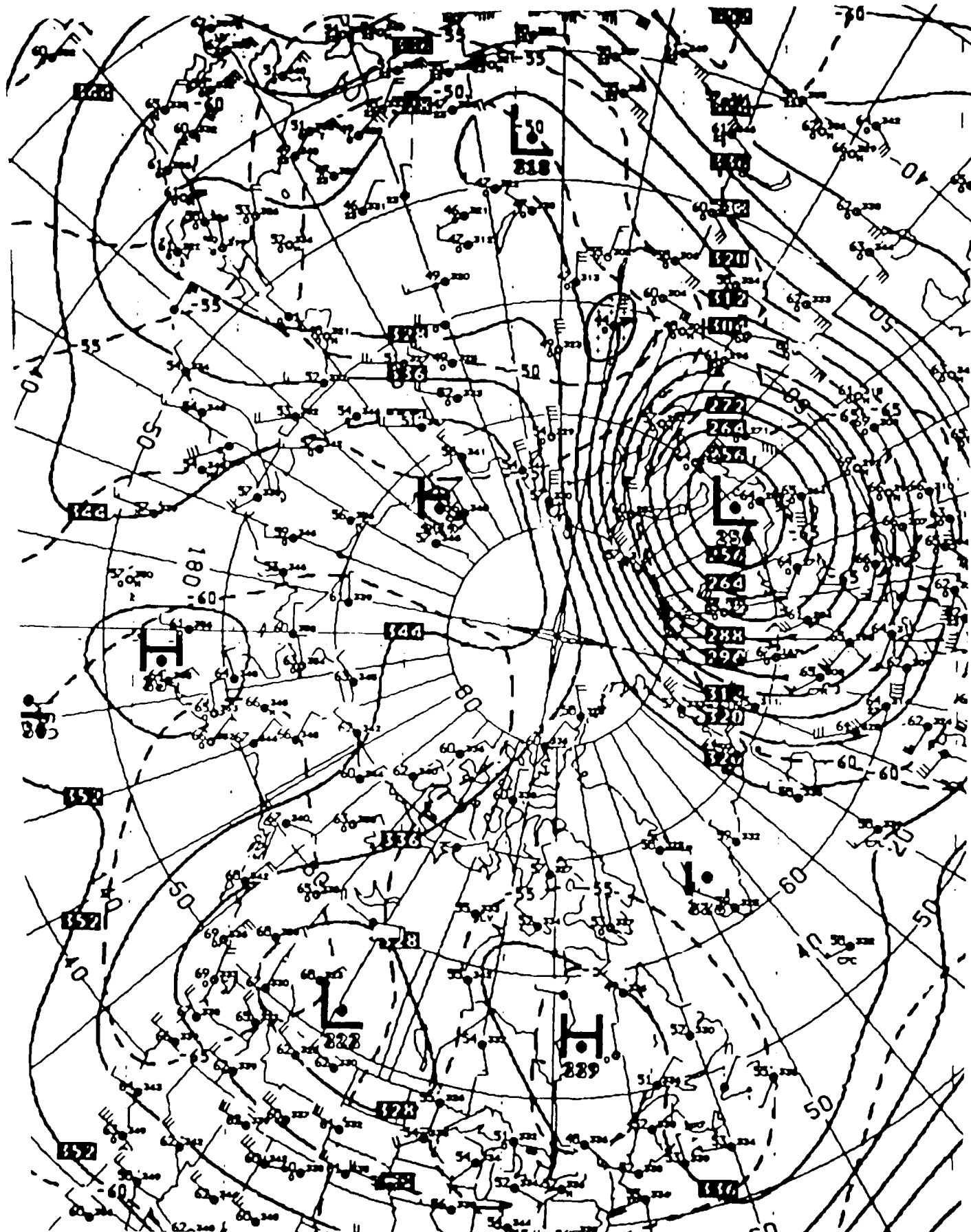


Fig. 43. 30 mb height/temperature for January 27, 1985.

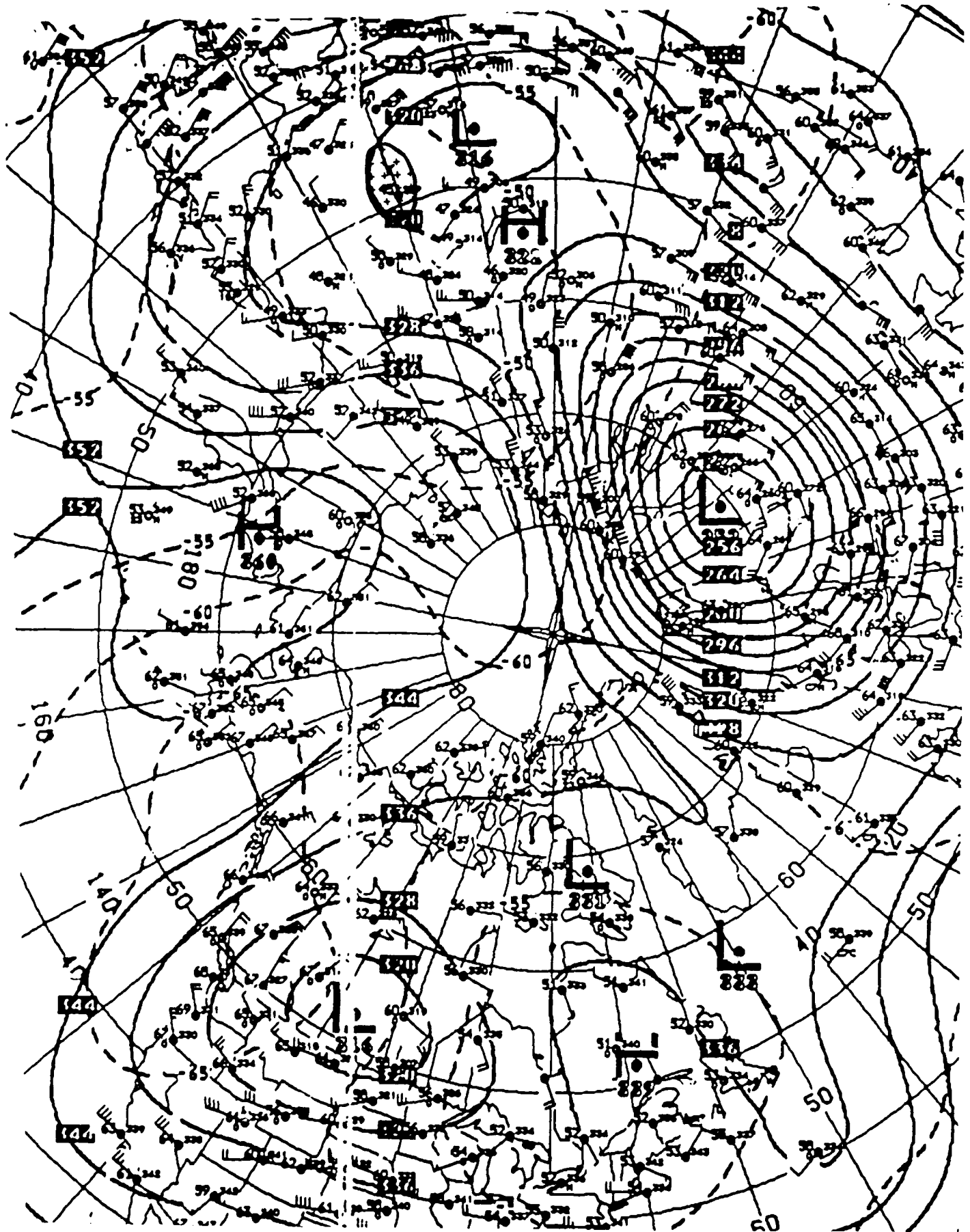


Fig. 44. 30 mb height/temperature for January 28, 1985.

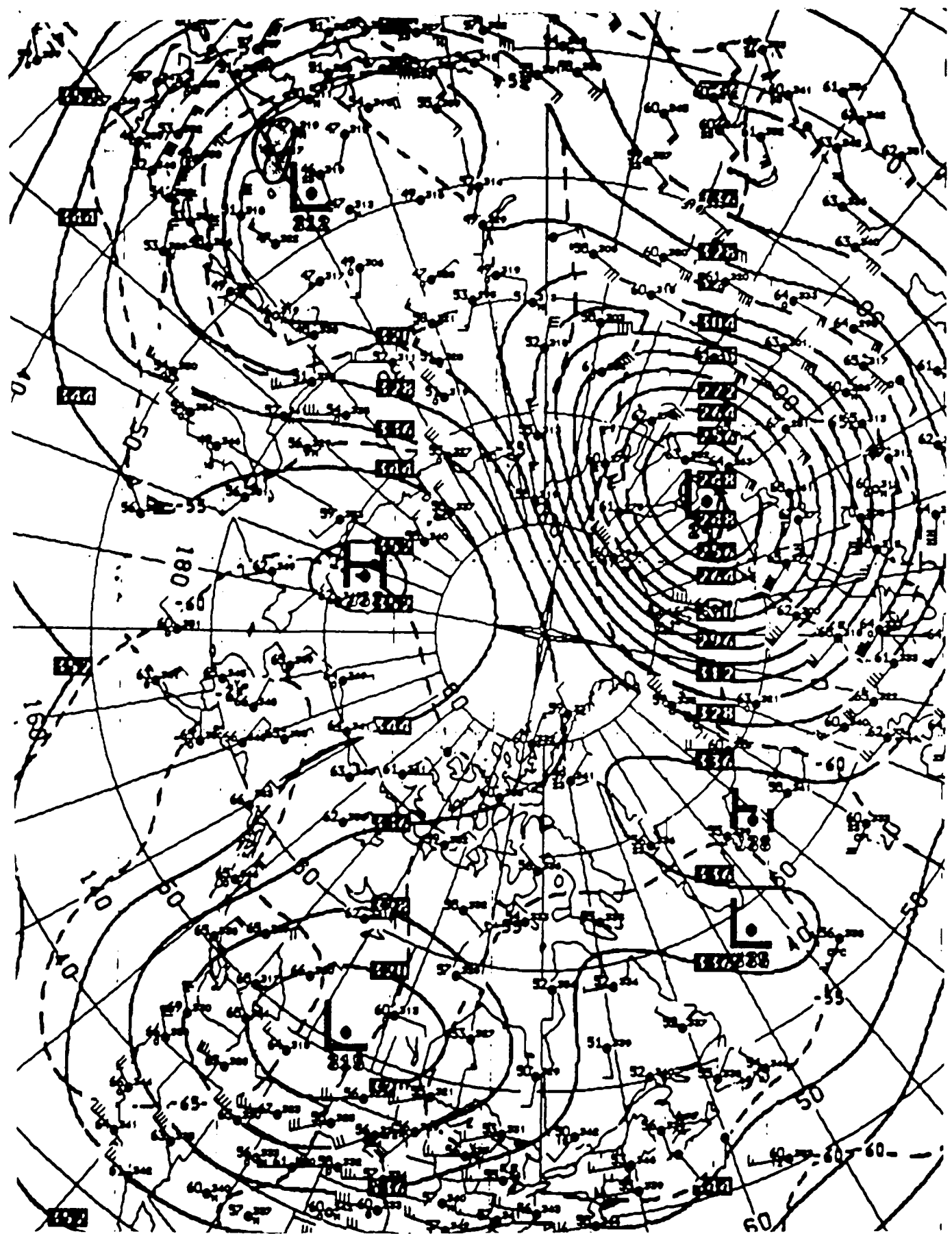


Fig. 45. 30 mb height/temperature for January 29, 1985.

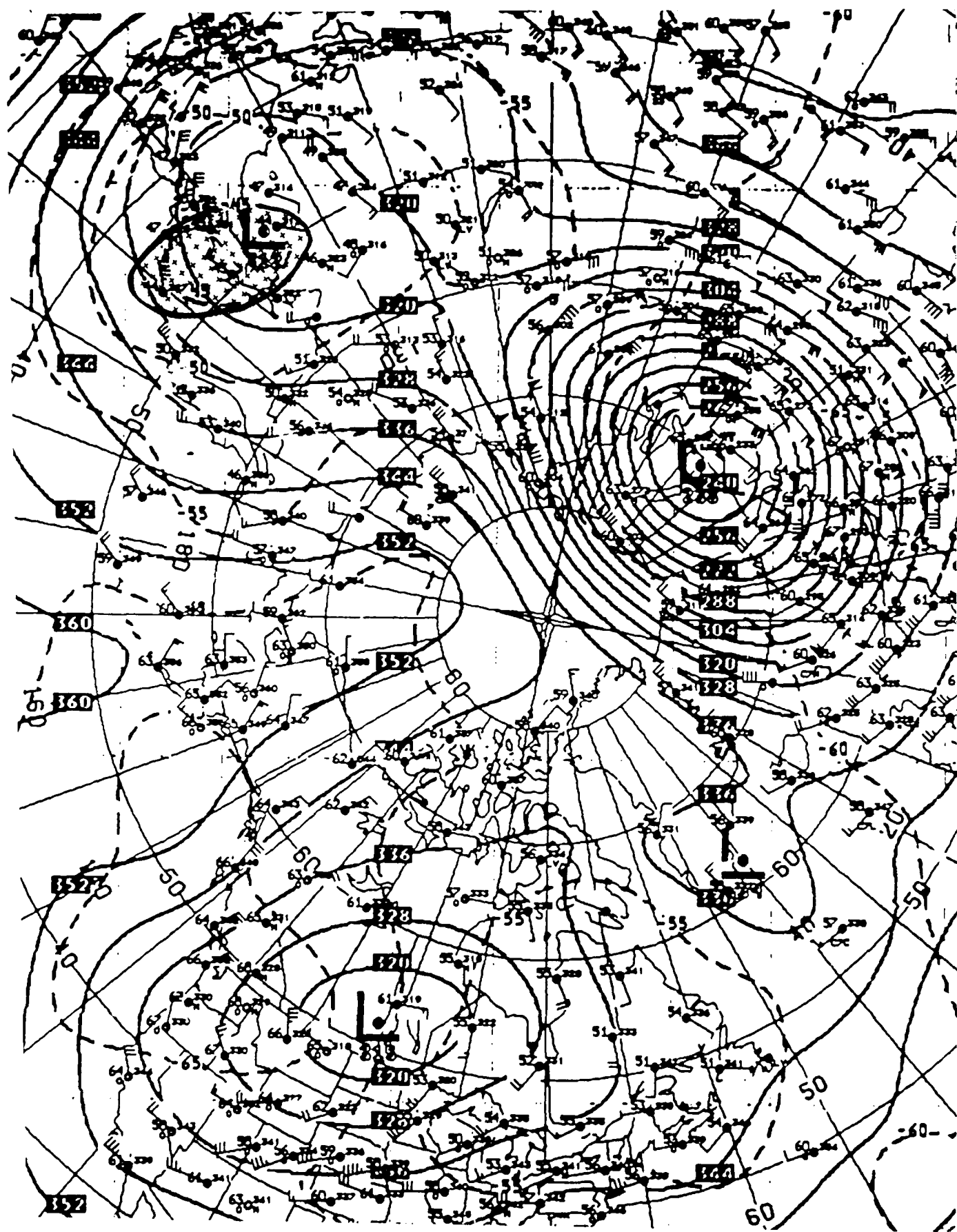
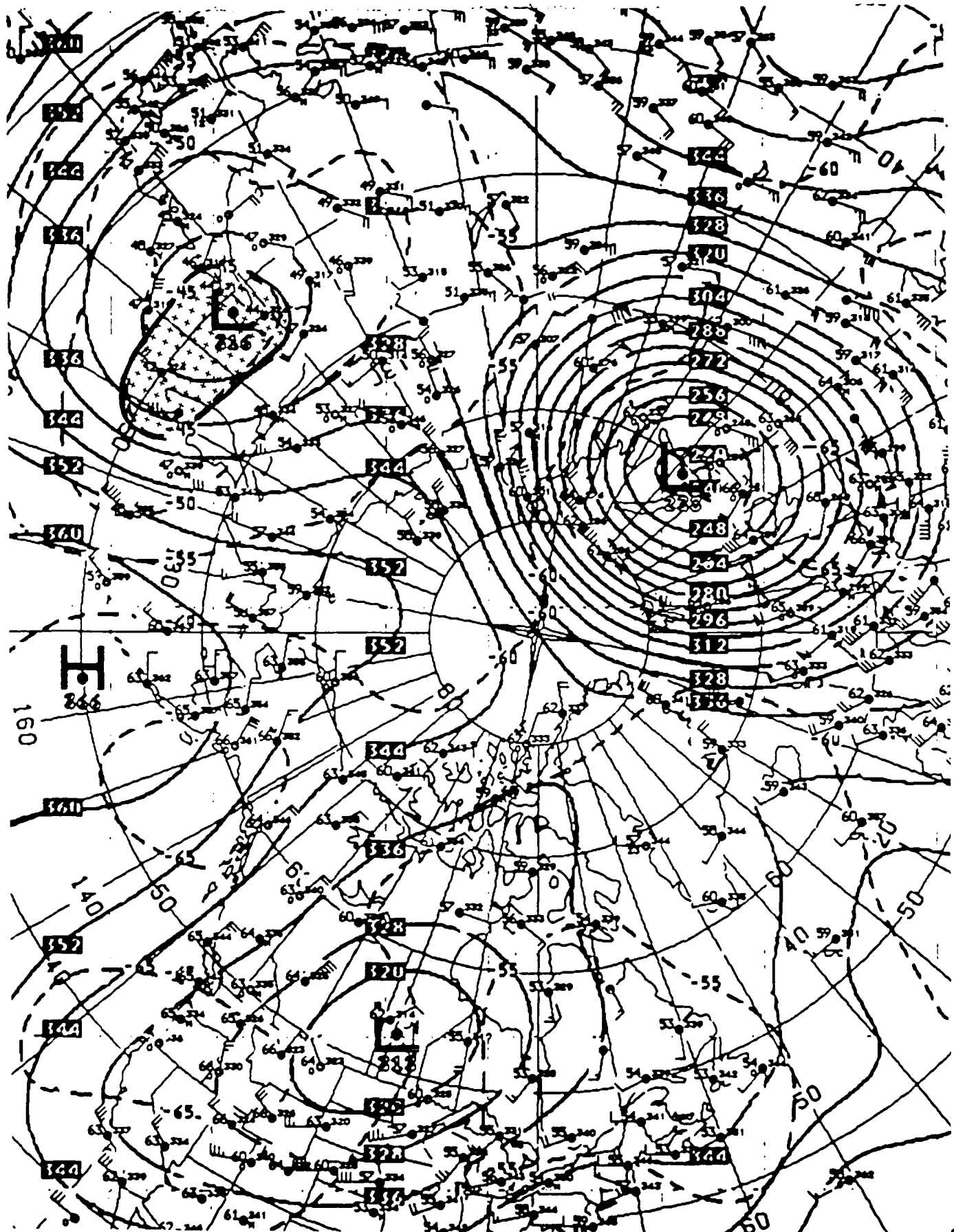


Fig. 46. 30 mb height/temperature for January 30, 1985.



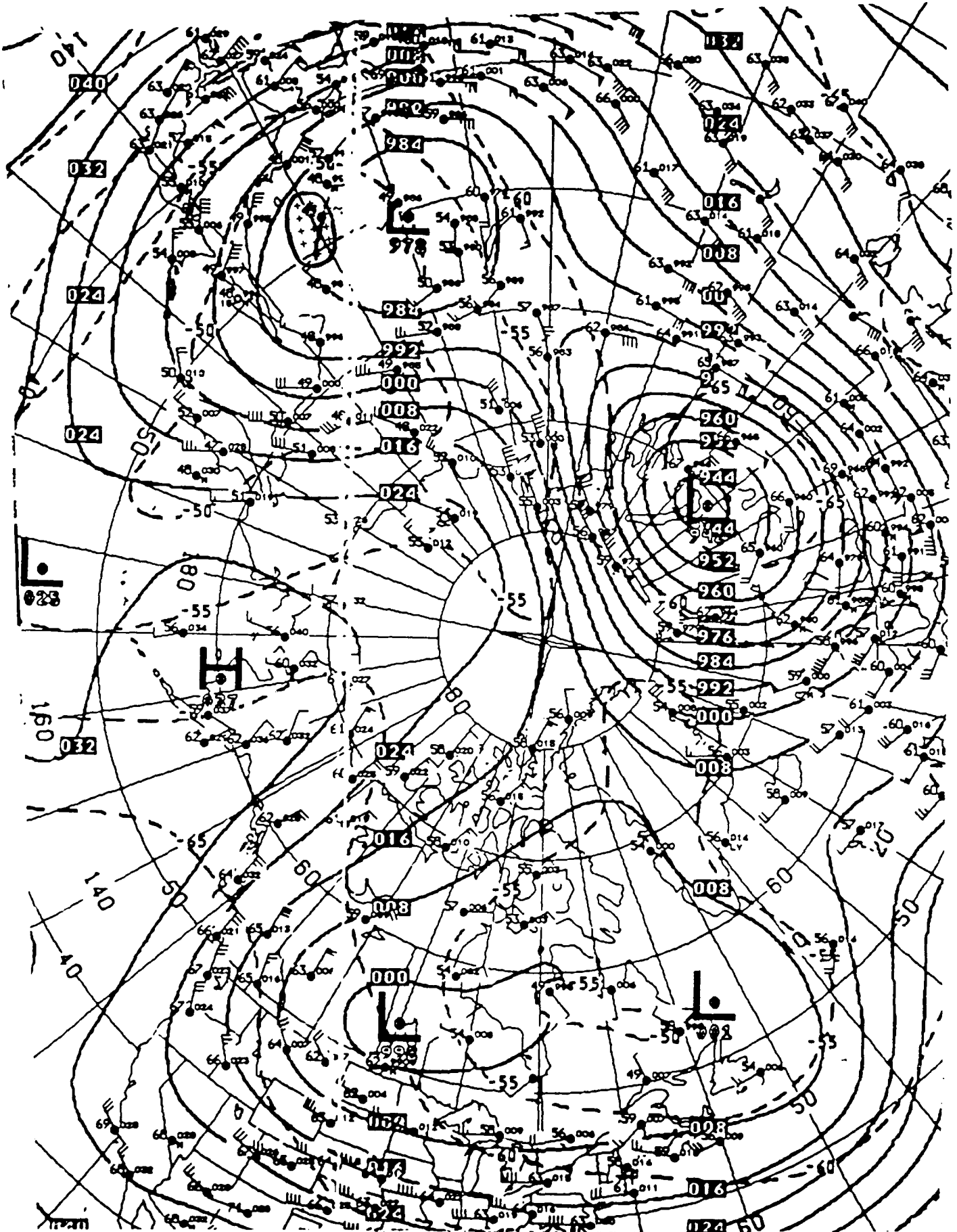


Fig. 48. 50 mb height/temperature for January 28, 1985.

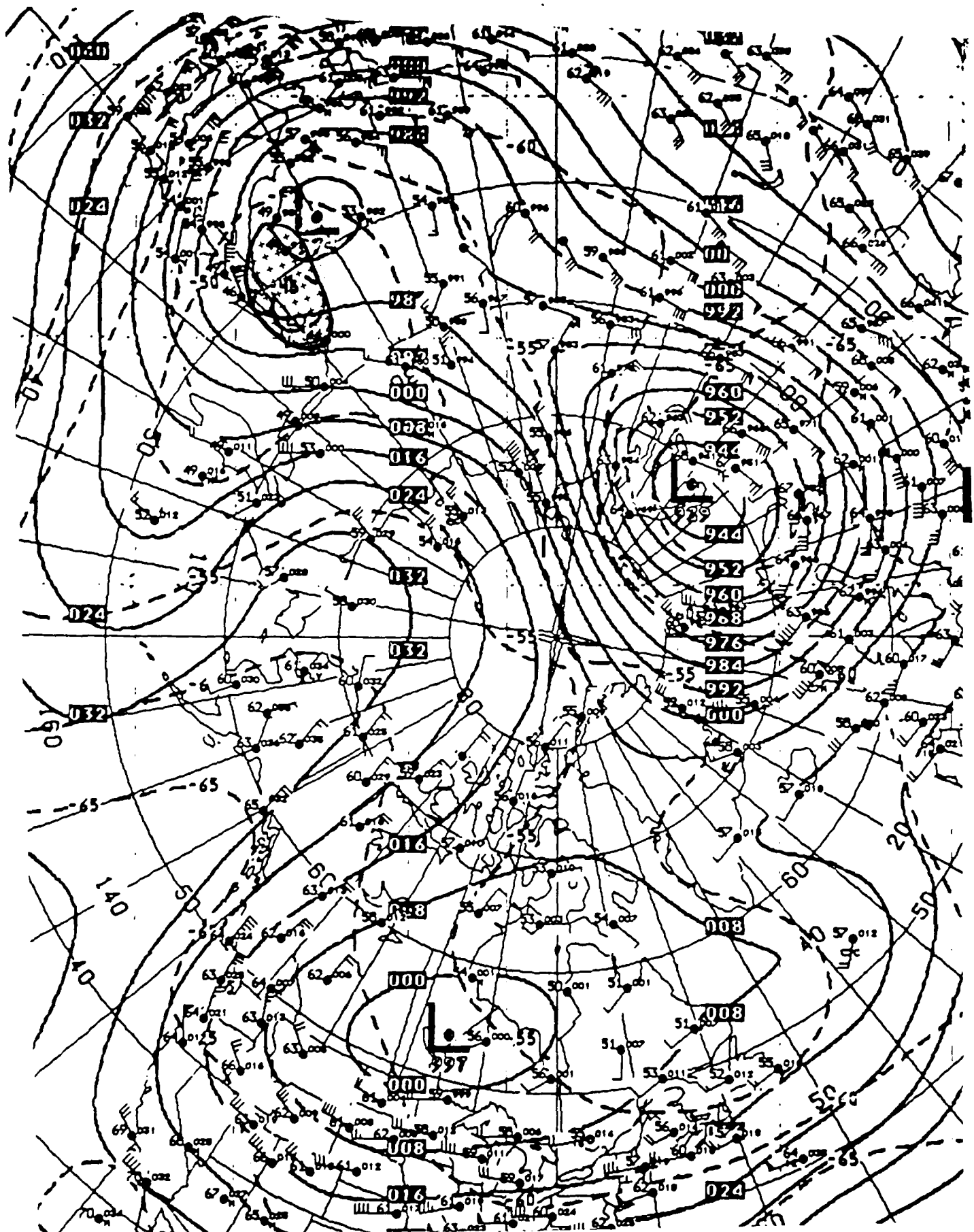


Fig. 49. 50 mb height/temperature for January 29, 1985.

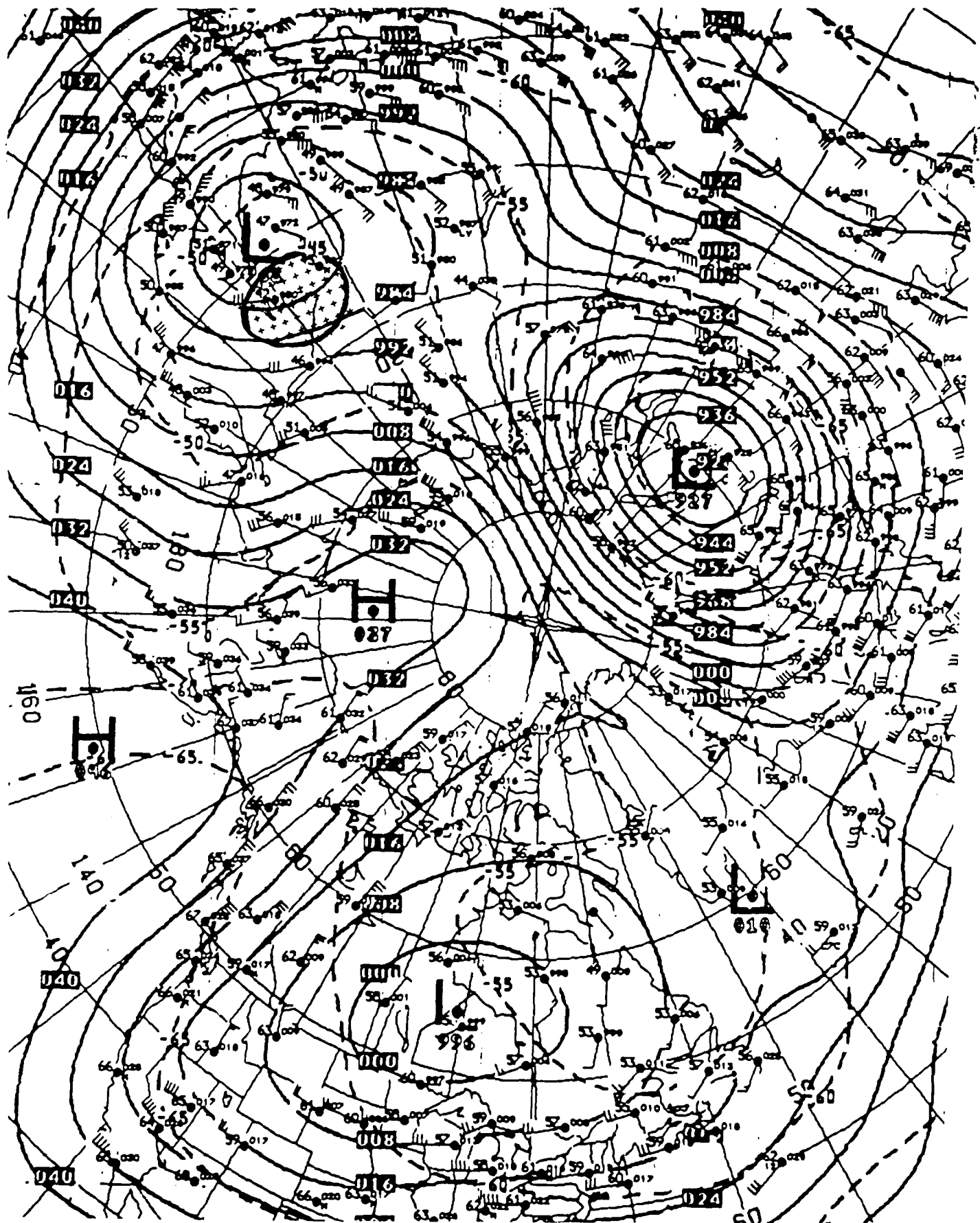


Fig. 50. 50 mb height/temperature for January 30, 1985.

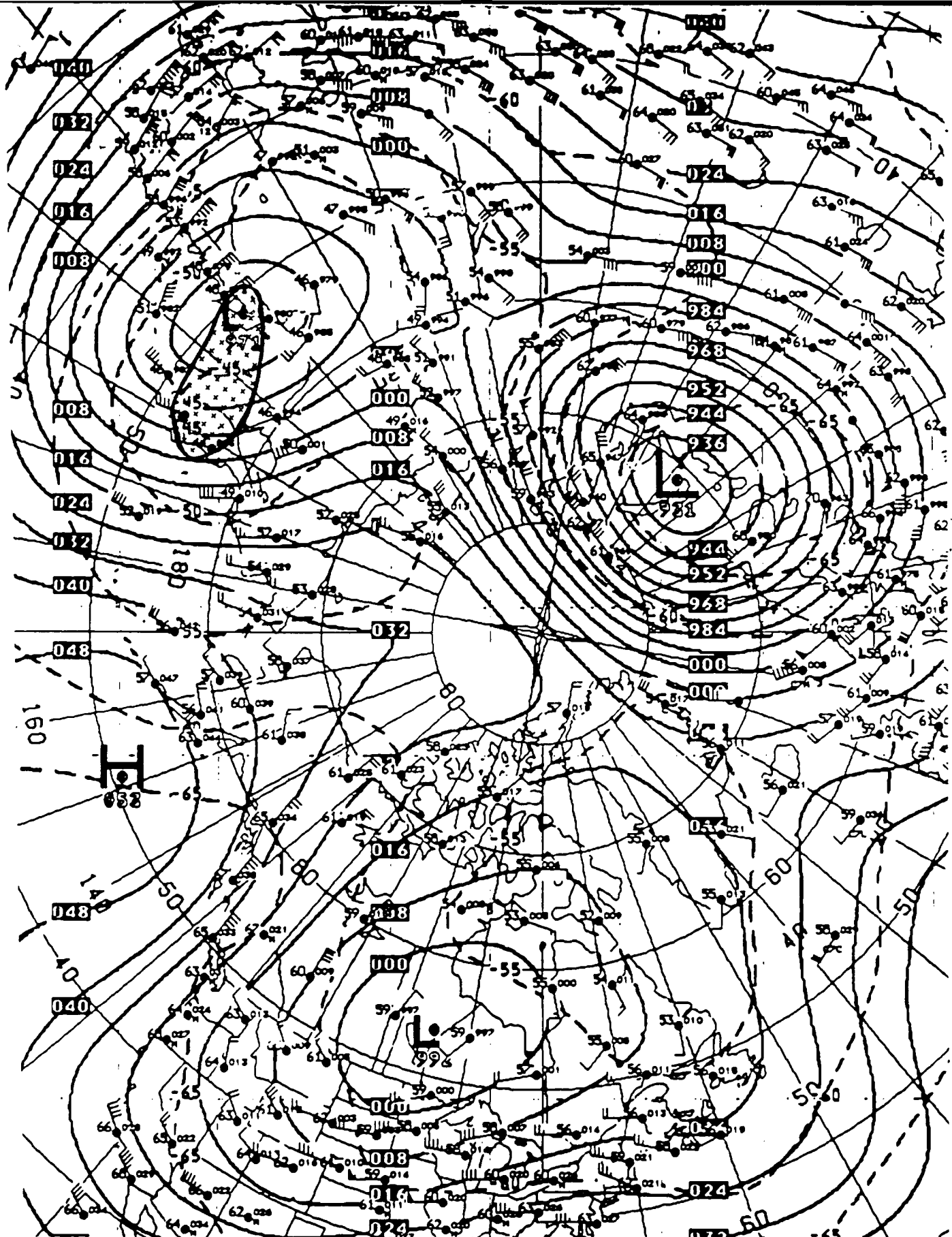


Fig. 51. 50 mb height/temperature for January 31, 1985.

Listed below are the significant data obtained from the 30 mb and 50 mb charts of the minor warming.

#### 30 mb Chart Results

<u>Date</u>	<u>Max Temp</u>	<u>Wind Dir &amp; Speed</u>	<u>Latitude</u>	<u>Longitude</u>	<u>Wave#</u>
Jan 20	-44° <sup>0</sup> C	S 40 kt	60N	105E	2
Jan 21	-36° <sup>0</sup> C	S 35 kt, W 35 kt	55-60N	110E-090E	2
Jan 22	-45° <sup>0</sup> C	W 40 kt	50-65N	120E-110E	Breaking
Jan 24	-45° <sup>0</sup> C	W 30 kt	45-50N	130E-120E	Breaking
Jan 25	-45° <sup>0</sup> C	S 30 kt	55-60N	095E-090E	1
Jan 26	-44° <sup>0</sup> C	S 20 kt	50-55N	110E-100E	1
Jan 27	-44° <sup>0</sup> C	S 40 kt	60-65N	090E	1
Jan 28	-45° <sup>0</sup> C	S 10 kt	45-50N	120E	Building
Jan 29	-45° <sup>0</sup> C	SW 10 kt	40-45N	130E	Building
Jan 30	-43° <sup>0</sup> C	S 30 kt, SW 30 kt	45-50N	150E-135E	Building
Jan 31	-44° <sup>0</sup> C	S 30 kt, E 15 kt	45-55N	160E-140E	2

#### 50 mb Chart Results

<u>Date</u>	<u>Max Temp</u>	<u>Wind Dir &amp; Speed</u>	<u>Latitude</u>	<u>Longitude</u>	<u>Wave#</u>
Jan 28	-45° <sup>0</sup> C	SW 20 kt	45-50N	130E	3
Jan 29	-44° <sup>0</sup> C	S 10 kt	45-55N	140E-135E	3
Jan 30	-42° <sup>0</sup> C	E 35 kt	50-60N	145E-130E	3
Jan 31	-44° <sup>0</sup> C	S 30 kt	50-60N	160E-140E	3

This warming is first seen at the 30 mb level on January 20, Fig. 37, but does not appear at the 50 mb level until January 28, Fig. 48. As with a major warming HF propagation was degraded throughout the warming. Aircraft transiting through the warming area at these altitudes would not have had to deal with sudden wind shift encountered in a major warming but would still have to be able to withstand the stress imposed by the steep temperature gradient. Turbulence created by these

sudden "hot spots" would still pose a probelm.

It is hard to say how or when this minor warming ended as it appeared to be peaking just as January 1985 ended, the end of this case study's data base. Again, the 30 mb and 50 mb charts displayed many of the same similarities and discontinuities seen during the major warming. Temperature profiles between the two levels were almost identical. The minor warming was located right where it was latitudinally supposed to occur, in the 45-65N belt. Winds in both levels were predominately westerly or southerly with the 50 mb winds being slightly weaker than the 30 mb winds. The major difference between the two levels is also a big difference bettwen the two types of warmings - the wave pattern. The 50 mb level was dominated by wave 3 throughout the warming while the 30 mb level experienced both wave 1 and wave 2.

### **Conclusion**

The purpose of this case study was to show some of the differences readily apparent between a major and minor warming and how these warmings vary at the 30 mb and 50 mb levels. January 1985 was chosen as a month that had data displaying both events. Information that would be pertinent to an operational forecaster was briefly discussed. One of the biggest obstacles facing the operational forecasters of the stratosphere is that no prognostic charts are readily available for their use, instead they must rely solely on analysis charts like the ones presented in this study to make their forecasts.

## References

- Andrews, D. G., J. R. Holton, C. B. Leovy, 1987: Stratospheric Sudden Warmings, **Middle Atmosphere Dynamics**, Academic Press, 489pp.
- Angell, J. K. and J. Korshover, 1970: Quasi-Biennial, Annual, and Semiannual Zonal Wind and Temperature Harmonic Amplitudes and Phases in the Stratosphere and Low Mesosphere, *J. Geophys. Res.*, **75**, 543-549
- Blackshear, W. T., W. L. Grose and R. E. Turner, 1987: Simulated Sudden Stratospheric Warmings: Synoptic Evolution, *Quart. J. Roy. Meteor. Soc.*, **113**, 815-846.
- Butchart, B., S. A. Clough, T. N. Palmer, and P. J. Trevelyan, 1982: Simulations of an Observed Stratospheric Warming with Quasi-geostrophic Refractive Index as a Model Diagnostic, *J. Roy. Meteor. Soc.*, **108**, 475-502.
- Charney, J. G. and P. G. Drazin, 1961: Propagation of Planetary-Scale Disturbances from the Lower into the Upper Atmosphere, *J. Geophys. Res.*, **66**, 83-109.
- Dunkerton, T., C-P F. Hsu, and M. E. McIntyre, 1981: Some Eulerian and Lagrangian Diagnostics for a Model Stratospheric Warming, *J. Atmos. Sci.*, **38**, 819-841.
- Grose, W. L. and K. V. Haggard, 1981: Numerical Simulation of a Sudden Stratospheric Warming with a Three-Dimensional, Spectral, Quasi-Geostrophic Model, *J. Atmos. Sci.*, **38**, 1480-1496.
- Haymond, Frederick B., 1967, High Altitude Clear Air Turbulence, **9WS/TR, 002**, Air Weather Service (MAC)United States Air Force, 147pp.
- Holton, J. R., 1976: A Semi-Spectral Numerical Model for Wave-Mean Flow Interactions in the Stratosphere: Applications to Sudden Stratospheric Warmings, *J. Atmos. Sci.*, **33**, 1639-1649.
- , 1977: Interannual Variability of the Winter Stratosphere in the Northern Hemisphere, *Mon. Wea. Rev.*, **106**, 762-770.
- , 1979: **An Introduction to Dynamic Meteorology**, Academic Press, 391pp.
- , 1981: The Amplification of Height Wave 1 in January 1979: A Characteristic Precondition for the Major Warming in February, *Mon. Wea. Rev.*, **109**, 983-987.
- , 1982: On the Interannual Variability of the Middle Stratosphere During the Northern Winters, *J. Meteor. Soc. Japan*, **60**, 124-139.

- Hsu, C-P F., 1981: A Numerical Study of the Role of Wave-Wave Interaction During Sudden Stratospheric Warmings, *J. Atmos. Sci.*, **38**, 189-216.
- Julian, P. R. and K. B. Labitzke, 1965: A Study of Atmospheric Energetics During the January - February 1963 Stratospheric Warming, *J. Atmos. Sci.*, **22**, 597-610.
- Kanazawa, H., 1980: The Behavior of Mean Zonal Wind and Planetary-Scale Disturbances in the Troposphere and Stratosphere during the 1973 Sudden Warming, *J. Meteor. Soc. Japan*, **58**, 329-356.
- Labitzke, K., 1965: On the Mutual Relation between Stratosphere and Troposphere during Periods of Stratospheric Warmings in Winter, *J. Appl. Meteor.*, **4**, 91-99.
- , 1977: Interannual Variability of the Winter Stratosphere in the Northern Hemisphere, *Mon. Wea. Rev.*, **105**, 762-770.
- Lee, 1Lt. David R., Capt. Roland B. Stull and Maj. William S. Irvine, 1979: Clear Air Turbulence Forecasting Techniques, *AFGWC/TN, 79/001*, Air Weather Service (MAC) United States Air Force, 119pp.
- Mahlman, J. D., 1969: Heat Balance and Mean Meridional Circulations in the Polar Stratosphere During the Sudden Warming of January 1958, *Mon. Wea. Rev.*, **97**, 534-539.
- Matsuno, T., 1971: A Dynamical Model of the Stratospheric Sudden Warming, *J. Atmos. Sci.*, **28**, 1470-1493.
- McGuirk, J. P. and D. A. Douglas, 1988: Sudden Stratospheric Warming and Anomalous U.S. Weather, *Mon. Wea. Rev.*, **116**, 162-174.
- McIntyre, M. E., 1982: How Well Do We Understand the Dynamics of Stratospheric Warmings?, *J. Meteor. Soc. Japan*, **60**, 37-60.
- Mechoso, C. R., A. Yamazaki, A. Kitah, and A. Arakawa, 1988: Numerical Forecasts of Stratospheric Warming Events During the Winter of 1979, *Mon. Wea. Rev.*, **113**, 1015-1029.
- Miyakoda, K., R. F. Strickler, and G. D. Hembree, 1970: Numerical Simulation of the Breakdown of a Polar-Night Vortex in the Stratosphere, *J. Atmos. Sci.*, **27**, 139-154.
- Muench, H. S., 1965: On the Dynamics of the Wintertime Stratospheric Circulation, *J. Atmos. Sci.*, **22**, 349-360.
- O'Neill, A., 1980: The Dynamics Of Stratospheric Warmings Generated by a General Circulation Model of the Troposphere and Stratosphere, *J. Roy. Meteor. Soc.*, **106**, 659-690.

- Palmer, T. N., 1981: Diagnostic Study of a Wavenumber-2 Stratospheric Sudden Warming in a Transformed Eulerian-Mean Formalism, *J. Atmos. Sci.*, **38**, 844-855.
- Perry, J. S., 1967: Long-Wave Energy Processes in the 1963 Sudden Stratospheric Warming, *J. Atmos. Sci.*, **24**, 539-550.
- Pick, D. R., 1979: Stratospheric Charts for Period 1 January - 31 March 1979, Document M019/SC/79/1/u, Meteorological Office, Bracknell, Berkshire, UK.
- Plumb, R. A., 1981: Instability of the Distorted Polar Night Vortex: A Theory of Stratospheric Warmings, *J. Atmos. Sci.*, **38**, 2514-2531.
- Quiroz, R. S., A. J. Miller, and R. M. Nagatani, 1975: A Comparison of Observed and Simulated Properties of Sudden Stratospheric Warmings, *J. Atmos. Sci.*, **32**, 1723-1736.
- Simmons, A. J., and R. Strufing, 1983: Numerical Forecasts of Stratospheric Warming Events Using a Model With a Hybrid Vertical Coordinate, *Quart. J. Roy. Meteor. Soc.*, **109**, 81-111.
- Tung, K. K., and R. S. Lindzen, 1979: A Theory of Stationary Long Waves, Part II: Resonant Rossby Waves in the Presence of Realistic Vertical Shears, *Mon. Wea. Rev.*, **107**, 735-749.
- , and H. Yang, 1988: Dynamical Component of Seasonal and Year-to-Year Changes in Arctic and Global Ozone, *J. Geophys. Res.*, **93**, 12537-12559.
- Welander, P., 1955: Studies on the General Development of Motion in a Two-Dimensional Ideal Fluid, *Tellus*, **7**, 141-156.